THE GEOLOGY, GEOCHEMISTRY AND GENESIS OF URANIUM MINERALIZATION AT DINYA - KOKING N.E. NIGERIA

BY

TAVERSHIMA NAJIME
B.SC. (Hons) A.B.U

THESIS SUBMITTED TO THE POSTGRADUATE SCHOOL AHMADU BEL LO UNIVERSITY, IN PARTIAL FULFILLMENT OE THE REQUIREMENTS FOR THE DEGREE OF MASTER OF SCIENCE (GEOLOGY)

Department of Geology
Faculty of Science
Ahmadu Bello University
Zaria, Nigeria

DECEMBER, 1992

DECLARATION

I declare that this thesis, is my own work and has not been submitted in any form for another degree or diploma to any other University or Institution. Information derived from published or unpublished work of other workers has been acknowledged in the text.



Signature

4/12/92

Date

CERTIFICATION

This thesis titled, The Geology, Geochemistry and Genesis of Uranium Mineralization at Dinya-Koking, N.E. Nigeria by Tavershima Najime meets the regulation governing the award of the degree of Masters of Science of Ahmadu Bello University, and is approved for its contribution to knowledge and literary presentation.

Chairman, Supervisory Committee	Date
Prof S.I. Abaa	16/03/93
Member, Supervisory Committee	Date
Member, Supervisory Committee	Date
Prof S.I. Abaa	16/03/93
Head of Department	Date
	2/2/94
Dean, Postgraduate School	Date

DEDICATION

To Dooshima Wife

Alueshima Daughter

Nashima Son

AND

To the Memory of Najime Ashwe.

ACKNOWLEDGEMENTS

My sincere gratitude to Dr. C. D. Okujeni for suggesting this work and his frank criticism during the work. The arrangement for the field work, samples analysis and computer data analysis he made for this work are very much appreciated. I thank Prof. S. I. Abaa for the suggestions, criticism and encouragement on this work.

I appreciate the help from Mr. O. Lawal of I.A.R. for sample analysis and Mr. Idris Funtua of C.E.R.I. for his help in data analysis.

I acknowledge the cooperation of technical staff of Geology and Microbiology departments for their assistance during the different stages of laboratory work.

Finally, I acknowledge the support of my mother Asaa Najime and the entire family of Najime Ashwe for their good prayers, and understanding towards the success of this work.

I cannot mention the names of all who contributed in various ways to make this work a success. This is not to say their contributions are forgotten or invaluable. From my heart, I still remember and I say 'Thank you all'.

ABSTRACT

The geology of Nigeria indicates possible areas of uranium mineralization. Radiometric anomalies have been found both within the sedimentary basins and the basement complex.

The Dinya-Koking area is one of these areas that have radiometric values above 5000 C.P.S.. The area falls within the Proterozoic basement rocks east of the Cretaceous Benue sedimentary basin.. Emplaced within the basement rocks are rhvolitic rocks of Cenozoic age. The rhyolite dykes lie along a North-South lineaments believed to be shear zones. The high radiometric values are found to be closely associated with the rhyolitic bodies.,

Alterations of rocks occur at the contact of the basement granites and rhyolites.. The alterations indicate secondary processes, which were due to the action of hydrothermal solution during or/and after the emplacement of the rhyolites.

The action of the hydrothermal solution is concentrated along the contact and shear zones which acted as channelways along which the fluid circulated.. Intact the shear zones and fractures were also the deep seated structures through which the supercritical fluid circulated and scavaged uranium and other metals that tend to be enriched together with Uranium.. The mineralizing fluid itself was generated by the magmatic activity *due* to gravitation and crystallization fractionazation-

Geochemistry of the rock samples reveals a constant depletion of the rock forming oxides Cao, mgo and Na_2o but. enrichment of uranium, potassium and other metals.. The enrichment and depletion trend match closely to the element correlation and element associations.. The trend of elements point to the fact that the mineralizing fluid was rich in uranium., Cr» Ni, Cu, Zn„ Fe, mn and P.. The presence of Ni and Fe in the mineralizing solution confirms its association with the volcanic activity that led to the rhvolites emplacements, while the association of uranium and the I. ithophil.es must, be *due* to leaching and concentration in the hydrothermal solutions.

TABLE OF CONTENTS

		Page
1.0	Introduction	1
1.1	Location and accessibility	2
1.2	Relief and Drainage	4
1.3	Climate and vegetation	6
1.4	Previous work	8
1.5	Present work	10
2.0	Geological setting	11
	Pan-African activity	11
	Cretaceous activity	12
	Cenozoic activity	12
2.1	Geology of the study area	13
2.1.1	Basement rocks (Precambrian)	14
	Migmatites	14
	Fine grained granite	18
	Porphyritic biotite granite	18
	Equigranular granite	20
	Microgranites	24

		Page
2.1.2	Volcanic rocks (Cenozoic)	25
	Rhyolites	25
2.2	Structures	27
2.2.1	Foliation	28
2.2.2	Faulting	28
2.2.3	Minor bodies	29
2.2.4	Joints	29
3.0	Mineralization	31
3.1	Secondary processes	37
	Altered rocks	37
	Mildy altered porphyritic biotite granite	39
	Intensely altered and sheared porphyritic biotite granite	39
	Mildy altered rhyolites	41
	Intensely altered and sheared rhyolites	43
	Alteration processes	43
	Chloritization	45
	Sericitization	45
	Carbonization	46
	Silicification	46
	Hematization	46

		Page
4.0	Methodology	49
4.1	Geochemical analysis	49
4.2	Analytical methods	49
4.2.1	Atomic Absorption Spectrophotometry for determination of Ca, Mg, Fe, Zn, Mn, Cu, Cr and Ni	52
4.2.2	Flame photometry for determination of Na and K	55
4.2.3	Spectrophotometry for determination of phosphorus, Titanium and Uranium	56
	Phosphorus determination	56
	Titanium determination	60
	Uranium determination	63
5.0	Element distribution	68
5.1	Major elements	68
5.2	Trace elements	88
5.3	Distribution trends	102
	Elements distribution	102
	Depletion and enrichment trends	107
5.4	Correlation Analysis	108
5.5	Principal component Analysis	113
	Element Associations	119

5.6	Comparison between correlation and enrichment enrichment - depletion trends	120
5.7	Comparison between element correlation element association and enrichment - depletion trends	122
6.0	Discussion	125
6.1	Origin of mineralizing fluid	127
6.2	Source of Uranium and other metals	128
6.3	Conclusion	131
6.4	Recommendation	132
	References	134

LIST OF FIGURES

Page

Fig. 1.1 Map of Nigeria showing probable areas of Uranium deposits 3

Fig. 1.2 Drainage, location and accessibility map of the study area 5

Fig. 2.1 Location, and geological setting of the study area 15

Fig. 2.2 Rose diagram of joints trends in the basement rocks 30

Fig. 3.1 Radiometric reading of sampled points using SPP^2 NP Scintilometer 32

Fig. 3.2 Histogram of radiometric values from the mineralized zone 33

Fig. 3.3 Areal distribution of radiometric values in the mineralized zone 34

Fig. 3.4 Cumulative frequency curves of radiometric values 35

Fig. 3.5 Zones of alteration intensity in rhyolites and porphyritic biotite granite 38

Fig. 3.6 Rhyolite outcrop showing mappable alteration 46

Fig. 4.1 Geological map of the study area APPENDIX III

Fig. 4.2 Geological and structural setting of the mineralized zone. 50

Page

Fig. 4.3 Calibration curve for colorimetric determination of phosphorus 59

Fig. 4.4 Calibration curve for colorimetric determination of titanium 62

Fig. 4.5 Calibration curve for colorimetric determination of uranium 66

Fig. 5.1 (a-m) Histograms of CaO, MgO, FeO, K_2O, Na_2O, P_2O_5, TiO_2, MnO, Zn, Cu, Cr, Ni and U frequency distribution. 72-99

Fig. 5.2 (a-m) Areal distribution of CaO, MgO, FeO, K_2O, Na_2O, P_2O_5, TiO_2, MnO, Zn Cu, Cr, Ni and U. 73-101

Fig. 5.3 Percentage element loss and gain in the mildly altered porphyritic biotite granite 105

Fig. 5.4 Percentage element loss and gain in the intensely altered porphyritic biotite granite 105

Fig. 5.5 Percentage element loss and gain in the mildly altered rhyolites 106

Fig. 5.6 Percentage elements loss and gain in the intensely altered rhyolites 106

Fig. 5.6 (a-f) Factor analysis plot for factors I to IV. 116-118

LIST OF TABLES

		Page
Table 2.1	Approximate modal analysis of the basement rocks and rhyolites	17
Table 2.2	Statistics of joints, rhyolite dykes and minor bodies trend.	27
Table 5.1	Range, mean and standard deviation for all the elements.	69
Table 5.2	Range, mean and Stand deviation for the unaltered, mildly altered and intensely altered granites and rhyolites	70
Table 5.3	Loss and gain in the mildly and intensely altered porphyritic biotite granite.	103
Table 5.4.	Loss and gain in the mildly and intensely altered rhyolites.	104
Table 5.5	Correlation matrix of the population data.	109
Table 5.6	Correlation matrix of values from the intensely altered porphyritic biotite granite.	111
Table 5.7	Correlation matrix of intensely altered rhyolites.	112
Table 5.8	Result of the principal component analysis at different percentage variance.	114
Table 5.9	Comparison of element association, element correlation and enrichment-depletion trends.	123

SOME ABBREVIATIONS USED IN THE TEXT

C.P.S	-	counts per seconds (Radioactive emissions)
P.P.M.	-	parts per million
%	-	percentage
V/V	-	volume per volume
E.h	-	Oxidation - Reduction potential
p.H.	-	Hydrogen ion activity in solution (scale of acidity and alkalinity)
EDTA	-	Ethylene diamine tetraacetic acid.
TBP	-	Tributyl phosphate
NH_4NO_3	-	Ammonium nitrate
H.F	-	Hydroflouric acid
$Hclo_3$	-	perchloric acid
H_3PO_3	-	phospheric acid
^oC	-	degrees centigrade
ml	-	milliliters
Cal	-	calories
µg	-	micro grammes
kg	-	kilogrammes
kj	-	kilojoules
nm	-	nanometres
cm	-	centimetres
ca (cao)	-	calcium (calcium oxide)
mg (mgo)	-	magnesium (magnesium oxide)
Na (Na_2O)	-	sodium (sodium oxide)
K (K_2O)	-	potassium (potassium oxide)
Fe (Fe_2O_3)	-	Iron (Iron oxide)
Mn (MnO)	-	Manganese (Maganese oxide)
Ti (TiO_2)	-	Titanium (Titanium oxide)
P (P_2O_5)	-	phosphorus (phosphorus oxide)
CU	-	Copper
Cr	-	Chromium
Ni	-	Nickel
Zn	-	Zinc
U	-	Uranium
N.E.	-	Northeast

APPENDEXES

Appendix I	Result of Analysis for the samples
Appendix II	Cumulative frequency curves for the elements analysed
Appendix III	Figure 4.1 (in pocket).

SOME ABBREVIATIONS USED IN THE TEXT

C.P.S	-	counts per seconds (Radioactive emissions)
P.P.M.	-	parts per million
%	-	percentage
V/V	-	volume per volume
E.h	-	Oxidation - Reduction potential
p.H.	-	Hydrogen ion activity in solution (scale of acidity and alkalinity)
EDTA	-	Ethylene diamine tetraacetic acid.
TBP	-	Tributyl phosphate
NH_4NO_3	-	Ammonium nitrate
H.F	-	Hydrofluoric acid
$HClO_3$	-	perchloric acid
H_3PO_3	-	phospheric acid
^oC	-	degrees centigrade
ml	-	milliliters
Cal	-	calories
µg	-	micro grammes
kg	-	kilogrammes
kj	-	kilojoules
nm	-	nanometres
cm	-	centimetres
ca (cao)	-	calcium (calcium oxide)
mg (mgo)	-	magnesium (magnesium oxide)
Na (Na_2O)	-	sodium (sodium oxide)
K (K_2O)	-	potassium (potassium oxide)
Fe (Fe_2O_3)	-	Iron (Iron oxide)
Mn (MnO)	-	Manganese (Maganese oxide)
Ti (TiO_2)	-	Titanium (Titanium oxide)
P (P_2O_5)	-	phosphorus (phosphorus oxide)
CU	-	Copper
Cr	-	Chromium
Ni	-	Nickel
Zn	-	Zinc
U	-	Uranium
N.E.	-	Northeast

Chapter 1

INTRODUCTION

Both economic and political considerations have become fundamentally important in the search for and exploitation of Uranium ores. The uranium derived from the ores is used as energy fuel in nuclear reactors. It is also used to produce radioactive isotopes for use in industry, agriculture and medicine. Due to the economic and strategic uses of uranium many countries have embarked on intensive search and exploitation of uranium ores.

In Nigeria research work on uranium mineralized areas aimed at delineating economic uranium ore have gained momentum over the past years. The government too has shown interest and given support to research institutions and other establishments, such as the Nigerian Uranium Mining Company (NUMCO), which are involved in exploration and research on uranium ores.

The works of Farrington, (1952); Ojo,(1980); Bowden et. al., (1981); Oshin, (1984); Oshin and Rahaman, (1986); Okujeni et. al.,(1988); Funtua (1988) and many others have indicated that the geographical location, geology and geological history of Nigeria provide for a possible deposition of

uranium ores within certain geochemical terrains (Fig.1.1). These terrains are areas within which some rock types have indicated anomalous abundances (above clark value) of uranium.

The result of these works which have indicated areas of uranium anomalies, have motivated a lot of interest and the need for further work in showings with reported high radiometric readings. The present work was undertaken to make a detailed study of one of such anomalies at the Dinya-Koking areas near Jalingo in Taraba State.

1.1 LOCATION AND ACCESSIBILITY

The Dinya-Koking area is located within Monkin Sheet 216 NW, which covers part of Taraba State, North eastern Nigeria. The area lies adjacent to and east of the Benue trough. It is bounded by Latitudes $8^{O}47'15"N$ and $8^{O}49'30"N$ and longtitudes $11^{O}36'25"E$ and $11^{O}40'15"E$.

The area is accessible from the Numan - Jalingo road where it branches eastward at Lankoviri village to Zing. It is also accessible from the northeastern part along the Yola-Zing road. From Zing the area is accessible along the southward road that leads through Monkin village to Dinya and Koking areas (Fig. 1.2). The road from Monkin to Dinya and Koking areas are seasonal being motorable only during the dry season.

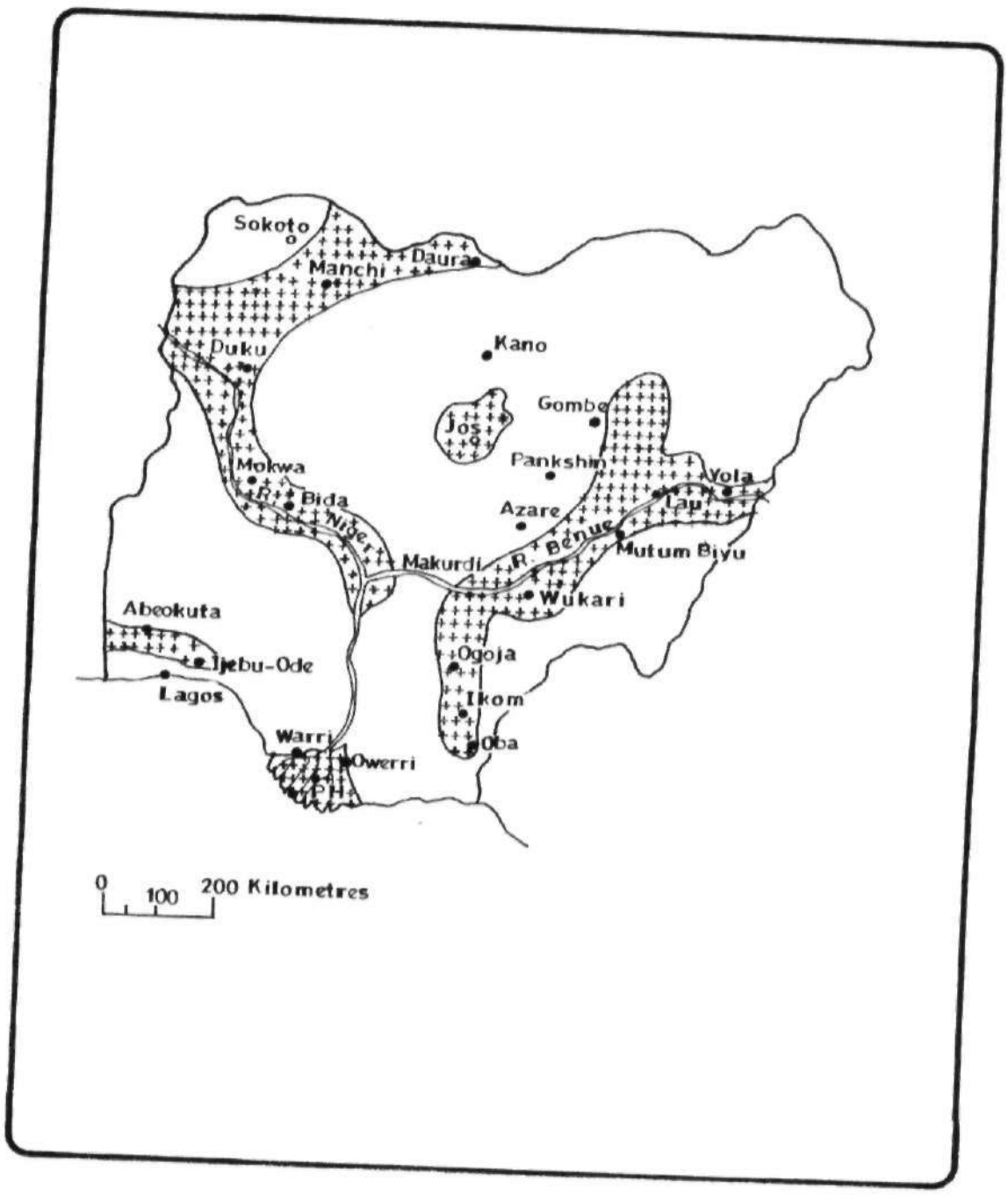


Fig. 1.1. Map of Nigeria showing probable areas for Uranium deposits.
(Ojo, 1980)

Other areas within the mapped area are accessible through numerous footpaths, connecting villages and hamlets.

1.2 Relief and Drainage

The area northeast and southeast of the Benue valley is underlain by basement rocks and scattered occurrences of volcanic rocks. The terrain rises somewhat regularly towards the Cameroon border, reaching maximum heights of 700 - 900 metres in the Mambila plateau region. It is an area of discontinous mountain ranges and dissected high level plateau surfaces.

Within the area of study, the landscape is generally flat and undulating with a few hills and low lying whalebacks and ridges. The lowest and highest points are 504 metres and 671 metres above sea level respectively. The area is however bounded by towering ranges reaching 910 metres and 844 metres above sea level in the northwestern and western part respectively.

The surrounding high lands are dissected by numerous steepsided river channels which radiate in all directions to join larger rivers. The area is well drained by numerous streams and rivers with a few areas in the southwestern part liable to flood during wet season. The streams and rivers are

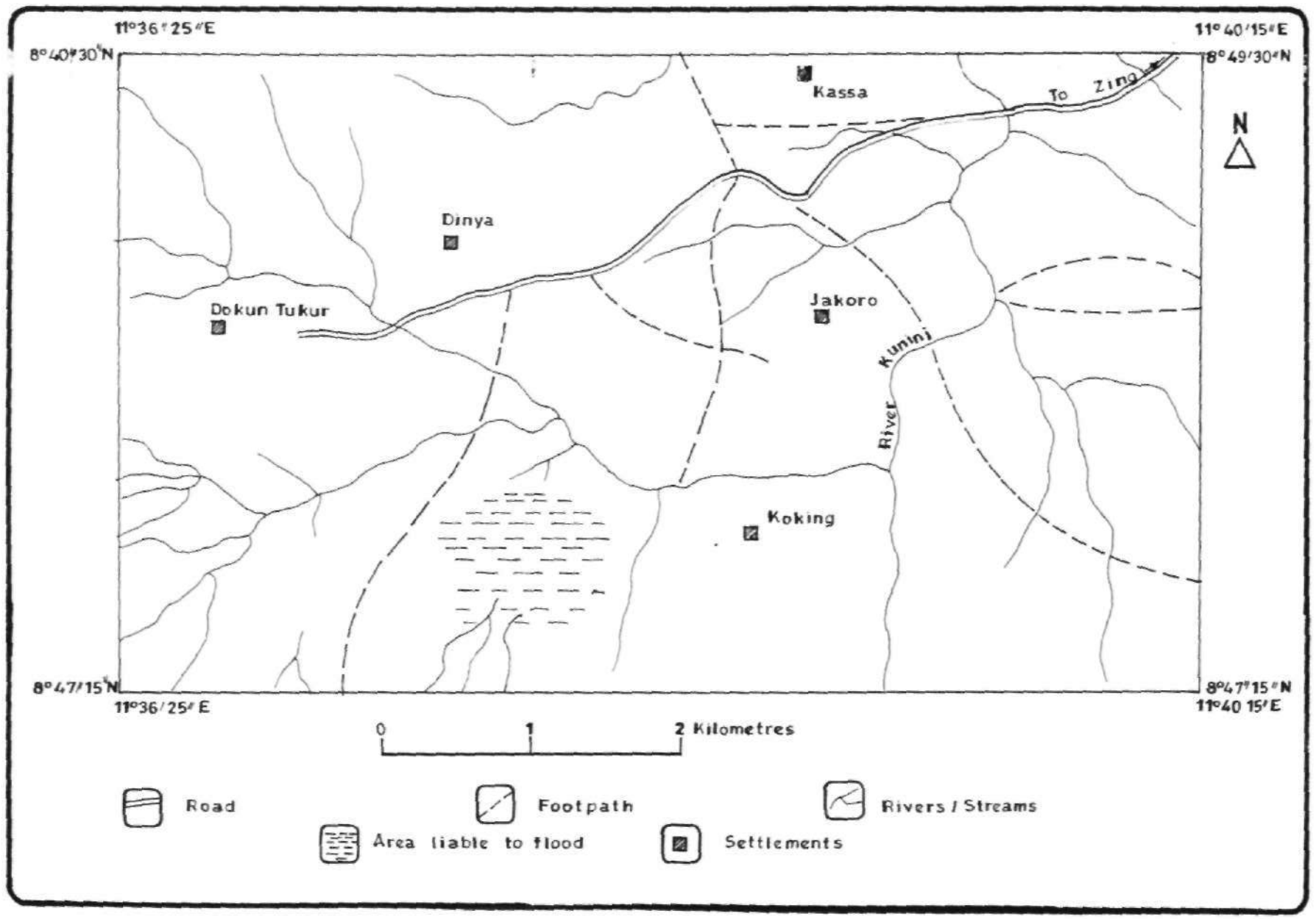


Fig. 1.2. Drainage, location and accessibility map of the study area.

all tributaries to river Kunini (Fig 1.2) which drains northward to join river Benue.

1.3 Climate and Vegetation

The climate of the area falls within the southern Savannah. The climatic zone which covers latitude $8^{O}N$ and $11^{O}N$ coincides with the Guinea Savannah Vegetation zone.

The wet season lasts for seven to eight months between March and November with 1270 mm to 1525mm Mean annual rainfall.

Temperatures in the zone are low and less variable, usually between $27^{O}C$ and $30^{O}C$ of the mean daily minimum and maximum. The relative humidity varies between 40% and 70% in the afternoon and evening respectively while the mean annual daylight radiation is between 80 - 90 kj^{-1} Cal cm^{-3} per year. The dry season in the zone lasts from November to March or April, during which there are no rainfalls. Temperatures are very high during the day while the relative humidity is generally low.

There are two marked seasonal winds direction in the area, the southeast trade wind blowing northeastwards during the wet season and the northeast trade winds (Harmattan winds), blowing southwestwards during the dry season.

The climate of the eastern borderlands comprising the area of study is influenced both by Latitudes and altitude. The change in altitude has resulted in constant humidity cloudiness, less sunshine, low temperatures and less evaporation. Line squall are quite common especially before and after the wet season.

The dorminant plant species of the northern Guinea Savannah, *Isoberlina doka* and *Isoberina dalzieli*, *Monotes kerstingii* and *Uapaca togoensis* (syn. U. Somon) occur where bush burning is not rampant. Useful trees such as the sheabutter or Karite (*Butryrospernum paradoxim. Sub. sp. parkii)* Tamarind (*Tamarindus Indica*) locust beans trees parkia sp. Vitex doniana, Afezelia Africana, Daniella Oliveri and the rubber Climber (*Landolphia huelotti*) are generally preserved.

The modification brought about by altitudes and hence climate has also influenced the vegetation of the eastern borderlands, which have plant species common to both temperate and tropical climates. Byrophytes (mosses), tree fern (cynthea spp.), epiphytes (orchid and bygonia) and lichen are abundant with other plant species of temperate affinities occuring together with the tropical plants.

1.4 PREVIOUS WORK

A review of the geology and concepts of genesis relating to important types of uranium deposits by Nash et.al.,(1981); gave rise to classification of uranium deposits into "Type deposits". These are deposits associated with certain geochemical provinces which demonstrate relationship to specified rock types. From the classification the following "Type deposits" were documented

(i) Quartz-pebble conglomeritic deposits

(ii) Unconformity Type deposits

(iii) Deposits in Ultramafic rocks

(iv) Vein type deposits

(v) Deposits associated with igneous rocks

(vi) Volcanogenic deposits

(vii) Deposits in Sandstones and

(viii) The yeelrie and calcrete type deposits

Previous work on Uranium Mineralization in Nigeria include that of Ojo, (1980) on the prospect of finding Uranium deposits in Nigeria. The work has indicated distribution of Uranium anomalies in the sedimentary and basement rocks. Oshin, (1984) worked on the distribution of uranium and thorium in the basement rocks. He indicated that some of the older granites have as high as 30ppm uranium. The work by

Oshin and Rahaman, (1986) on the favourability of uranium in Nigeria also indicated that the pegmatites around Adada in Adamawa and Bauchi State have as high as 72ppm Uranium concentration while work on Niger-Nigeria Younger Granites province by Bowden et.al., (1981) has shown that the albite granite from Ririwai and Afu within the region has uranium concentration of 100-145ppm.

Other works are those of Okujeni, (1987) on the biogeochemical investigation into use of leaf and bark of some Savannah trees in prospecting for uranium in the Upper Benue Trough; Okujeni, et.al., (1988) did a geochemical orientation survey for uranium in peta syncline and Gubrunde horst of the Upper Benue trough; Elegba et.al., (1988) carried out a feasibility of the geobotanical uranium exploration based on bark samples from Savannah trees; while Lancelot and Maurin (1985) Funtua, 1988; Funtua et.al., (1992a and b) and Ogunleye, (1991) worked on the geology and genesis of uranium mineralization in Northeastern Nigeria.

Other geological works covering the study area include those of Carter et. al., (1963); Oyawoye, (1970) and McCurry,(1970) on the geology of the Nigerian basement complex. Bawden and Tuley, (1966) worked on the land resources of southern Sardauna and Southern Adamawa provinces. Other workers include Ofoegbu, (1976) who worked on the

interpretation of aeromagnetic profiles across the Benue trough; Benkhilil, (1982) worked on the evolution and origin of the Benue trough while Wright, (1976); Burke 1970 and Ofoegbu, (1985) did a review of the geology and structural setting of the Benue trough.

1.5 PRESENT WORK

The aim of the present work includes: A comprehensive geological field mapping and production of a geological map of the study area; To study the detailed geology and structural setting of mineralized rocks, followed by a careful sampling of rocks in the ore zone and to undertake a study of the petrology and mineralogy of the rock samples in both handspecimen and thin sections together with a full petrographic description of the different rock types and their altered varieties.

Further work includes geochemical analysis of the rock samples for determination of major and minor elements; statistical treatment of data to show enrichment or depletion of elements in altered and unaltered rocks and interpretation of the data based on trends of elements in the rock related to uranium mineralization.

Chapter 2

GEOLOGY

2.0 Geological Setting

The Benue trough of Nigeria is a Cretaceous Intracratonic Sedimentary basin of about 800km long and 130-150 kms. wide. It is filled with rocks ranging from middle Albian to Maestrichtian (Ofoegbu 1985). The Cretaceous rocks within the trough are bordered on either side by the metamorphic basement rocks. The basement complex is Precambrian in age (Oyawoye 1972). It consists of quartzo-feldpathic migmatites and gneisses with occasional quartzites, marbles and amphibolites. According to Carter et. al.,(1963) the quartzo-feldspathic migmatites are scattered remnants of highly metamorphosed rocks which have entirely been transformed to anactectic migmatites and granites by granitization.

Pan African activity: - The crystalline basement bordering the Benue trough as in many parts of Nigeria, contains many major and minor intrusives (Carter et. al., 1963; Cratchley and Jones, (1965); Reyment (1965); Oyawoye, (1972). McCurry, 1976). The older intrusives are the older granites while the Younger intrusives include granitic, basic and

dibasic rock types associated with dykes-like bodies. (Falconer, 1911; Oyawoye, 1972; McCurry, 1976; Wright 1976).

The older granities which are product of the Pan-African Orogeny represent a cycle of granite evolution in which anatexis and stages of granitization and magmatic activity were displayed. (Carter et.al., 1963). The younger intrusives within the basement complex are mainly granitic pegmatites, although diorites, dolerites and some syenite occur. (Ofoegbu, 1985).

Cretaceous activity: The extensive igneous activity that took place in the lower Cretaceous was concentrated within the Benue trough. The igneous phase was apparently most intensive during the late Albian times and had ceased by the end of Turonian.

Within the Benue trough extensive Cretaceous volcanism occurred from Albian to late Cretaceous. Another volcanic activity covering the trough extended from Cretaceous to Recent times.

Cenozoic activity - The most recent magmatic activity that has affected some parts of the Nigerian basement is the Tertiary to Quarternary Volcanism. Within the Benue trough the younger of these volcanic intrusions are of Miocene-to Quatenary in age

and are mainly basaltic. The product of the Cenozoic Volcanism found within the trough and east of the trough are considered to be the western extension of the abundant and diverse Cenozoic Volcanism of the Cameroon chains. (Wright, 1976).

East of the Benue trough the basement consists of scattered occurrences of volcanic rocks which mainly are basalts, but probably include trachtytes, phonolites, rhyolites, tuffs and agglomerates (Bowden and Turley, 1966).

Age determination for the trachytes and rhyolites around the study area gave Rb-Sr whole rock ages between 51.2 M.A. to 45.5 M.A. (Okeke, 1980; Dunlop, 1983) respectively.

2.1 Geology of the Study Area

The geology of the area which lies immediately east of the Benue trough is represented by the Precambrian basement. The crystalline basement rocks consist of migmatites, fine grained granites, porphyritic biotite granites, equigranular granites, microgranites and pegmatites.

Volcanic activity in the area is linked to the Cenozoic volcanism; the volcanic activity has produced lenticular dyke-like bodies of rhyolites.

Other important geological features in the area are structures such as shear zones, joints and the dyke like rhyolite bodies. fig (2.1).

2.1.1 Basement rocks (Precambrian)

Migmatites

Migmatites are not extensively exposed in the study area. They occur as relicts ratts and xenoliths within the granites. The xenoliths form sharp boundaries with the porphyritic biotite granite and the fine grained granite.

The contact relationship between the migmatites and the granites suggest that the migmatites are older and were the initial basement rock into which the granites were emplaced. A later event was the emplacement of microgranites dykes which cut across the migmatites and granites (Plate 2.1).

The migmatites are evenly fine grained with discontinous or nebulous foliations defined by alternating ptygmatic folding of leucocratic granite components and basic gneissic components which tend to give the rock a banding structure.

The mineralogical composition of the rock shows that the basic gneissic bands consist of biotite, muscovite, ilmenite

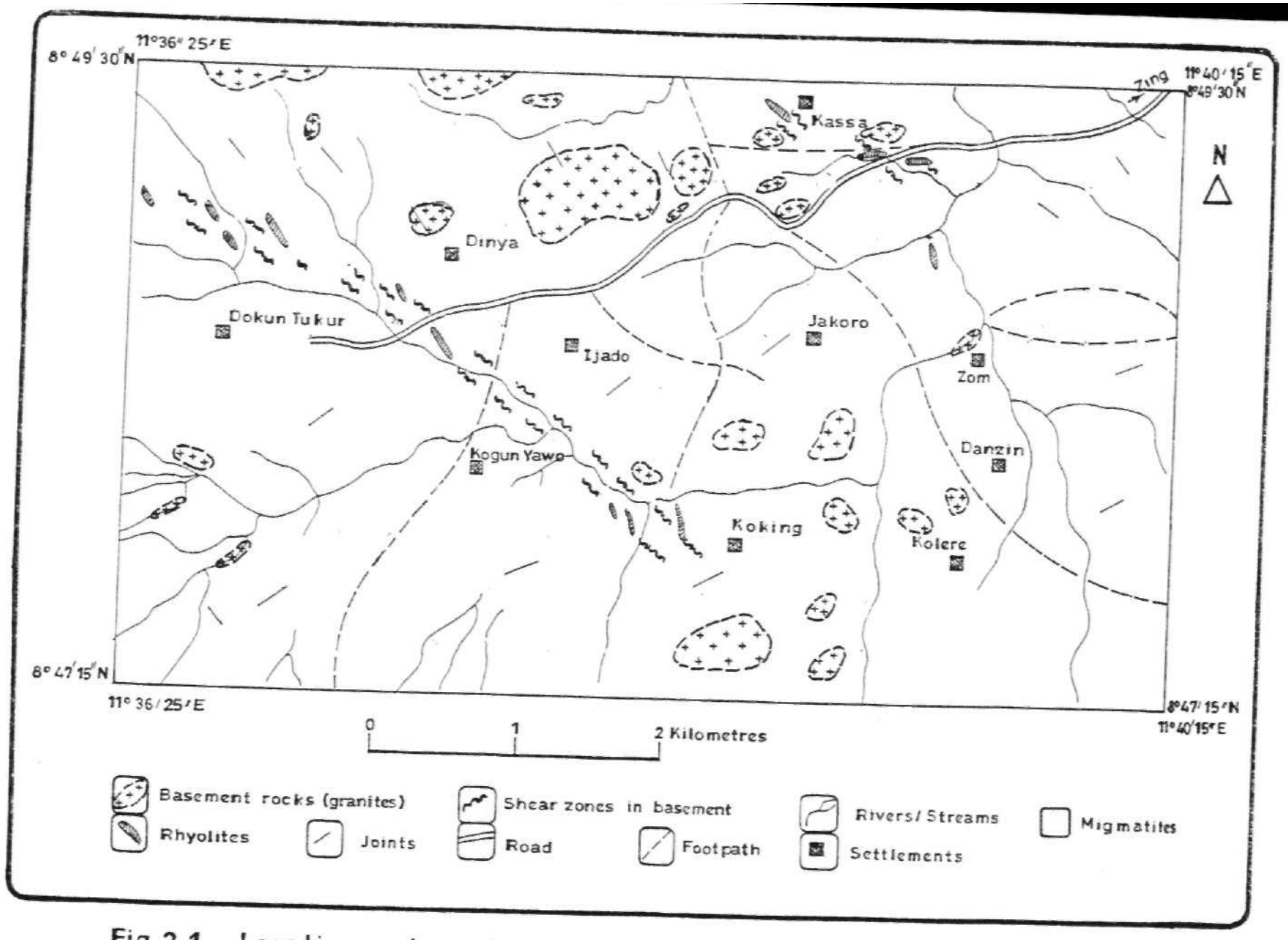


Fig. 2.1. Location and geological setting of the study area.

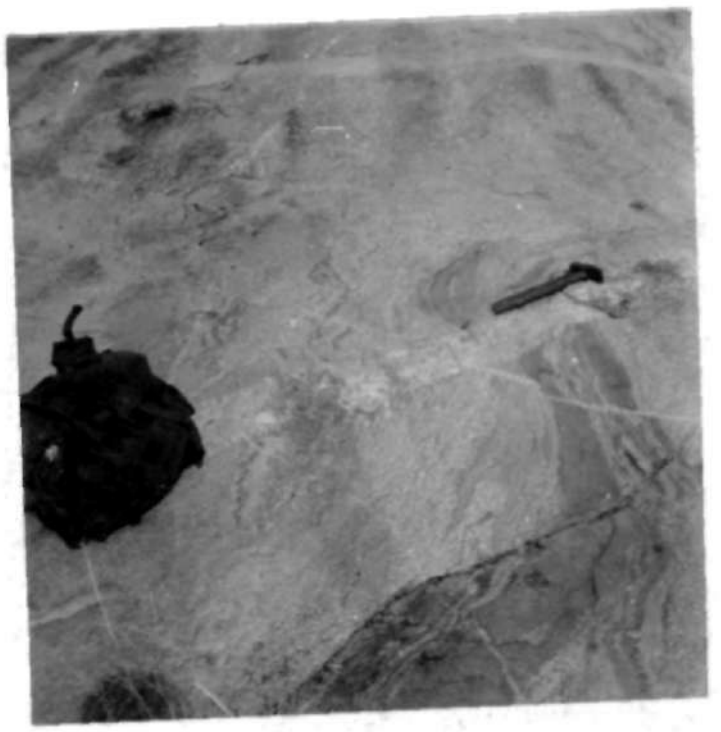


Plate 2.1 - Microgranite vein cuts across porphyritic biotite granite and migmatite xenolith

and magnetite while the leucocratic granitic components are essentially quartz, feldspars and a few grains of magnetite. Biotite, muscovite and the iron-minerals are evenly distributed in the gneissic component; while the leucocratic granite component has sub-hedral aggregates of quartz and feldspars mainly microcline evenly distributed. A careful study indicate that a greater number of the biotite grains are altered to chlorite while muscovite is altered to magnetite. An approximate visual modal analysis of the rock is shown in (Table 2.1).

Minerals	1	2	3	4	5	6	7	8
Quartz	35-40	35-40	35-40	35-40	20-25	30.32	35-37	50-60
Orthoclase	40-45	40-45	28-30	45-48	20-25	31-33	38-42	rare
Microcline	5-8	2-3	2-3	rare	3-5	rare	rare	rare
Plagioclase	2-3	8-13	22-25	rare	17-20	3-4	rare	rare
Biotite	8-10	2-4	7-9	12-14	21-24	27-30	rare	rare
Muscovite	trace	rare	rare	rare	rare	rare	rare	rare
Hematite	rare	trace	rare	trace	trace	trace	24-27	40-50
Magnetite	trace	trace	rare	trace	trace	trace	trace	trace

Table 2.1 Approximate modal analysis of the basement rocks and rhyolites

(1) Fine grained granite (2) Equigranular granite (3 & 4) microgranit

(5 and 6) porphyritic biotite granite (7 and 8) Rhyolites.

Fine grained granite

The fine grained granites occur as irregular bodies and large pendants scattered within the porphyritic biotite granite. They are represented in a few outcrops near Zom in the southeastern part of the area and in the southwestern parts. They rarely extend beyond individual outcrops.

The fine grained granite are equigranular and fine grained. The quartz crystals with little signs of strain are sawn together with the feldspars. The feldspars are mainly orthoclase with a few grains of albite and microcline. The albite has fine lamellae of twinning, while microcline exhibit poor outlines of tartan twinning.

Between the interstices of quartz and feldspar occur biotite aggregates which are partially or completely altered to chlorite. The chlorite and biotite aggregates form interlocking network that define a poor foliation. Other minerals in the rock include muscovite and ilmenite as accessory minerals. A modal analysis of the rock is given in (Table 2.1).

Porphyritic biotite granite

The porphyritic biotite granite is the most exposed and widely distributed rock in the study area. It is represented in

90% of the exposed outcrops mapped. They occur as hemogeneous masses having sharp boundaries with the xenoliths of migmatites and rhyolites but disconcordant boundaries with the fine grained granites. The porphyritic biotite granites were emplaced during the late stages of the Older Granites cycle Carter et. al., (1963) but before the emplacement of the microgranites and pegmatites.

The rock consists of large phenocrysts of feldspars evenly distributed in the rock. The phenocryst are responsible for the porphyritic texture of the rock. In some outcrops the feldspar phenocryst grade from large to medium sizes. Weak foliation in the rock is due to distribution of streaky mica minerals around the quartz and feldspar minerals.

Thin Section shows that the feldspars are mainly orthoclase, microcline and albite. The orthoclase and microcline form the phenocrysts. The orthoclase feldspars occur as anhedral to sub-hedral aggregates having string microperthites and inclusion of biotite and iron-rich minerals. The few albite aggregates were observed to display intermediate twinning. The microclines feldspars generally show weak outlines of twinning.

Medium grained quartz of subhedral shapes are widely distributed in between the feldspars. The quartz grains are

fractured and cracked giving rise to undulose extinction.

The mafic minerals in the rock consist of Prismatic biotite aggregates, a few grains of muscovite and ilmenite. The biotite grains show pleochroism, well developed cleavage planes and has patchy edges. The pleochroism display greenish, brownish and reddish brown colours. A few of the grains have inclusion of allanite, sphene and chlorite, giving rise to pleochroic haloes. The biotite and muscovite aggregates form clusters and alignment in between the feldspars and quartz aggregates (plate 2.2). The alignments of the minerals results to weak foliation in the rock and suggest post-depositional deformation.

Ilmenite, allanite, sphene and zircon which are sparsely distributed in the rock form the accessory minerals. A modal analysis of the rock is given in (Table 2.1).

Equigranular granites

The equigranular granites occur as small outcrops exposed along river Kunini near Jakoro in the Central part of the area. The contact relationship between the equigranular granites and other rocks could not be established due to their restricted exposure. According to Carter et. al., (1963), the equigranular granites represent a phase of granitization

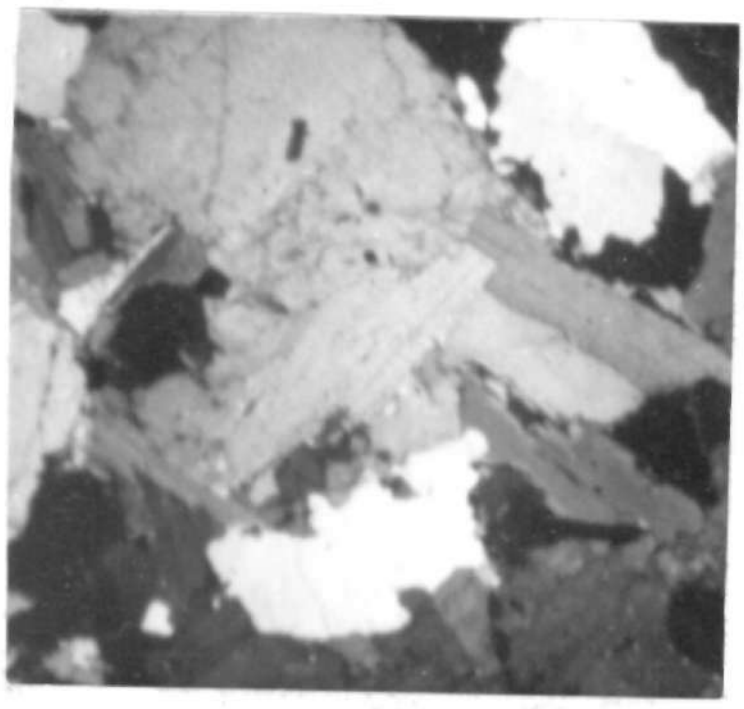


Plate 2.2 - Porphyritic biotite granite showing interlocking crystals with prismatic aggregates of biotite and strained quartz crystals (photomicrograph)

intermediate between the migmatites and formation of the porphyritic biotite granite. The equigranular granites are medium size grained and occur as massive bodies due to silicification.

The rock is composed of quartz, orthoclase, albite, microcline, biotite, muscovite with magnetite and ilmenite as accessory minerals Table (2.1). Two generations of quartz are identified in the rock. The small rounded crystals, show undulose extinction due to strain while the large quartz crystals that have resulted from recrystallization and silicification, (Secondary quartz) show no evidences of strain.

The most extensively distributed feldspars are the orthoclase feldspars. They show micro-perthitic texture with some grains exsolved to well formed lamellae. Exsolution in orthoclase to albite and microcline is well displayed in some of the grains. The orthoclase feldspars have inclusions of chlorite and quartz (plate 2.3).

A few grains of chlorite occur between the interlocking crystals of quartz and feldspars. Other minerals include muscovite and allanite which form the accessory minerals.

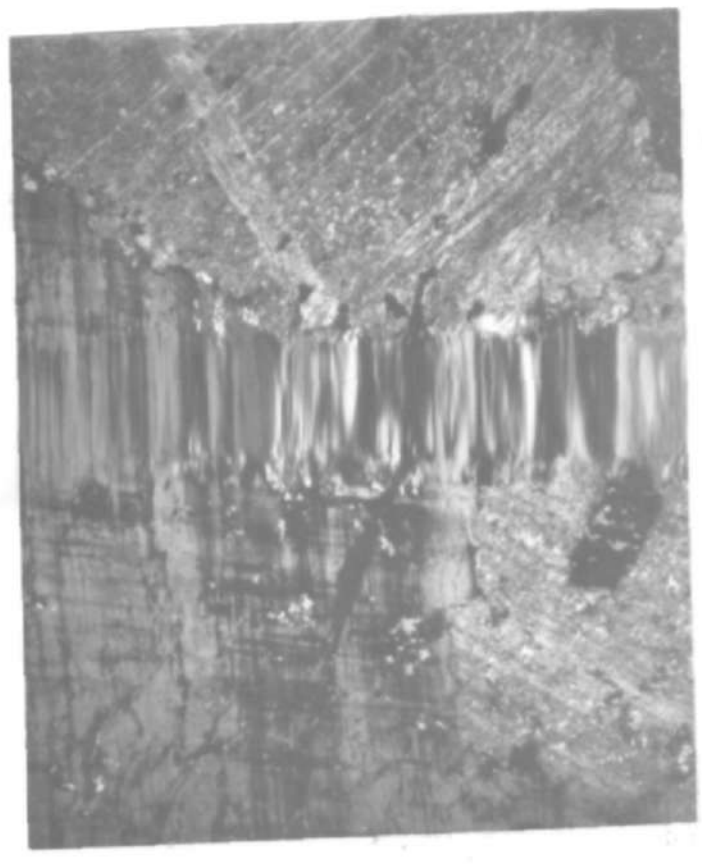


Plate 2.3 - Equigranular granites, showing feldspars with twinning, alteration at the edges and inclusion of mafic minerals including accessory minerals (photomicrograph)

Microgranites

The microgranites are a distinctive group of granites that occur as dyke-like bodies. The microgranites cut across all the other basement rocks. This indicate the late emplacement of microgranites during the final stages of granitization.

The microgranite are a fine grained rock with equigranular aggregates of quartz feldspar and sparsely distributed matic minerals. Microscopically the rock is composed of quartz, albite, orthoclase, microcline and biotite with a few aggregates of ilmenite and allanite as accessory minerals. (Table 2.1).

The quartz crystals have rounded to sub-hedral shapes, widely and evenly distributed in the rock. The quartz crystals show little or no strain. The feldspars mainly orthoclase are a little larger in size than the quartz crystals, they are also widely and evenly distributed in the rock. Albite and microcline are also present in the rock. The quartz and feldspars are closely interlocked while the matic minerals are twisted around the interstices.

A few prismatic crystals of biotite are sparsely distributed in the rock while a few chlorite aggregates occur around the interstices of the felsic minerals. Accessory

minerals in the rock include ilmenite and allanite.

2.1.2 Volcanic rocks (Cenozoic)

Rhyolites

Volcanic rocks in the study area are identified as rhyolites. They occur as lenses and dyke bodies along an approximate N-S linear trend. The individual lenses or dykes have average strike length of 50 metres. They are separated over short distances and show changes in strike directions.

The rhyolites are massive, fine grained and brownish in colour with spotty smoky stains due to hematization. The rocks are brecciated and sheared (plate 2.4). Hematization and silicification of the rock are clearly observed in handspecimen especially around the sheared and mineralized zones.

Microscopically the rhyolites are cryptocrystalline, with occassional microphenocryst of quartz, feldspar, ilmenite and magnetite set in a cryptocrystalline groundmass. It is evident that the microphenocrysts of quartz, feldspars and the mafic minerals grade in size to fine aggregates that form the cryptocrystalline groundmass. Quartz is the dominant mineral in the groundmass. Other minerals that occur in the rock are



Plate 2.4 - Breciated and sheared rhyolites, silicification and hematization is very conspicous

ilmenite, zircon, apatite which form the accessory minerals (Table 2.1).

Some of the rhyolites show a network of veinlets which are either filled with silica or hematite. The deposition of silica and hematite is responsible for the silicification and hematization observed in handspecimen.

2.2 Structures

The Structural features of the study area consist of foliation, fault, trends of minor bodies and joints. Table 2.2 show the reading of structural trends obtained from the area.

Strike in Degrees	No. of Joints	No. of Rhyolite Dykes	Quartz and felsic veins
0-20	27	6	5
20-40	7	-	2
40-60	9	-	-
60-80	2	-	1
80-100	3	-	-
100-120	3	6	1
120-140	22	8	2
140-160	22	4	7
160-180	7	1	1

Table 2.2 Statistics of joints, rhyolite dykes and minor bodies trend.

2.2.1 Foliations

Foliation trends in basement rocks occur in the fine grained granite, the porphyritic biotite granite and microgranite. Foliations in the migmatites are disoriented while the rhyolites show no foliation trend.

Foliations in the basement rocks are generally weak, the trends are defined by minerals alignment especially the mica mineral while the felsic minerals show no particular orientation. The foliation trend in the basement rocks fall between 60^{O}NE and 85^{O}NE. Foliation trends in the microgranite are concordant with their strike directions and also fall within the general bearing of the foliation trend.

2.2.2 Faulting

Faulting in the basement rocks was not observed. The basement however has been intruded by rhyolitic dykes, along a north, Northeast lineament, they occur as disjointed bodies which display changes in strike directions. The changes in strike and displacement are probably fault displacements (Okujeni pers. Communication).

2.2.3 Minor bodies

A number of minor bodies such as quartz veins and felsic veins run across the basement rocks in two prominent directions. Quartz veins in the area show a predominant North and Northwest Orientation, while the felsic veins run predominantly in the northwest directions. The quartz veins occur mostly as fracture filling bodies while felsic veins occur as intrusive bodies.

2.2.4 Joints

Joints are the most widely distributed structural feature in the area. They occur mostly in the basement rocks. A statistical display of the joints trend from the area has shown that the northeast-southwest and northwest-southeast are the two prominent joints trends (Fig 2.2).

Field observation show that several joints run parallel over several metres. Some of the joints are occasionally filled with quartz at intervals. 102 joints readings were recorded during the study (Table 2.2).

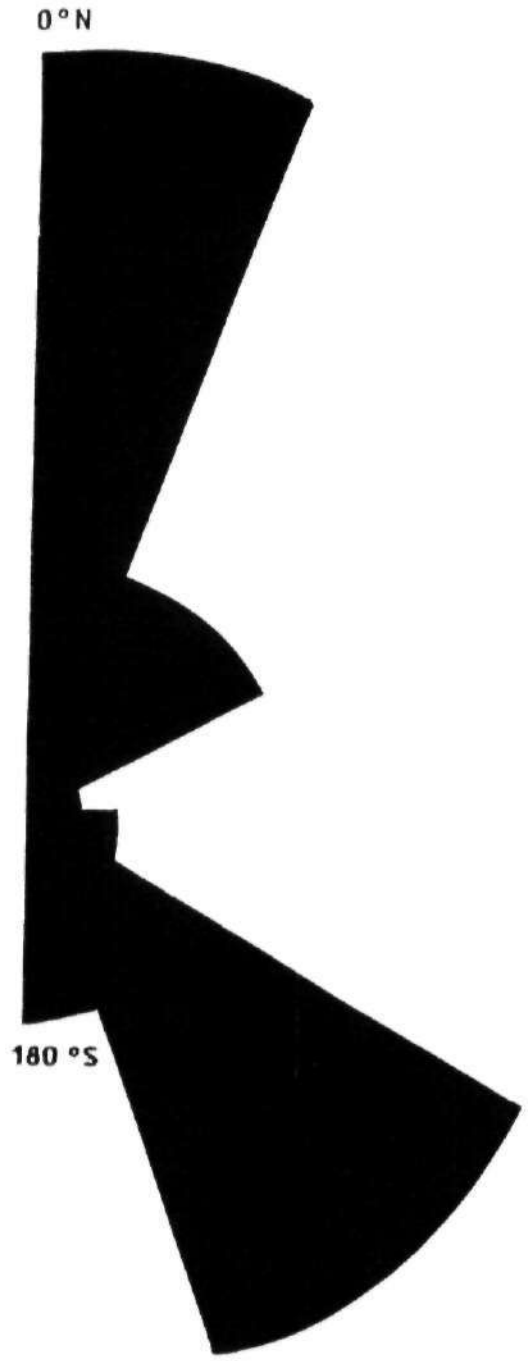


Fig.2.2. Rose diagram of joints trend in the basement rocks.

Chapter 3

MINERALIZATION AND ALTERATIONS

3.0 Mineralization

A radiometric survey was conducted in the study area using an Spp^2 N.P. scintillometer. The survey indicated certain area with very high radiometric readings. The values ranged between 500 C.P.S to 15000 C.P.S with an average of 1611 C.P.S. and a Standard deviation of 2398.

Areas that indicated very high radiometric counts were found to be associated with two rhyolite dykes. The dykes were carefully sampled with radiometric counts recorded at those points. (Fig. 3.1).

Figure (3.2) show the distribution of radiometric values plotted into histograms. Figure (3.3) shows the areal distribution pattern of radiometric counts. Figure (3.4) is a plot of the cumulative curve, using the raw data.

From the distribution of values in the histogram, values from eleven points sampled occur above the average value while about thirty-six values occur below the average value. The areal distribution pattern on the other hand show that the

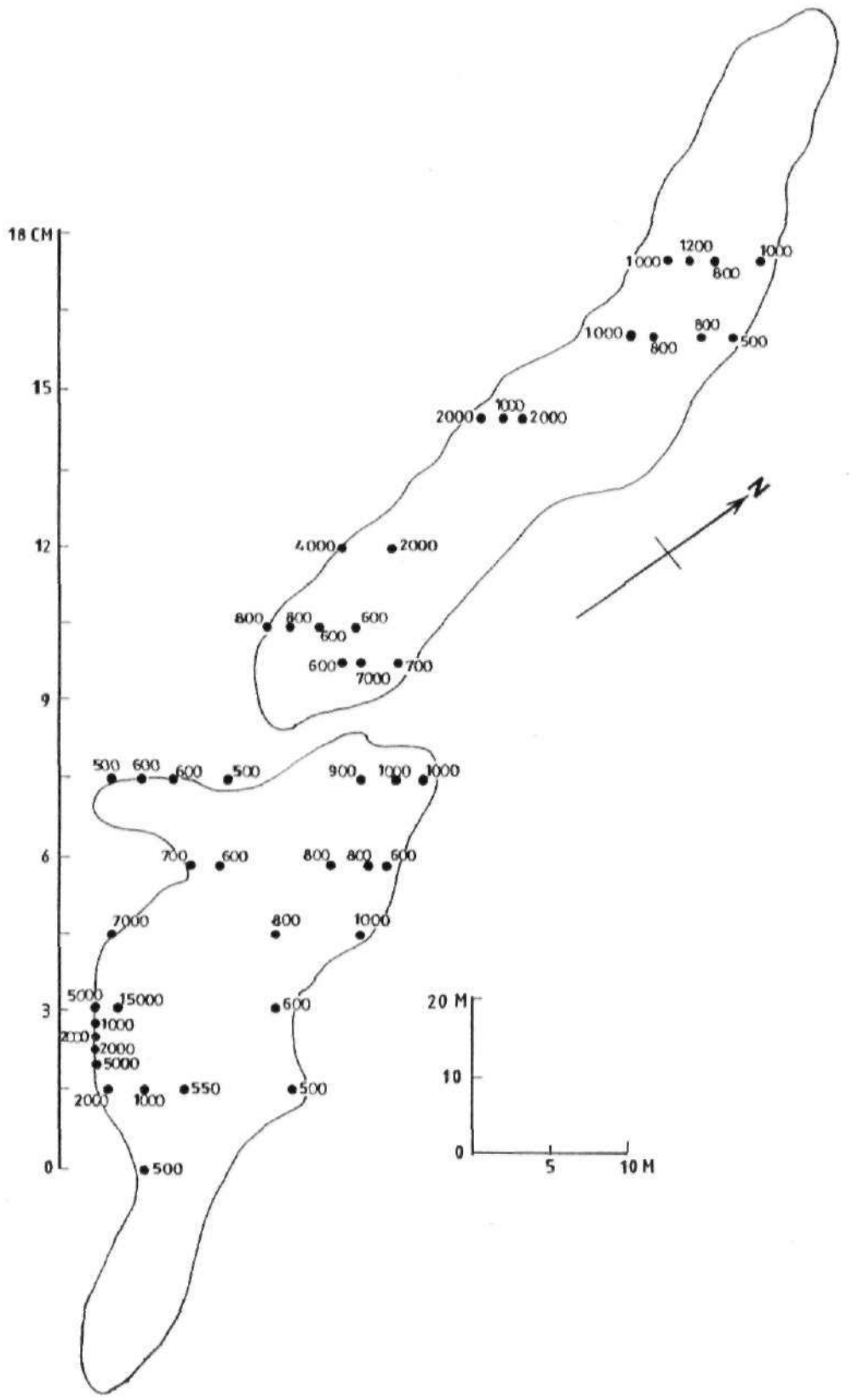


Fig. 3.1. Radiometric reading at sampled points using SPP² NP scintilometer .

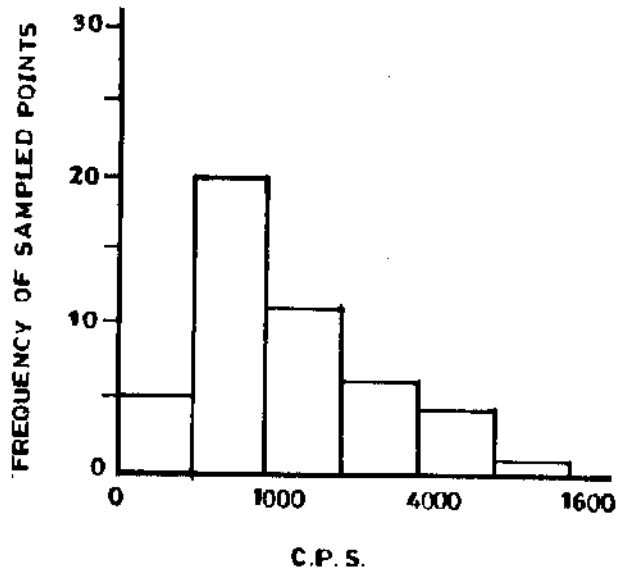


Fig.3.2. Histogram of radiometric values from the mineralized zone.

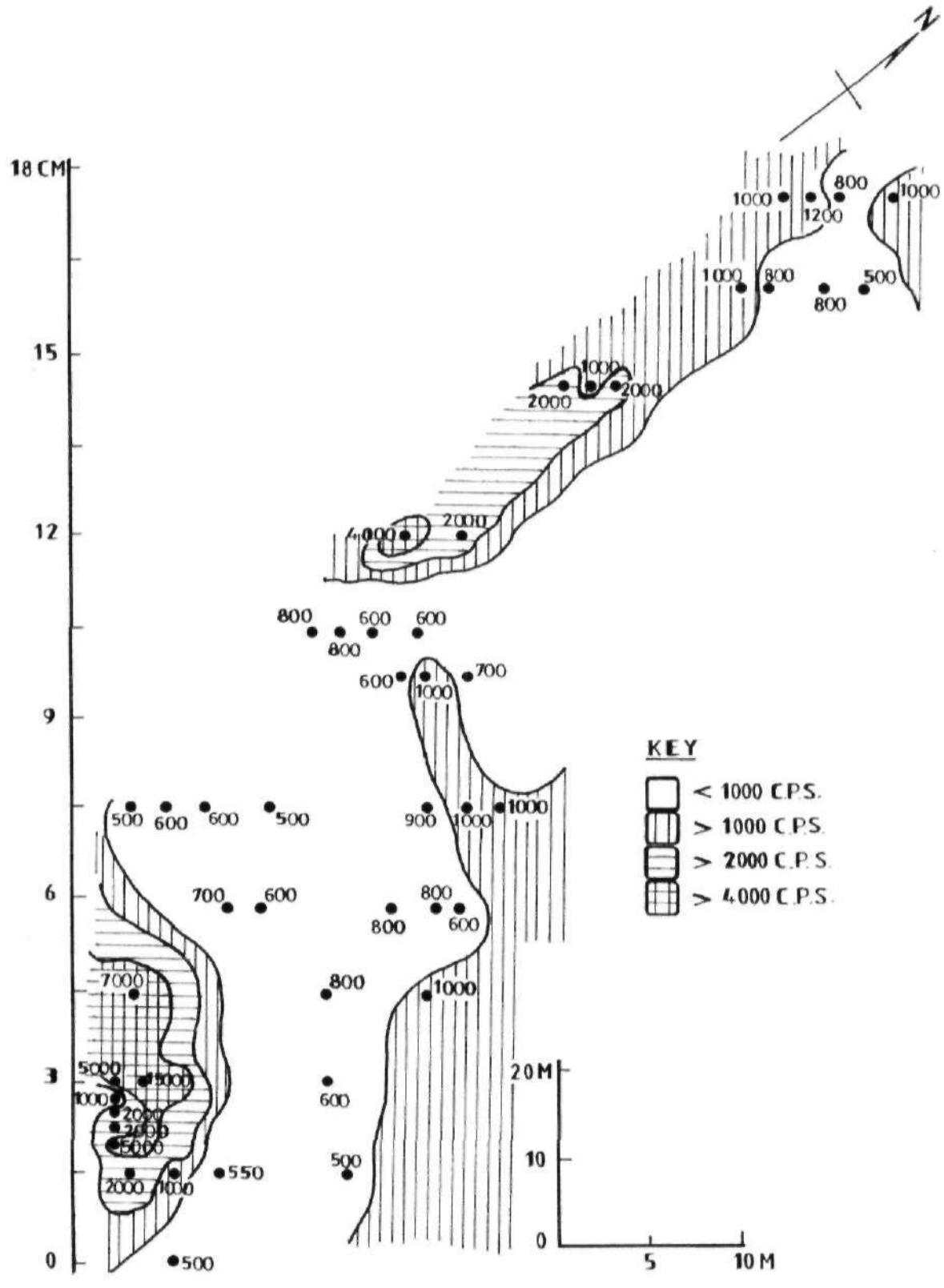


Fig. 3.3. Areal distribution of radiometric values in the mineralized zone .

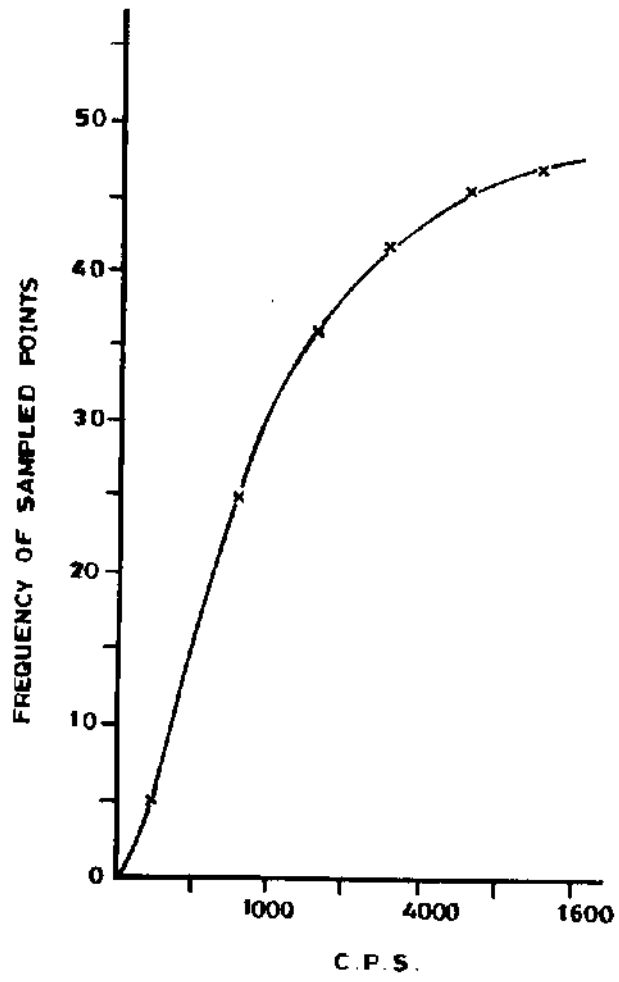


Fig. 3.4. Cumulative frequency curves of radiometric values.

high radiometric occur close to the contact zones of the rhyolites and granites.

The plot of cumulative frequency of the radiometric values, present values that give a straight line up to values of 2000 C.P.S., above this value, the curve changed abruptly.

The radiometric counts above the average values obtained from the area together with the nature of the frequency curve obtained indicate that some of the values were anomolous. The anomolous values are possible indications that the rocks are mineralized.

3.1 SECONDARY PROCESSES

Other evidences of mineralization in the study area were observed from the effect of secondary processes on the rocks.

The pervasive alterations of the host rocks is seen as effect from hydrothermal solutions that must have brought about mineralization. The nature and extent of alteration of the host rocks is discussed below. This is followed by the alteration processes that took place during alteration of the rocks.

Altered rocks

Due to the action of the hydrothermal solutions, along the contact of the rhyolites and granites, the two rock responded by changes in petrology and mineralogy. The alteration decrease with distance from the contact areas. The changes in the alteration density with reference to distance from the contacts of the two rocks has given rise to the classification of the rocks into four alteration zones (Fig 3.5). The zones are:

(i) mildly altered porphyritic biotite granite

(ii) intensely altered and sheared porphyritic biotite granite

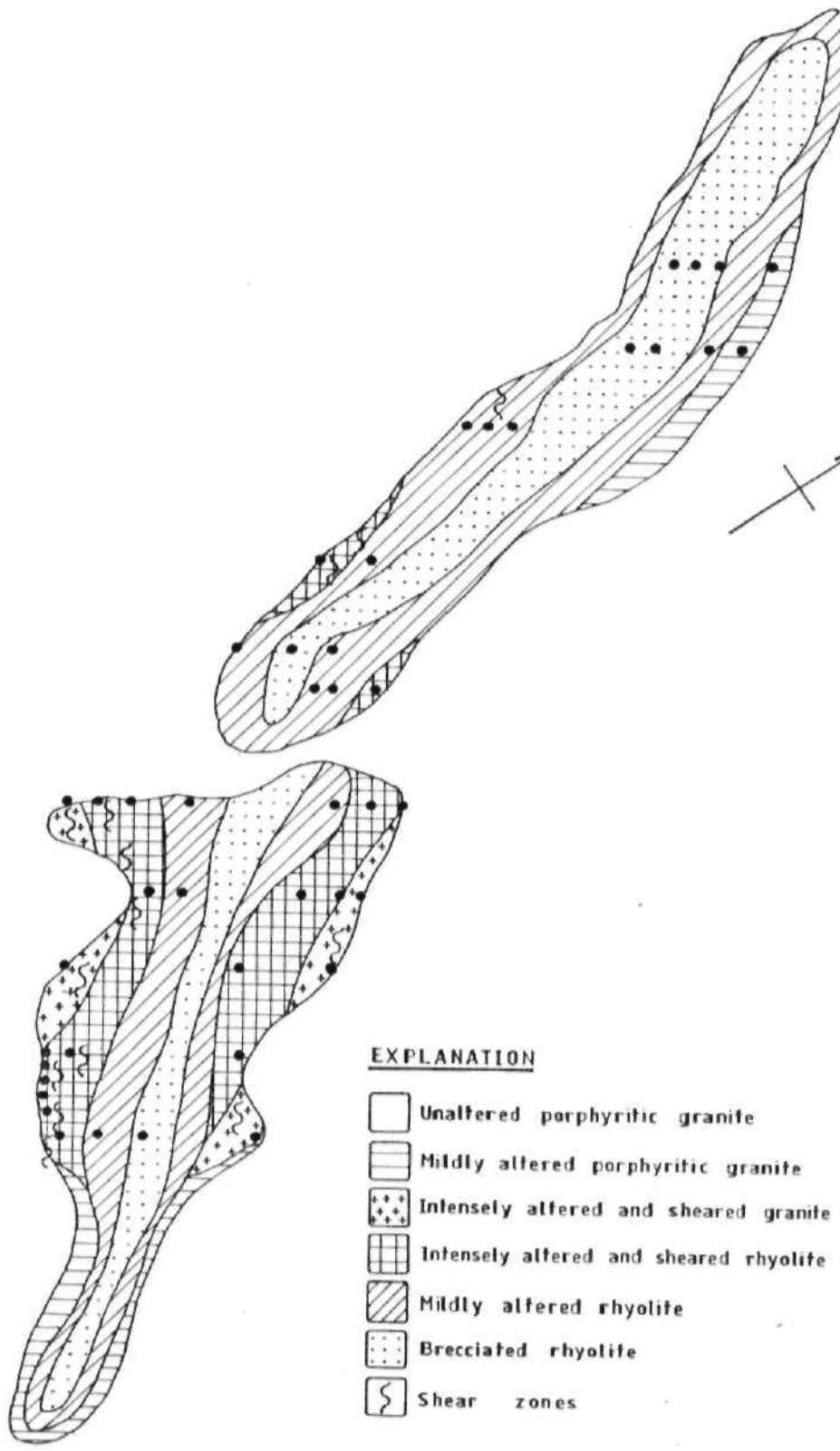


Fig.35. Zones of alteration intensity in rhyolites and porphyritic granite.

(iii) midly altered rhyolites

(iv) intensely altered and sheared rhyolites

Mildly altered porphyritic biotite granite

From the fresh unaltered porphyritic biotite granite towards the contact of the granite and rhyolites, the granite show a gradual increase in alteration intensity. This area is classified as the mildly altered zone.

Alteration in this zone include recrystallization of quartz to smaller aggregates and filling of veinlets, quartz grains that were yet recrystallized show evidences of strain and fracturing. The orthoclase feldspars are less exsolved with little microperthitic texture, while microcline and albite show shadow outlines. The feldspars generally have cloudly outlines and exhibit alteration to sericite around the edges. (Plate 3.1). Biotite is partially or completely altered to chlorite, other iron-rich minerals are also altered to hematite and introduced into veinlets.

Intensely altered and Sheared Porphyritic biotite granite

The porphyritic biotite granite along the contact with rhyolites fall under the intensely altered and sheared zone.

In this zone all the quartz aggregates are recrystallized to smaller aggregates that form the medium

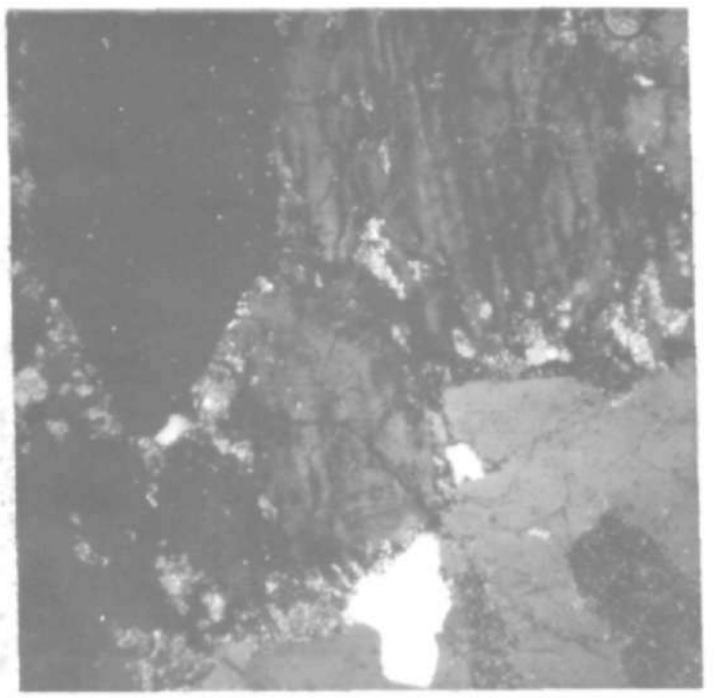


Plate 3.1 - Mildly altered granites. The biotite crystals are completely destroyed with the feldspars showing perthitic texture and alteration to sericite (photomicrograph)

grained groundmass. The feldspars are completely altered to sericite while biotite and chlorite are no longer preserved.

Magnetite and hematite derived from the alterations are widely distributed in this zone. A network of veinlets filled with hematite and silica is common. Other veinlets are those of fine groundmass which cut across the medium grained groundmass and the quartz and hematite veinlets (plate 3.2).

Mildly altered rhyolites

Further away into rhyolites, the alteration intensity is less than the rhyolites at the contact. Alteration in this zone is mild and is characterized by a continuous crysptocrystalline groundmass of quartz, feldspar and a few iron-rich minerals.

Common evidences of alteration are recrystallization of quartz and in filling of veinlets. A network of hematite veinlets are common. Some of the veinlets are characterized by formation of a silica core and an outer layer of hematite or vice-versa (plate 3.3).

Alteration in this zone also involve introduction of veinlets infilled with a finer grained groundmass. The veinlets cut across the earlier formed quartz and hematite veinlets. The introduction of fine grained groundmass

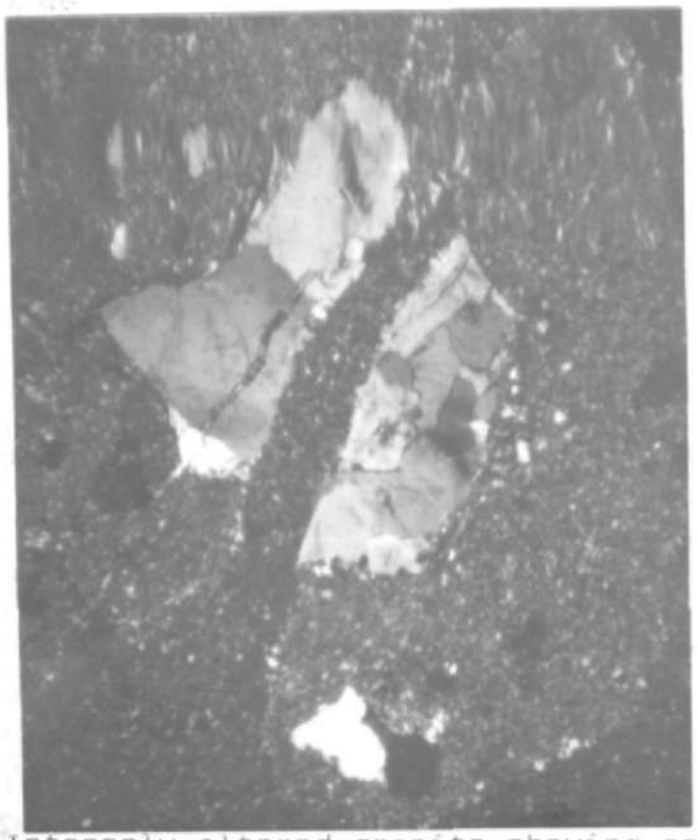


Plate 3.2 - Intensely altered granite showing complete alteration of mineral aggregates, except a few quartz grains and introduction of veinlets in the rock (photomicrograph)

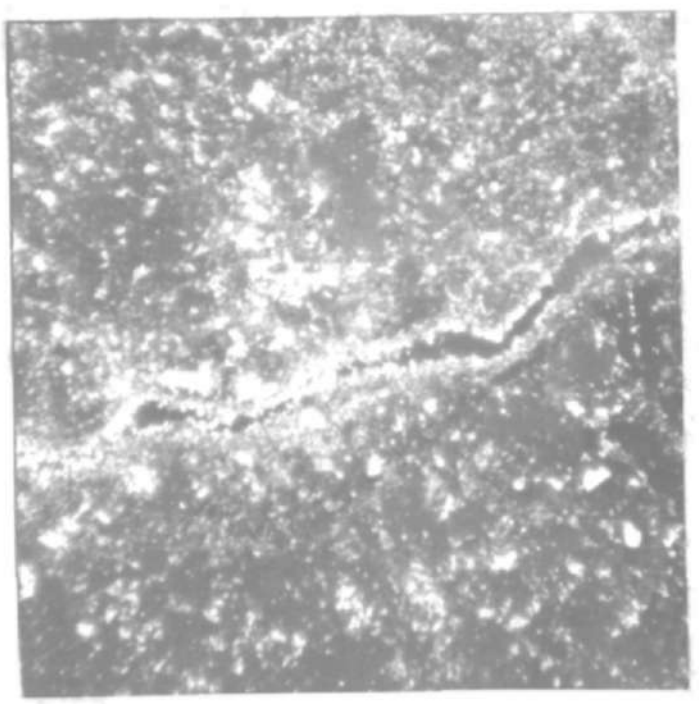


Plate 3.3 - Mildly altered rhyolites. Cryptocrystalline texture, with introduction of hematite and quartz veinlets

veinlets tend to give the rock a flow texture.

Intensely altered and Sheared rhyolites

The rhyolites in contact with the granites are the mos intensely altered and sheared. The rock consists of a crysptocrystalline groundmass made up of quartz, ilmenite, magnetite and sericite.

Alteration in this zone is characterized by recrystallization and devitrification of quartz to glass rods and shards. The devitrified glass and shards form clusters which have given the rock a spherulitic texture (plate 3.4). The devitrified glass also occurs as fracture filling grains in veinlets.

An extensive network of skeletal hematite covers a large part of the rock and occurs as core or outer layers bodering devitrified quartz veinlets. Some specimens in the zone have a large network of hematite, while the remaining part is composed of amorphous mass which is believed to be Opal.

Alteration processes

The wall-rock alteration was primarily due to some certain processes during upward migration of hydrothermal solutions. The effect of some of these processes such as silicification and hematization were mappable in the field (Fig. 3.6).

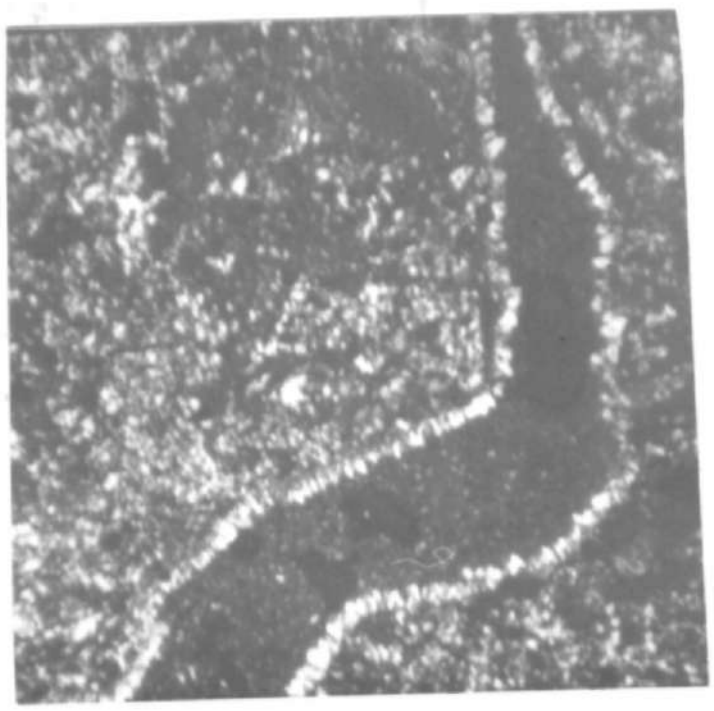


Plate 3.4 - Intensely altered granite. Cryptocrystalline. Clusters of devitrified glass giving rise to spherulitic texture in the rock. The glass rods and shards also line the outer boundary of veinlets composed of a finer grained groundmass

CHLORITIZATION

Chloritization of the wall rocks resulted from introduction of H_2O and CO_2 while Fe_3O_4, MnO and mgO were gained and Na_2O and CaO lost. The reaction was due to hydrogen metasomatism.

In thin section the chlorite occurs as patchy grains filling interstices, fractures or veinlets. Chloritization in the porphyritic biotite granite resulted from the supply of mineralizing fluid rich in Fe^{2+}, Mg^{2+} and H^+ to the wall rock.

SERICITIZATION

Sericitization of plagioclase around the margin occurred in a few crystals and increased with intensity of alteration. Sericitization of the plagioclase resulted from the introduction of H_2O and CO_2 and the redistribution of K_2O. The reaction was due to potash metasomatism with sericite and K-feldspars as the mineral products.

The alteration of biotite and other ferromagnesium minerals became complete in intensely altered and sheared rocks. This means that the exchange reaction between potassium and sodium increased with alteration. This

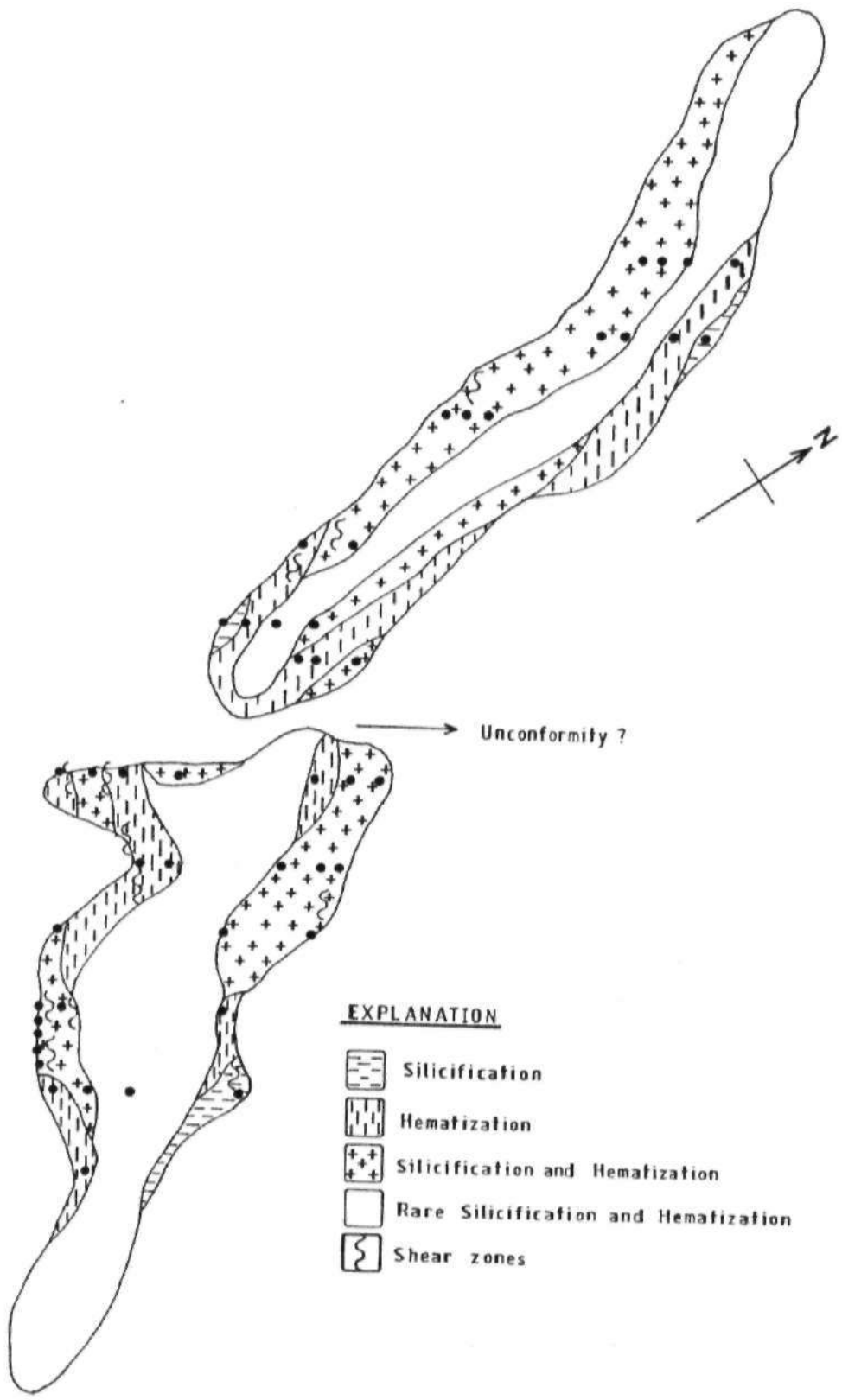


Fig.3.6; Rhyolite outcrop showing mappable alterations.

justifies the fact that the K_2O/Na_2O ratio increases with alteration towards the foci of mineralization.

CARBONIZATION

With introduction of CO_2 in the wall rock SiO_2 was liberated and driven off to be recrystallized in fractures and veinlets. Generally the silicate structures were attacked by CO_2, forming carbonates and releasing SiO_2 which eventually migrated into the vein and lode sites where it was reprecipitated as quartz. (Boyle (1961; 1979).

SILIFICATIONS

The process of silicification is recognized by an increase in silica, manifested mainly by presence of fine grained quartz, chert or opal in the wall rock and by precipitation of quartz in stringers, veinlets, fractures and along the border zone of other veinlets as was commonly observed.

During silification, quartz is replaced and liberated to be reprecipitated in adjacent structures and may be reintroduced in the wall rock where it replaces carbonate minerals.

HEMATIZATION

Hematization is characteristics of many uranium mineralization. Increase in hematite with proximity to

mineralization is a common phenomena. A shift in Fe^{2+}/Fe^{3+} ratio is as a result of hematization.

Hematization was observed both macroscopically and microscopically. It is pervasive especially along the sheared and mineralized zones. In thin section, hematite form patchy and skeletal intergrowth, that covers a larger percentage of some samples. It occurs in association with magnetite and ilmenite and tend to be deposited in stringers, fractures and veinlets.

DEVITRIFICATION

Devitrification may have resulted from either spontaneous or gradual recrystallization in the intensely altered zones. The devitrified glass shards and rods occupy veinlets or form clusters. The clusters have given rise to spherulitic texture in the intensely altered rocks.

Devitrification in the rhyolites resulted from either initial recrystallization or due to later processes of shearing and/or introduction of mineralizing fluids. In some of the intensely altered and sheared rhyolites, there are precipitation of amorphous material, formed by recrystallization of silica to opal.

Chapter 4

4.0 METHODOLOGY

A general geological mapping of the study area covering 28 square kilometres was conducted on a scale of 1:25,000. A detailed geological map of the area Fig.(4.1) has been drawn and attached as appendix III.

Within the area two dykes were mapped in detail (Fig. 4.2) and sampled along East-west cross profiles. Representative samples across the rhyolite outcrops and bordering basement rocks were taken along these profiles at close intervals.

Thin sections of the samples collected from the study area were made for petrographic studies.

4.1 Geochemical Analysis

The rock samples collected from the study area were prepared for geochemical analysis; first, the samples were broken to bits and pulverized into powder using a tungsten Carbide Spex Mill. The powdered samples were then stored in labelled sample bottles.



Fig. 4.2. Geological and structural setting of the mineralized zone.

The digestion of the powdered samples into liquid form were done so as to utilize such techniques as Atomic Absorption Spectrophotometry (AAS), Spectrophotometry and Flame photometry, for determination of major and trace elements.

The $HF/HClO_3$ method of digestion was used, most silicate minerals normally dissolve in acids and mixtures containing $HClO_3$.

0.5 grammes of rock samples powder was placed into clean 25 ml teflon crucibles 2ml of perchloric acid ($Hclo_3$) "Analar" grade 60% v/v was added to the crucibles from a springe pipette to wet the samples. 10 ml. of hydroflouric acid (HF) "analar"grade 40% was finally added to the crucibles. A blank solution was prepared by addition of same quantities of perchloric acid and hydroflouric acid to an empty crucible. The crucibles containing the samples and the blank were all covered and kept overnight.

The next day all the crucibles were heated on a boiling waterbath for four hours, after which the lids were removed to allow all the hydroflouric acid and silicon to fume off. When no more white fumes were visible and only the few millimetres of perchloric acid

remained, the crucibles were transfered to a sandbath set at 140^{O} centigrade, for the remaining perchaloric acid to fume off.

When the crystal mush was yet moist and no more fumes were produced, 1ml perchloric acid was pipetted into all the crucibles and the evaporation repeated. When the content were again just moist and no more white fumes were visible the crucibles were half filled with distilled water and the crystal mush allowed to dissolve while on the sandbath.

After the crystals had dissolved, the clear solution were removed and left to cool. After cooling they were filtered into 100ml volumetric flask and diluted to volume with distilled water then shaken on a 100^{SM} machine for five hours.

4.2 Analytical Methods

4.2.1 Atomic Absorption Spectrophotometry for determination of Ca, Mg, Fe, Zn, Mn, Cu, Cr and Ni

Analysis of the digested samples for determination of the above outlined major and trace elements was done using Perkin Elmer^{R} Model 2908 Spectrophotometre. The machine was set in absorbance mode, with other settings such as

wavelength, lamp current and spectral band selected to correspond with the element analysed.

An air/acetylene flame was used during the analysis. The sample solutions were aspirated through the atomizer or nebulizer to pass the air/acetylene flame, where the atomic vapour of the sample analysed was nebulized.

Light from a modulated hallow cathode Lamp Corresponding with the element analysed was selected. The light which is a sharp spectral line was fixed to pass a monochromatic wave selector, which isolated the resonance line required.

The resonance line which passed through the flame aspirated with the sample solutions were partially absorbed. The resulting beam that went through was finally directed to pass a photomultipher tube detector and amplifier. The amount of absorption was indicated on the readout facility and recorded as percentage absorption. Reading for all the samples, four standards and the blank were done and recorded.

The working principle of Atomic Absorption Spectrophotometry is based on the theory that the amount of percentage absorption of the resonance light for a

specific element in a sample solution is proportional to the concentration of the element in solution.

The concentration of the elements determined were calculated using the following formulae and given as Parts Per Million (PPM) and percentage (%) for element oxides.

$$\text{Element Concentration (ppm)} = \frac{X-Y(a+b).d}{(h+l).w} \quad - - - - \quad I$$

$$\text{\% Concentration of element oxides} = \frac{X-Y\ (a+b).d.100}{(h+l).w.10^{6}} \quad - - \quad II$$

X = % Absorbance of sample

Y = % Absorbance of blank

h = Absorbance of higher standard "a" µg/ml

l = Absorbance of lower Standard "b" µg/ml

d = dilution

w = weight of sample

Result of the analysis for the all the samples is attached in appendix I.

BELLO UNIVERSITY
IBRAHIM IBRAHIM LIBRARY

4.2.2 Flame Photometry for determination of Na and K

The EEL^{R} Flame Photometer Model A was used for determination of (Na) sodium and (K) potassium. The flame photometer utilized air/butane gas which produced a flame of 700^{O}C to 900^{O}C. The heat produced by the flame was most suitable for determination of alkali elements.

The machine was run by aspiration of the sample solution into the air/butane flame. This excited the atoms of elements in solution to high energy level, and as they reverted back to the ground energy levels, they emitted rays of lights.

For determination of Na and K, corresponding photocells filters for sodium and potassium were used to filter and allow passage of colour emissions from the flame which corresponded to the respective elements. The emitted rays transmitted through the photocells emerged as spectral lines, and subsequently went to the detector for registration.

Measurement of the light transmitted was read at a readout facility calibrated into 100 units. The readings are therefore recorded as percentage transmission. Measurements were done for all the samples, the four

standards and the blank solution.

The working principle of Flame photometry is based on the theory that the atoms of the measured elements are energized to high energy levels, while in the flame, and as they fall back to the ground energy states, they emit light or photons that are characteristics of those elements. The amount of percentage emission are also proportional to the concentration of those elements in solution.

After the measurements the percentage concentration of sodium and potassium were calculated using formula II for element oxides as in Atomic Absorption Spectrophotometry. The results for all the samples are attached in appendix I.

4.2.3 Spectrophotometry for determination of phosphorus, Titanium and Uranium

Phosphorus determination: The Baush and lomb^{R} spectronic 20 was used for determination of phosphorus ($P_2 O_5$). Using a blue phosphomolybdate complex method as decribed by Riley (1958).

Reagents were prepared using 168ml of 50% v/v "Aristar" sulpheric acid diluted to 1 litre; 5 grammes of

powdered amonium molybdate was dissolved and diluted in distilled water to 250ml and 4.4 grammes of ascorbic acid was also dissolved and diluted to 250ml in distilled water.

From the reagents a reducing solution was prepared by mixing 762.5ml of 3N Sulpheric acid, 232 ml ammonium molybdate, 366 ascorbic acid and 164.5ml of distilled water to make 1525ml of the reducing solution.

0.047 grammes of potassium dihydrogen phosphate was dissolved and diluted to 500ml with distilled water to make 50 µg/ml (P_2O_5) Standard Stock Solution. A working Standard solution was prepared by pipetting 1ml, 3ml, 6ml and 9ml of the 50 µg/ml Stock Standard Solution into clean 50ml volumetric flask. 25ml of the reducing solution were added to each and diluted to volume with distilled water.

For the sample solutions and blank, 5ml of the solution were pipetted into clean 50ml volumetric flask, and 25 ml of the reducing solution was added and diluted to volume with distilled water. Measurements of the samples, four standards and a blank solution were carried out on the Spectrophotometry using a red photocell at a wavelength of 827 nm.

Readings on the instrument were recorded as percentage transmission and converted to percentage absorbance by the equation:-

$$\text{Absorption (A)} = \frac{\text{Log } I_o}{\text{Log } I_1} \qquad \text{Log } I_o - \text{log } I, \text{ - - - III}$$

$\text{Log } I_o$ = Transmission of blank (log transformed)

$\text{Log } I_1$ = Transmission of sample (log transformed)

A = Absorption.

A plot of converted absorption values of the Standards plotted against concentration on a graph formed a straight line through the origin. (Fig 4.3). The plot obeyed Beer's Law and was used for calibration of phosphorus.

Calculation of the percentage concentration (P_2O_5) was determined using Beer's factor:-

$$\text{Beer's factor} = \frac{\mu g/ml \text{ of } P_2O_5 \text{ in Standard solution}}{\text{Optical density of Standard solution}} =$$

$$= \frac{1}{\text{Optical density of standard solution}} \text{ - - IV}$$

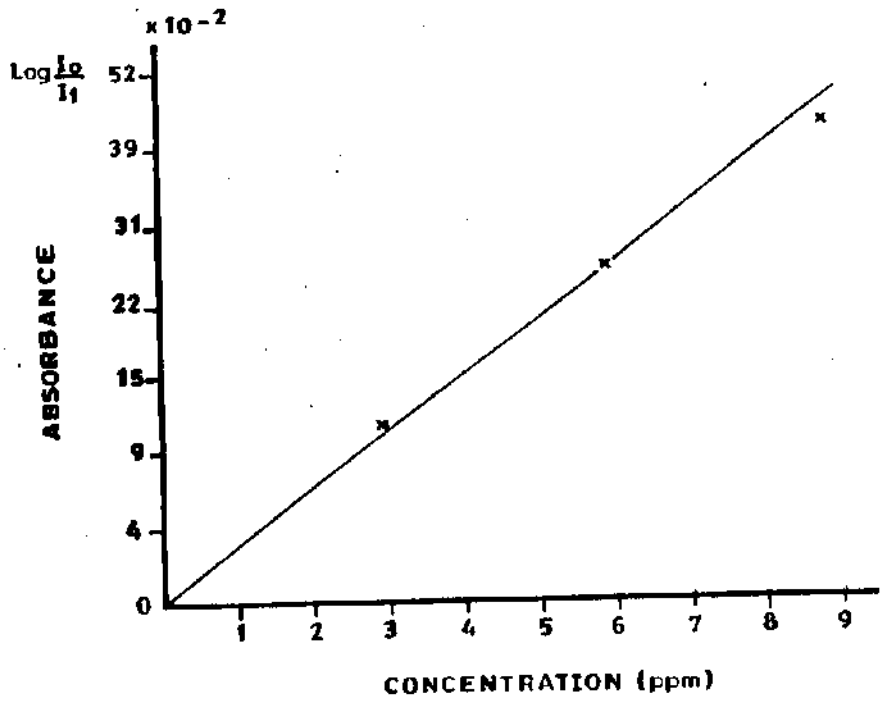


Fig.4.3. Calibration curve for colorimetric determination for phosphorus.

$$\% P_2O_5 = \frac{\mu g/ml\ (P_2O_5) \times dilution \times Beer's\ factor \times 100}{Weight\ of\ sample \times 10^6} - V$$

The calculated values of percentage (P_2O_5) are attached in appendix I.

Titanium determination - Titanium was determined on a W.P.A. S100 Spectrophotometer using a yellow titanium (IV) Sulphate complex formed by hydrogenperoxide and sulphuric acid as described by Riley (1958).

A colour reagent was prepared by mixing 200ml of 50% sulphuric acid (H_2SO_4) "Aristar", 200ml phospheric acid (H_3PO_4) (BDH) and 200ml 30% H_2O_2 "BDH" hydrogen peroxide in a 1 litre volumetric flask and diluted to volume with distilled water.

A standard stock solution was prepared by fusing 0.10 grammes of TiO_2 with 2 grammes potassium pyrosulphate in a silica crucible. The mixture was heated until no more fumes were given off. The cooled melt was dissolved into 50ml of 50% sulphuric acid, warmed and diluted to one litre volume with distilled water.

Three Standard working solutions were prepared by pipetting 2ml, 3ml and 5ml of the 100 µg/ml standard stock solution into three 50 ml volumetric flask. 15 ml of the

reducing solution were added to each of the standard solution and diluted to volume with distilled water. This produced 4 µg/ml, 6 µg/ml and 10 µg/ml TiO_2 solution respectively.

A plot of the converted absorption values were done using equation III and the Standard absorption values were plotted against concentration on a graph (fig.4.4). The curve passed through the origin. Beer's Law is obeyed and the curve was used for calibration of Titanium.

$$\text{Beer's factor} = \frac{\mu g/ml\ (TiO_2)\ \text{in Standard solution}}{\text{Optical density of standard solution}}$$

$$= \frac{1}{\text{Optical density of standard solution}} \quad - \quad - \text{VI}$$

$$\%\ TiO_2 = \frac{\mu g/ml(TiO_2) \times \text{dilution} \times \text{Beer's factor} \times 100}{\text{Weight of sample} \times 10^6} \quad - \quad \text{VII}$$

The calculated values of percentage TiO_2 Titanium Oxide are attached in Appendix (I).

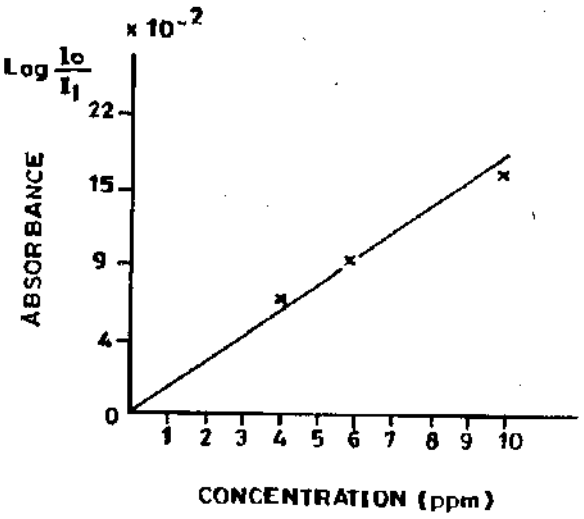


Fig.4.4. Calibration curve for colorimetric determination of Titanium.

Uranium determination:- Uranium was determined on a W.P.A. S100 spectrophotometer using a method described by Okujeni, (1987).

Preparation of reagents include a strong oxidizing agent of 50% ammonium nitrate (G.P.R) 0.005% EDTA prepared by measuring 3.5 grammes of EDTA and 175 grammes of ammonium nitrate, mixed together dissolved and diluted to 700ml with distilled water. The solution was acidified with 15ml of 1.4 nitric acid solution to maintain a low p.H.

Other reagents were 0.001% arsenzo III used as a colour reagent and an extraction solution prepared by mixing 1:4 part of tributyl phosphate (TBP) and kerosine.

0.1915 grammes of UO_2 $(NO_3)_2$ was dissolved and diluted to 100 µg/ml uranium standard stock solution. Three working standard solutions were prepared by pipetting 2 ml, 5 ml and 10ml of the standard stock solution into conical flask and diluted to 100ml with distilled water. Each of the diluted solutions gave 2µg/ml, 5µg/ml and 10µg/ml uranium concentration.

10ml of the sample Standard and blank solution were

separately pipetted into a separating flask, together with 10ml of NH_4NO_3/ EDTA solution and 5ml of Tributyl phosphate/kerosine. The mixture was shaken and the aqueous phase separated from the remaining non-aqueous phase. 5ml of arsenzo III was later added to the separated aqueous solution and allowed to stand for thirty minutes in order to achieve maximum colour development.

The samples, standards and blank solutions were measured on the Spectrophotometer set at a wavelength of 655 nm and the percentage transmission were read.

The method used involved oxidation of uranium in solution by a strong oxidizing agent NH_4NO_3/EDTA, acidified to maintain a low p.H. necessary for uranyl ion solubility. The tributyl phosphate/kerosine solution was used to separate the aqueous phase from the non-aqueous phase, while arsenzo III was added as a colour reagent.

A plot of the converted absorption values (using Equation III) of the standard solutions were plotted against concentration on a graph as in the case of phosphorus and Titanium. The curve obeyed Beer's Law and was used for Uranium calibration (Fig. 4.5).

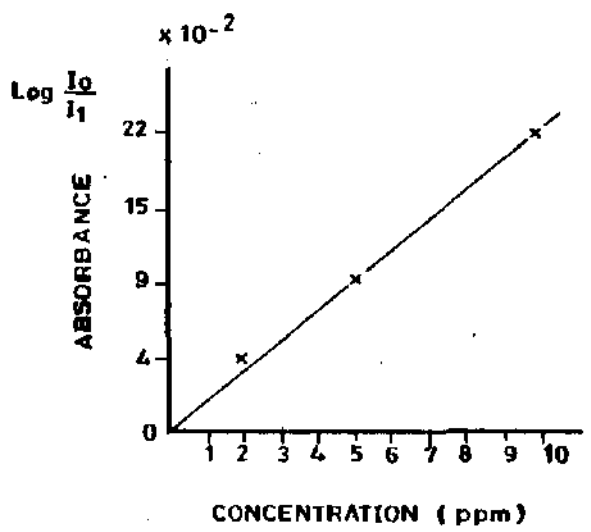


Fig.4.5. Calibration curve for colorimetric determination of Uranium.

$$\text{Beer's factor} = \frac{\mu g/ml(U) \text{ in standard solution}}{\text{Optical density of Standard solution}}$$

$$= \frac{1}{\text{Optical density of standard solution}} \quad - - - \text{VIII}$$

P.P.M (U) Concentration =

$$= \frac{\mu g/ml(U) \times \text{dilution} \times \text{Beer's factor}}{W} \quad - - - \text{IX}$$

The calculated values of uranium concentration are attached in Appendix I.

The general principle of Spectrophotometry is based on colour reaction. Colour development in a solution may be formed independently or by addition of a colour reagent. Element concentration are measured by transmission of corresponding spectral wavelength through the solution. The instrument measures the percentage light transmission from a monochromatic radiation through a given solution. A corresponding photocell is used to measure the optical density of the given solution. (That is the amount of absorption during transmission through the solution).

Elements in solution are responsible for the absorption of the light during transmission in the solution. It is shown that for a certain element, the number of absorbed atoms in a beam is proportional to the product of the pathlength (l) and concentration (c) expressed as:

$$\log \frac{I_o}{Io_1} = E\ l\ c - - - X$$

or $$A = E\ l\ c - - - XI$$

The formula is generally known as Beer's Law

E = constant

l = length light is transmitted through a solution

c = concentration

A = Absorbance.

Chapter 5

GEOCHEMISTRY

5.0 Element Distribution

Analysis of the following major and trace elements, CaO, mgO, FeO, K_2O, Na_2O, P_2O_5, TiO_2, mnO, Zn, Cu, Cr, Ni and U was carried out on all the samples (60).

Table (5.1) shows the range, mean and standard deviation for all the elements. Table (5.2) shows the range, mean and standard deviation for all the unaltered, mildly altered and intensely altered granites and rhyolites.

Figure (5.1) shows the distribution of elements concentration in the samples using histograms. The histograms were plotted using log transformed values converted from the raw data. Cumulative frequency curves for all the elements have also been plotted and is attached in appendix II.

5.1 Major elements

Calcium/(CaO)

Analysis of the samples shows that calcium oxide has a range of 0.02% to 1.23%, an average of 0.034% and no standard

Element	Range	Mean	Standard Deviation
CaO	0.020 - 1.230%	0.037%	-
MgO	0.006 - 0.820%	0.084%	0.193
FeO	0.480 - 17.40%	3.984%	3.648
K_2O	0.050 - 2.180%	0.186%	0.310
Na_2O	0.054 - 3.00%	0.195%	0.413
P_2O_5	0.005 - 0.734%	0.118%	0.131
TiO_2	0.02 - 0.32%	0.09%	0.06
MnO	0.002 - 0.180%	0.017%	0.030
Zn	7.5 - 235ppm	44.24 ppm	49.42
Cu	1 - 79 ppm	20.41 ppm	14.65
Cr	11 - 165ppm	56.10 ppm	37.31
Ni	5 - 40 ppm	16.43 ppm	9.67
U	5.6 - 170.9ppm	47.19 ppm	26.57

Table 5.1 Range mean and standard deviation for all the samples analysed (60)

	Unaltered biotite granite			Mildly altered Porphyritic porphyritic biotite			Intensely altered porphyritic biotite granite			Unaltered Rhyolites			Mildly Altered Rhyolite			Intensely Altered Rhyolite		
	Range	Mean	St.Dev	Range	Mean	St.dev.	Range	Mean	St.dev	Range	Mean	St.dev	Range	Mean	St.Dev	Range	Mean	St.dev
CaO	0.03-1.10	0.565	0.756	0.03-0.03,	0.03	-	0.03-1.230,	0.28	0.531	0.03-1.08,	0.206,	0.427	0.02-0.07,	0.038	0.013	0.03-1.20	0.197	0.371
MgO	0.014-0.530	0.272	0.364	0.10-0.012,	0.011	0.001	0.011-0.820,	0.175	0.360	0.006-0.70,	0.131,	0.278	0.006-0.042,	0.019	0.010	0.008-0.70	0.114	0.224
FeO	0.920-2.950	1.935	1.435	2.29-4.200,	3.245	1.350	0.750-3450	0.94	1.059	0.48 -6.750	2.946,	2.540	0.70-17.40 ,	5.68	5.021	1.00-13.06	4.50	3.62
K_2O	1.000-2.18,	1.590	0.834	0.145-0.180,	0.161	0.026	0.082-0.480,	0.231	0.166	0.058-0.266	0.108	0.080	0.48-0.420	0.113	0.091	0.05-0.76	0.136	0.167
Na_2O	0.092-3.00	1.546	2.056	0.066-0.251	0.158	0.130	0.080-0.480	0.286	0.316	0.066-0.84	0.232	0.309	0.058-0.254	0.088	0.053	0.056-0.80	0.175	0.221
P_2O_5	0.052-0.197	0.124	0.102	0.066-164	0.115	0.069	0.004-0.088	0.055	0.033	0.005-0.333	0.123	0.121	0.009-0.501	0.141	0.141	0.049-0.734	0.133	0.169
TiO_2	0.02-0.02	0.02	-	0.08-0.32	0.20	0.16	0.02-0.18	0.04	0.07	0.02-0.16	0.09	0.05	0.02 -0.11	0.10	0.05	0.01 - 0.12	0.06	-
mnO	0.004-0.074	0.039	0.049	0.03-0.008	0.005	0.003	0.002-0.008	0.007	1.784	0.007-0.011	0.005	0.003	0.002-0.06	0.18	0.021	0.002-0.124	0.016	0.027
Rb	7.5 - 24	15.7	11.66	16 - 23.5	197.5	53	10 - 30.5	18.7	8.26	17.5 - 90	39.58	28.55	12.5 - 100	37.8	21.33	13.5 - 23.5	59.25	
Cu	11 - 16	13.5	3.53	11 - 11	11	-	11 - 39	17.4	11.7	1 - 23	13	7.34	6 - 79	20.18	17.9	1 - 76	26.7	16.87
Cr	20 - 55	37.5	24.7	35 - 85	60	35.3	20 - 55	37	16.43	20 - 100	68.6	34.7	15 - 165	66.7	45.9	11 - 137	60.65	39.97
Ni	5.0 - 15.0	100	7.07	10 - 25	17.5	10.6	5 - 20	12.4	5.59	5 - 20	14.83	6.17	5 - 40	21.0	11	10 - 55	19.78	9.54
U	5.6-23.1	14.35	12.37	41.2-66.1	53.6	57.6	23.1 - 35	29.0	4.20	23.1 - 66.1	49.6	19.7	29-133.6	53.49	23.98	23.1-170.9	55.07	34.0

Table 5.4: Range, mean and Standard deviation of unaltered, mildly and intensely altered granites and rhyolites.

deviation. The average values for the unaltered rhyolites is 0.206% and 0.565% for the unaltered porphyritic biotite granite.

The average abundance (Clark value) of calcium in rhyolites and granites is 1.13% and 1.33% (Nockolds 1954) respectively. The average values of the unaltered rhyolites and granite in the study area indicate lower values than the clark values for rhyolites and granites.

Figure 5.1a shows the distribution of calcium and figure 5.2 shows the areal distribution pattern of calcium in the mineralized zone. The distribution pattern shows decrease in concentration towards the contact zones of rhyolites and granites. The distribution pattern of calcium is similar to the distribution of mgO and cu.

Magnesium/(MgO)

Magnesium values calculated as Magnesium oxide have a range of 0.006% to 0.820%, an average of 0.084% and a standard deviation of 0.193. The average values for the unaltered rhyolite is 0.131% and 0.272% for the unaltered porphyritic biotite granite.

The clark values of magnesium oxide in rhyolites and granites are 0.32% and 0.52% (Nockolds, 1954) respectively.

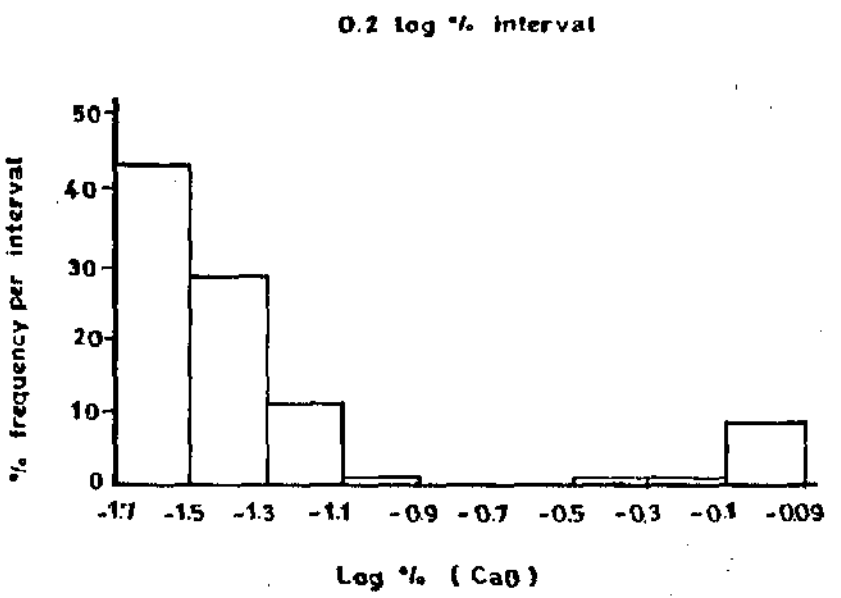


Fig 5.1a. Histogram of (CaO) frequency distribution.

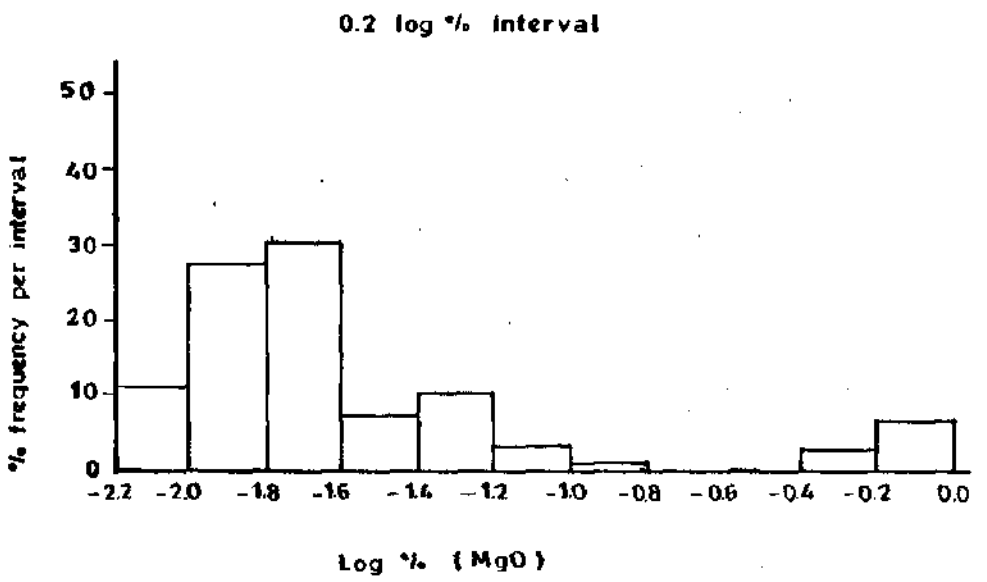


Fig. 5.1b. Histogram of (MgO) frequency distribution.

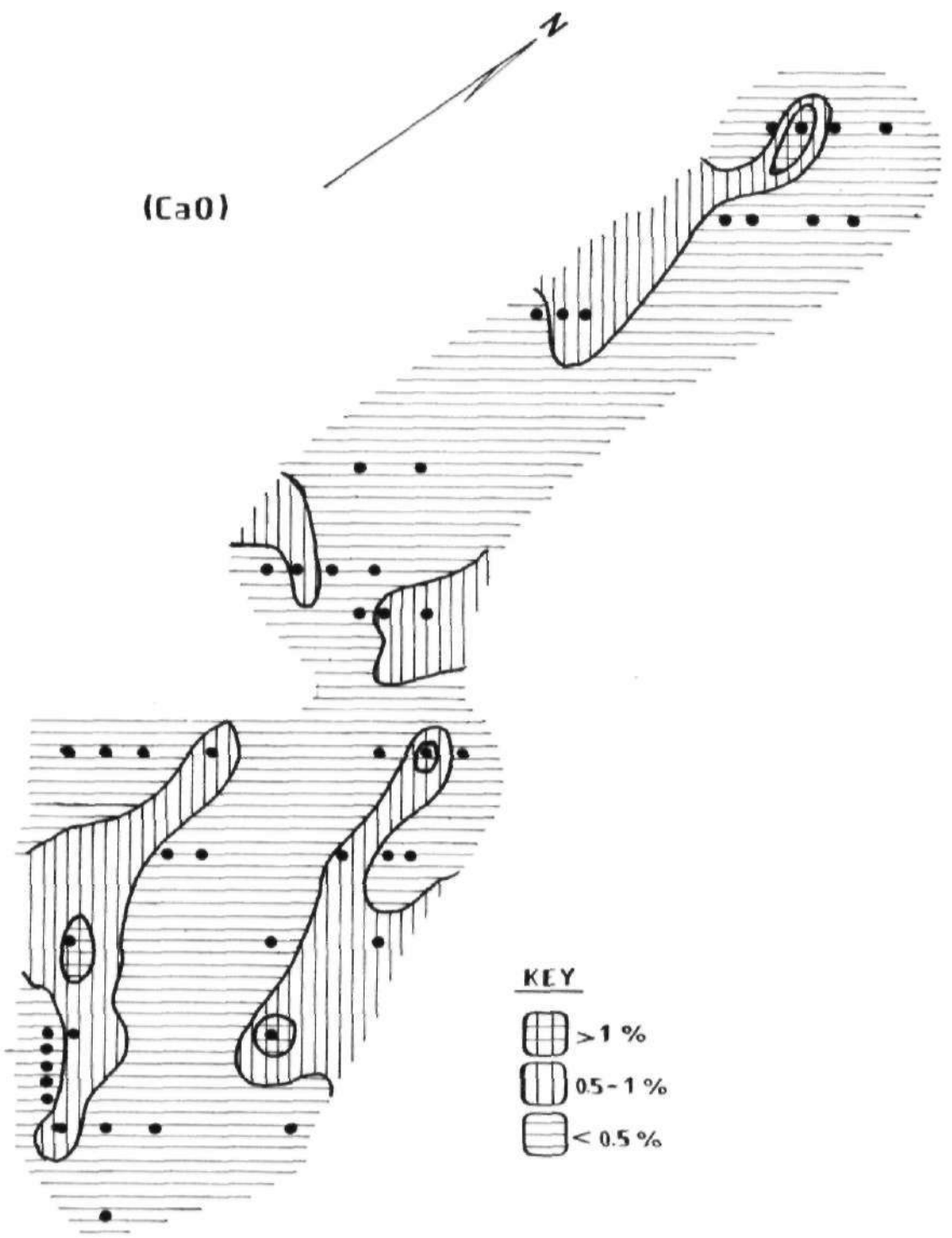


Fig. 5.2a. Areal distribution of Calcium (CaO) at Dinya-Koking mineralized zone.

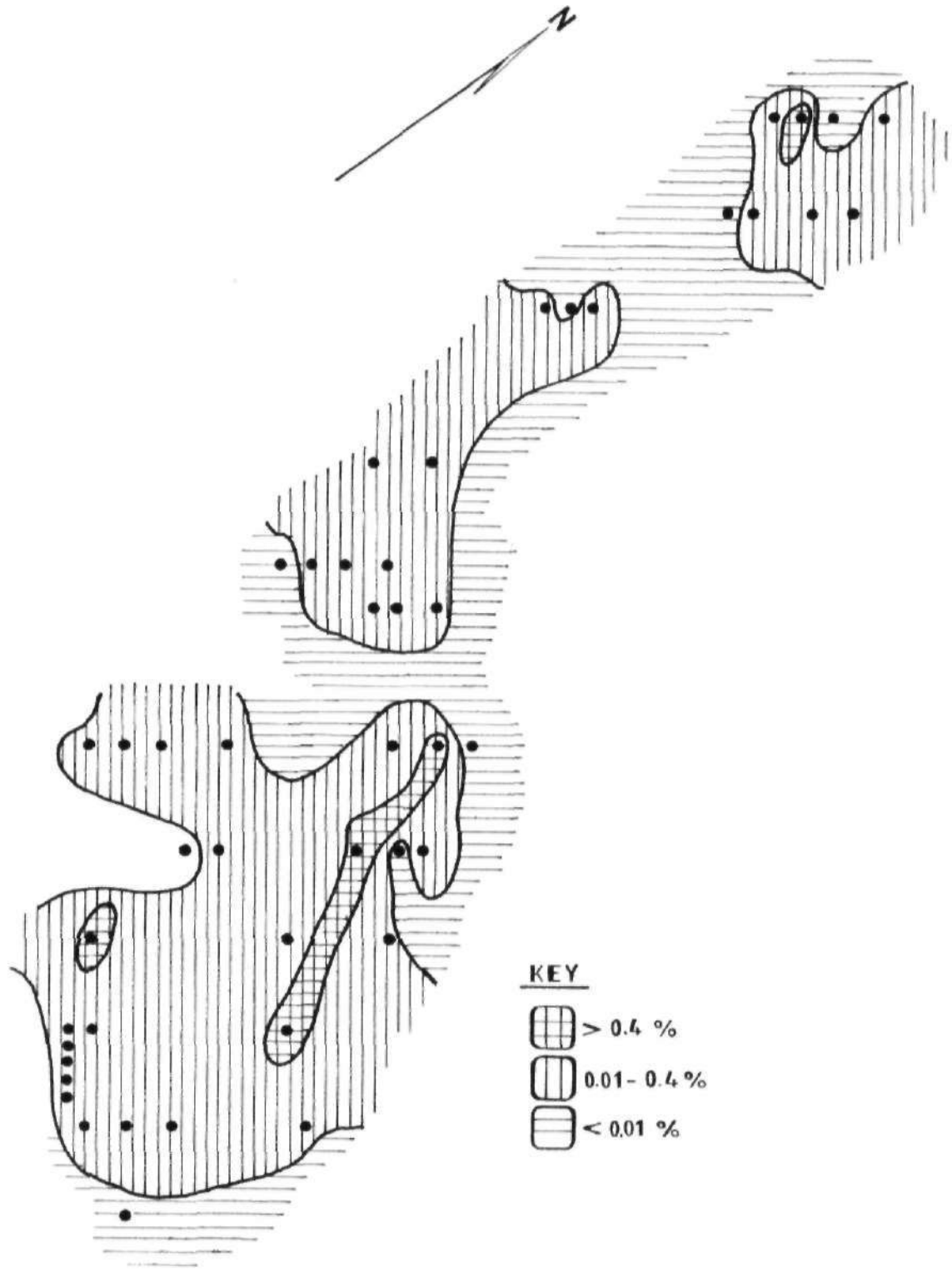


Fig. 5.2b. Areal distribution of Magnesium (MgO) at Dinya-Koking mineralized zone .

the values are higher compared to values obtained for the rhyolites and granites in the study area.

Figure (5.1b) shows the distribution of magnesium composition and figure (5.2b) shows the areal distribution pattern of magnesium in the mineralized zone. The distribution show higher values of concentration in rhyolites and along the contact between rhyolites and granites. The distribution is similar to that of calcium and copper.

Iron/(Fe_2O_3)

The total iron content calculated as Fe_2O_3 was determined for all the samples. Results of the analysis have shown that iron oxide concentration in the rocks has a range of 0.480% to 17.40%, an average of 3.984% and a standard deviation of 3.648. The average value of iron in the unaltered rhyolites is 2.946% and 1.935% for the unaltered porphyritic biotite granite.

The clark value of iron in rhyolites and granites are 0.860% and 1.25% (Nockolds, 1954) respectively. The unaltered rhyolites and granite in the study area show higher average concentration than the clark values in rhyolites and granites.

Figure (5.1c) show the distribution of iron oxide

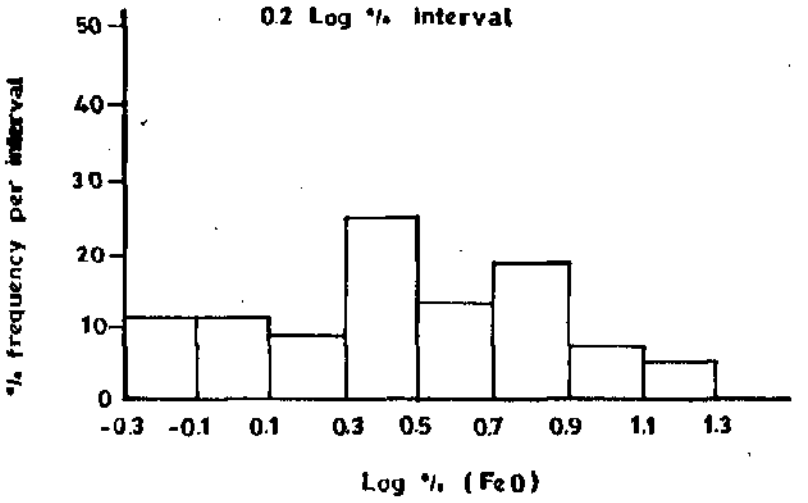


Fig. 5.1c. Histogram of (FeO) frequency distribution .

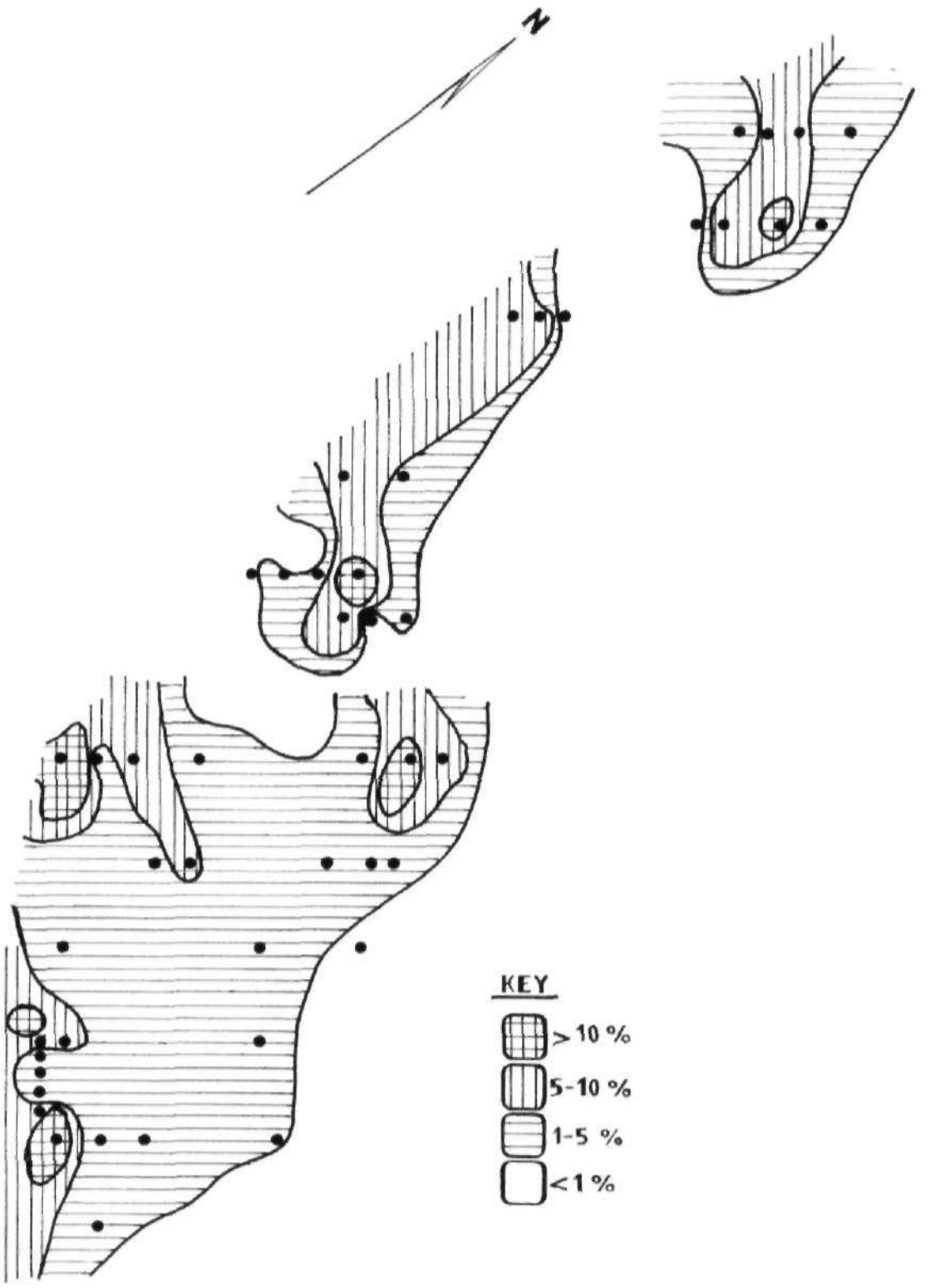


Fig.5.2c. Areal distribution of total Iron (Fe_2O_3) at Dinya-Koking mineralization zone.

concentration and figure (5.2c), shows the areal distribution pattern of iron oxide in the mineralized zone. The distribution of iron oxide shows increase towards the contact of the rhyolites and granites and is similar to the distribution of titanium oxide.

Potassium/(K_2O)

Potassium oxide values have a range of 0.05% to 2.18%, an average of 0.186% and a standard deviation of 0.310. The average values of potassium oxide in unaltered rhyolites is 0.108% and 1.590% for the unaltered porphyritic biotite granite.

The Clark values of potassium in rhyolites and granites are 5.35% and 5.45% (Nockolds, 1959) respectively. The clark values as compared to the rocks in the study area show higher values of concentration.

Figure (5.1d) show the distribution of potassium concentration and figure (5.2d) shows the areal distribution pattern in the mineralized zone which is generally related to the rhyolites. The high concentration in the rhyolites is similar to that of sodium oxide.

Sodium/(Na_2O)

Sodium oxide values range from 0.054% to 3.00%, with an

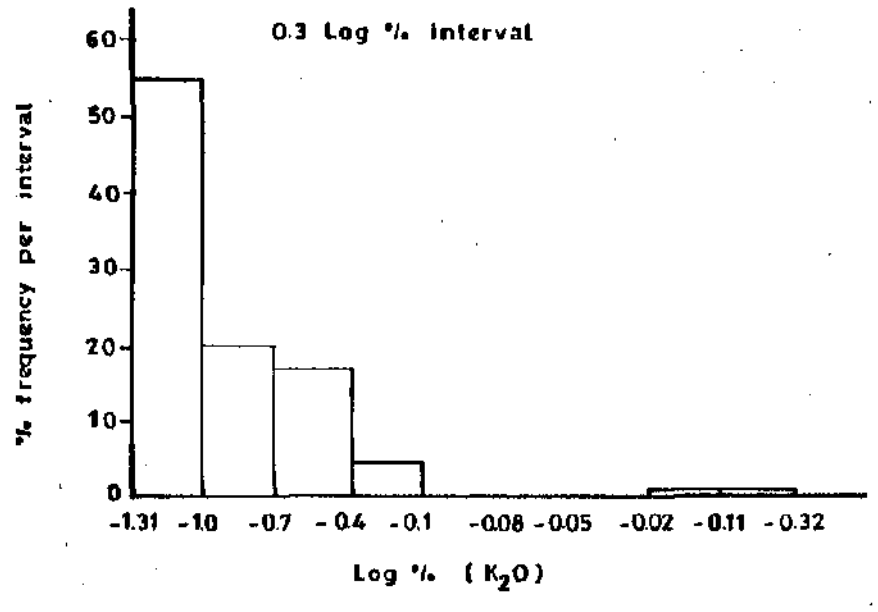


Fig. 5.1d. Histogram of (K_2O) frequency distribution.

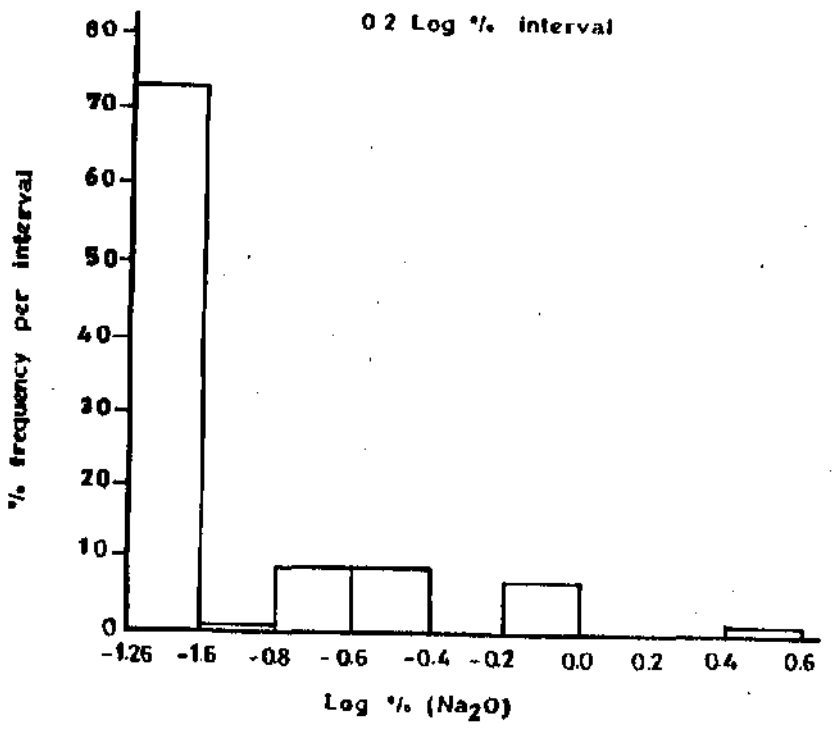


Fig. 5.1e. Histogram of (Na_2O) frequency distribution.

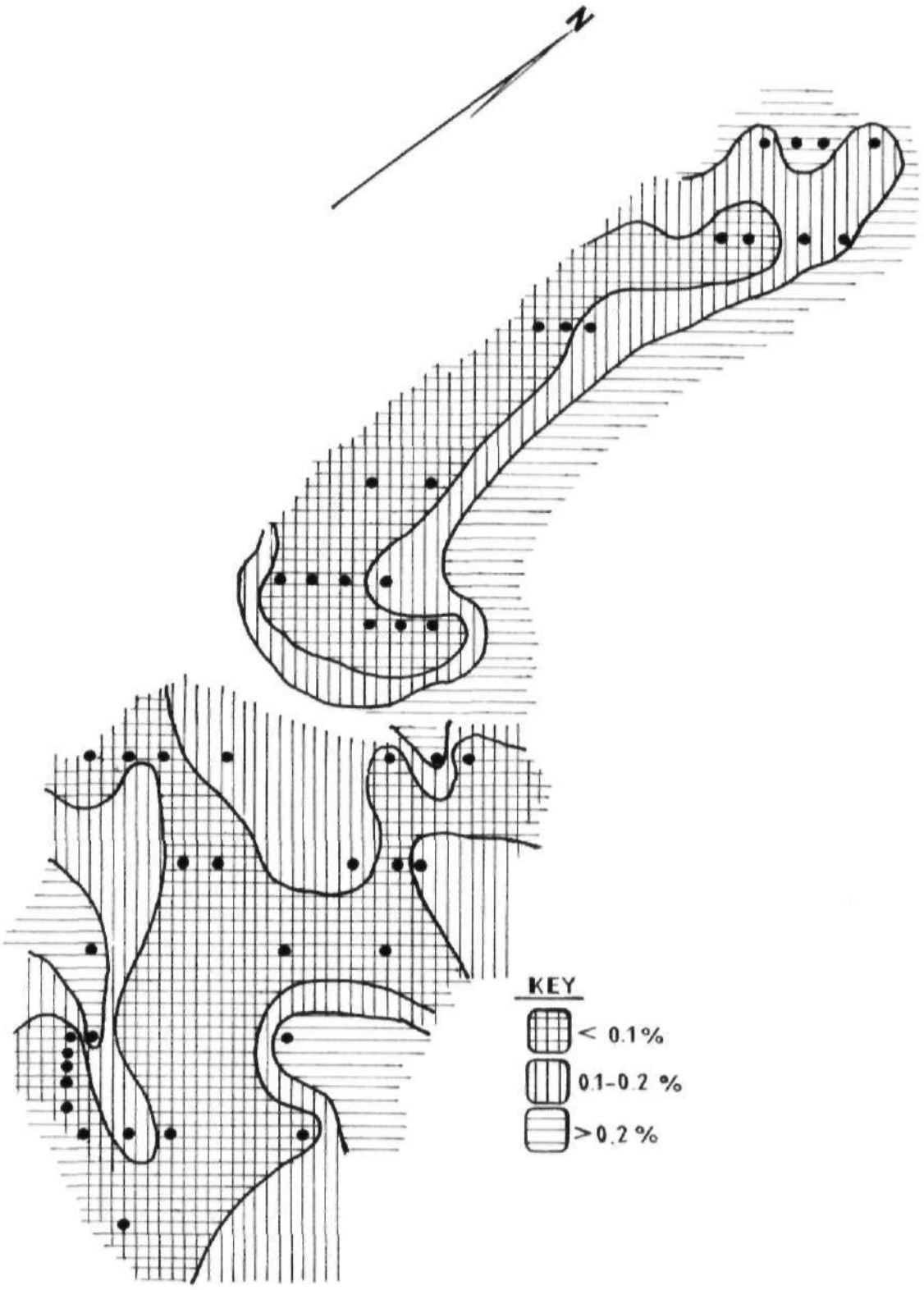


Fig. 5.2d. Areal distribution of Potassium (K_2O) at Dinya-Koking mineralized zone.

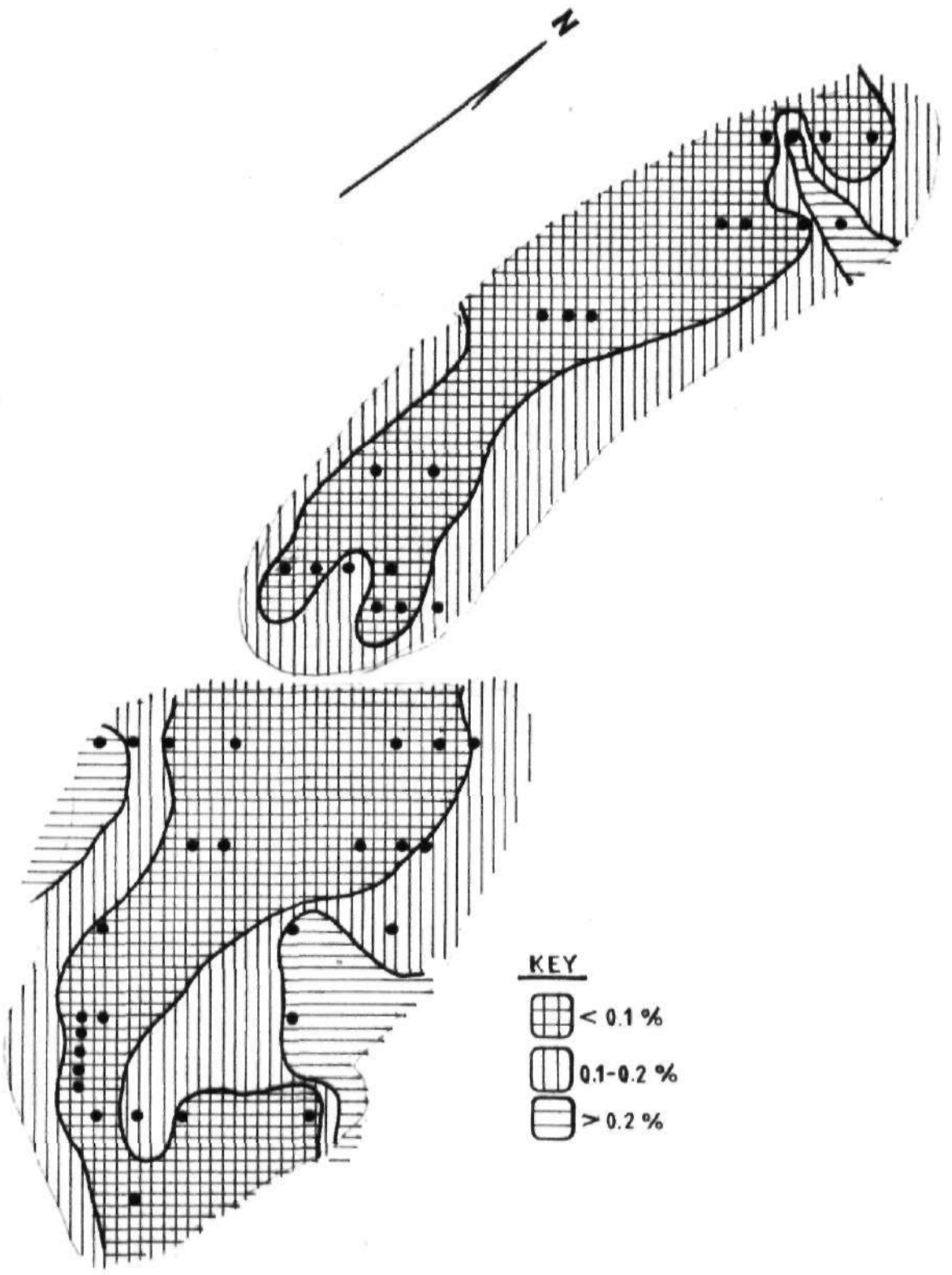


Fig. 5.2e. Areal distribution of Sodium (Na_2O) at Dinya-Koking mineralized zone.

average of 0.195% and a standard deviation of 0.413. The average values for the unaltered rhyolites and unaltered porphyritic biotite granite are 0.232% and 1.546% respectively.

The clark values of sodium in rhyolites and granites are 2.99% and 3.08% (Nockolds, 1954) respectively. The clark values indicate higher values compared to the granites and rhyolites in the study area.

Figure (5.1e) shows the areal distribution of sodium concentration and figure (5.2e) shows the areal distribution pattern in the mineralized zone. The distribution pattern shows higher values in the rhyolites and is similar to the distribution of potassium oxide.

Phosphorus/(P_2 O_5)

The values of phosphorus have a range of 0.005% to 0.734%, with an average of 0.118% and a standard deviation of 0.131. The average values for the unaltered rhyolites and unaltered porphyritic biotite granite are 0.123% and 0.102% respectively

The clark value of phosphorus in rhyolites and granites is 0.07% and 0.18% (Nockolds, 1954) respectively. The clark value of rhyolites indicates higher values than the average

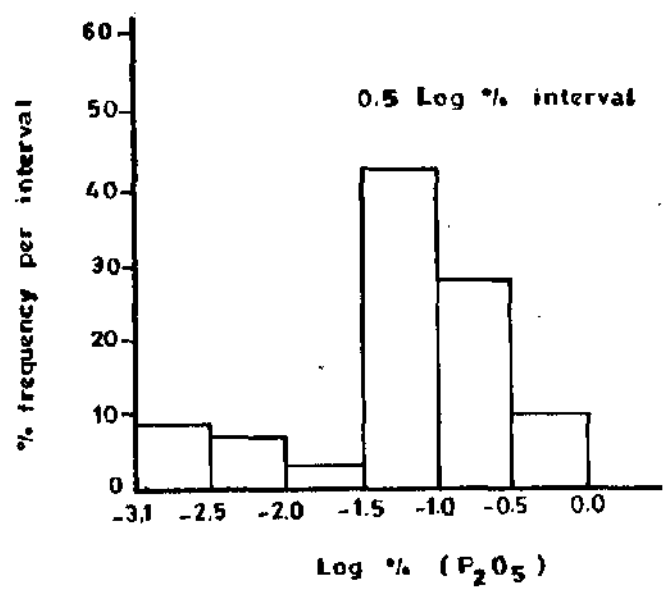


Fig. 5.1f. Histogram of (P_2O_5) frequency distribution.

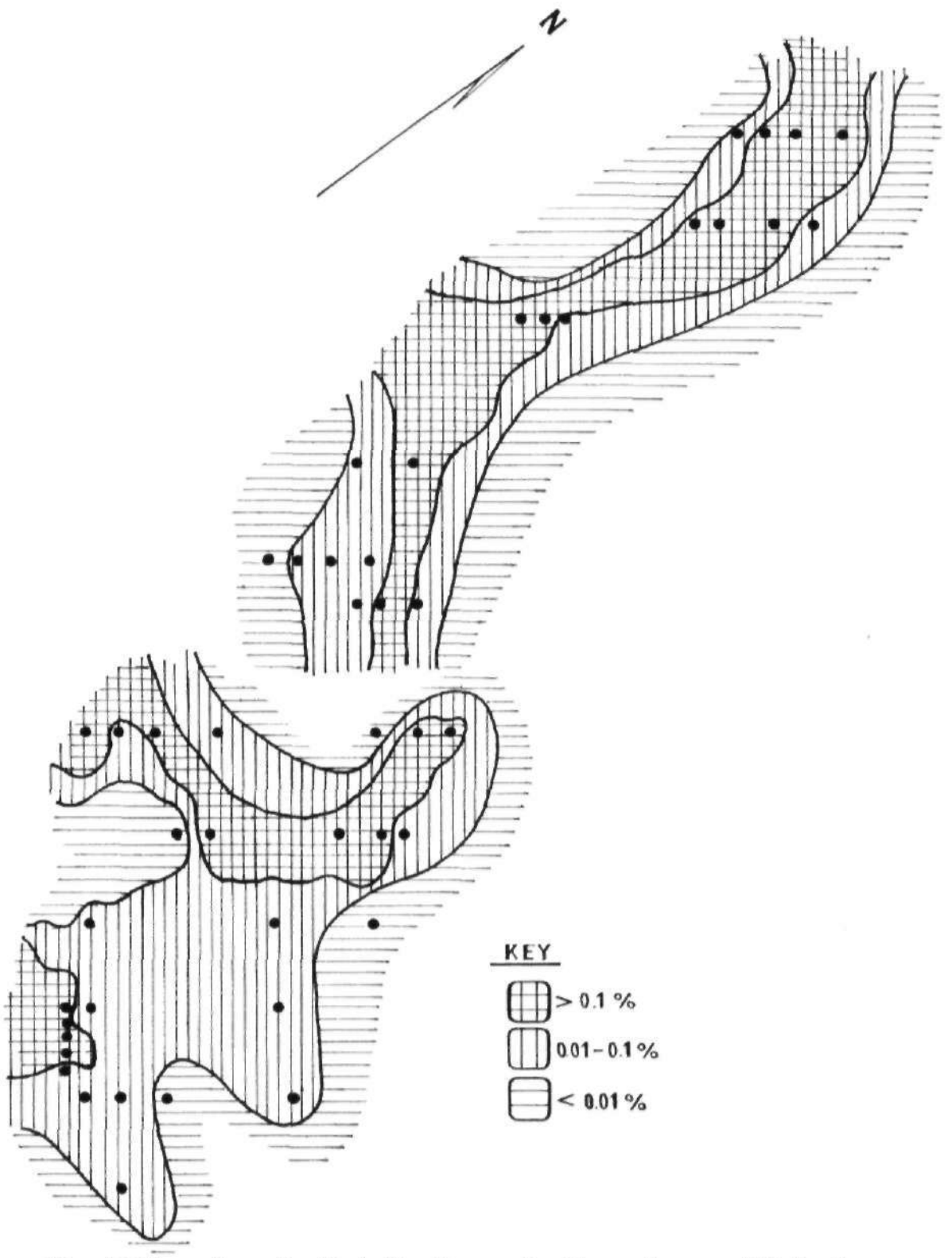


Fig. 5.2f. Areal distribution of Phosphorus (P_2O_5) at Dinya-Koking mineralized zone .

value of rhyolites in the study area, while the granite in the study area has higher average value than the clark value.

Figure (5.1 f) shows the distribution of phosphorus concentration and figure (5.2f) show the areal distribution pattern of phosphorus in the mineralized zone. The distribution show higher values in the rhyolites and along the contact. The distribution pattern is similar to the distribution pattern of nickel.

Titanium/(TiO_2)

Titanium values range from 0.02% to 0.32% with an average of 0.09% and a standard deviation of 0.06. The average values of unaltered rhyolites and unaltered porphyritic biotite granite are 0.16% and 0.20% respectively.

The clark values of titanium in rhyolites and granites are 0.22% and 0.37% (Nockolds 1954) respectively. The average values of rhyolites and porphyritic biotite granite show lower values than the clark values in rhyolites and granites.

Figure (5.1g) shows the distribution of Titanium values and figure (5.2g) shows the areal distribution pattern in the mineralized zone. The distribution indicate higher values of concentration along the contact of the granites and rhyolites. The distribution pattern is similar to that of iron oxide.

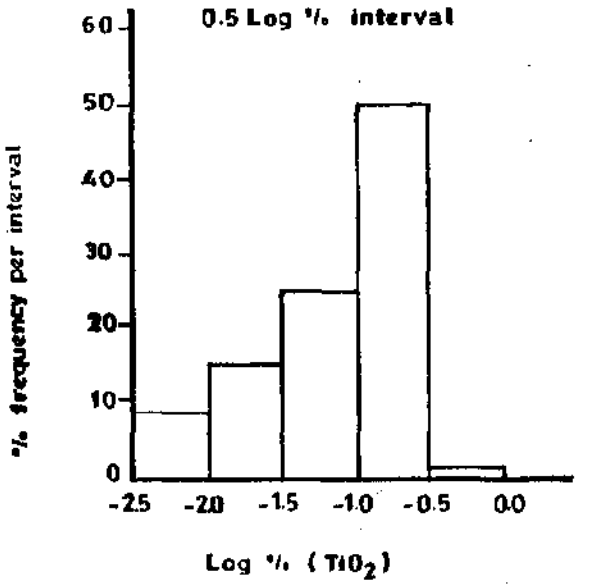


Fig. 5.1g. Histogram of (TiO_2) frequency distribution.

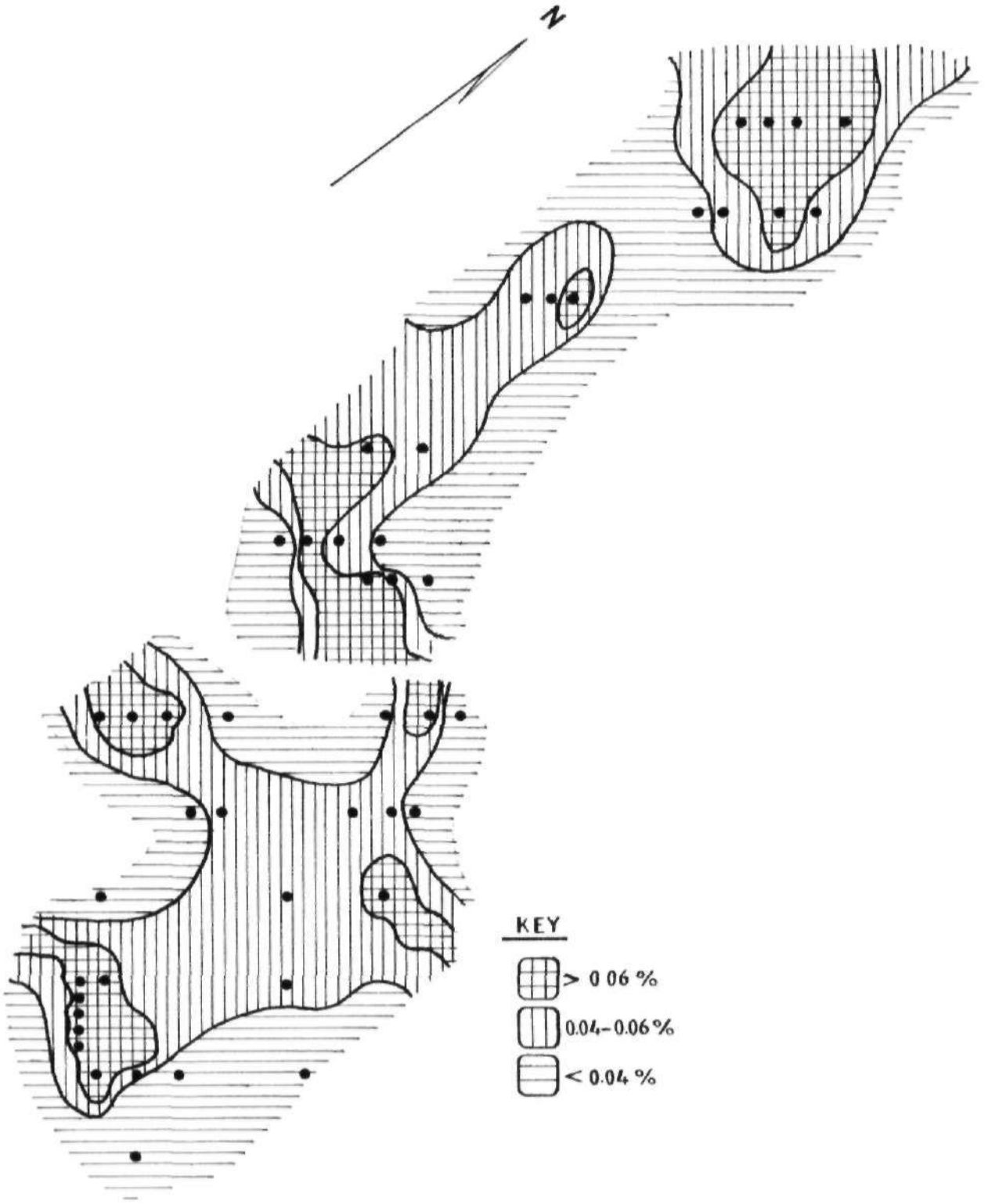


Fig. 5.2g. Areal distribution of Titanium (TiO_2) at Dinya-Koking mineralized zone.

Manganese (MnO)

Manganese values have a range of 0.0025% to 0.180%, and average of 0.017% and a standard deviation of 0.030. The average values of manganese in the unaltered rhyolites and porphyritic biotite granites are 0.005% and 0.039% respectively.

The clark value of Manganese in rhyolites and granites 0.03% and 0.06% (Nockolds, 1954) respectively. The clark value indicates higher values than similar rocks in the study area.

Figure (5.1h) shows the distribution of manganese values and figure (5.2h) shows the areal distribution pattern in the mineralized zone. The distribution shows higher values along the contact and is similar to the distribution of calcium and copper.

5.2 Trace elements

Zinc (Zn)

Zinc values range from 7.5ppm to 235ppm, with an average of 44.24ppm and a standard deviation of 49.42. The average values of zinc in unaltered rhyolites and porphyritic biotite

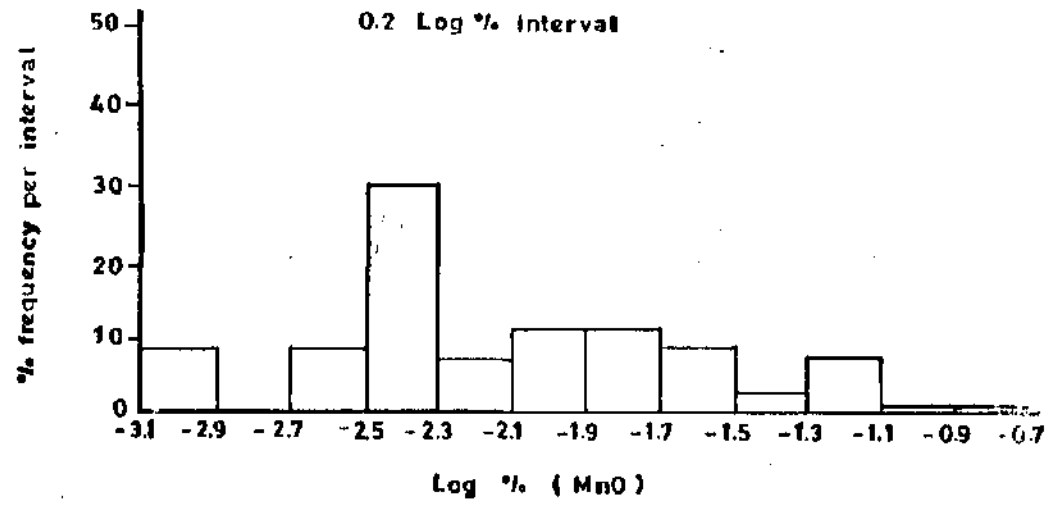


Fig. 5.1h. Histogram of (MnO) frequency distribution.

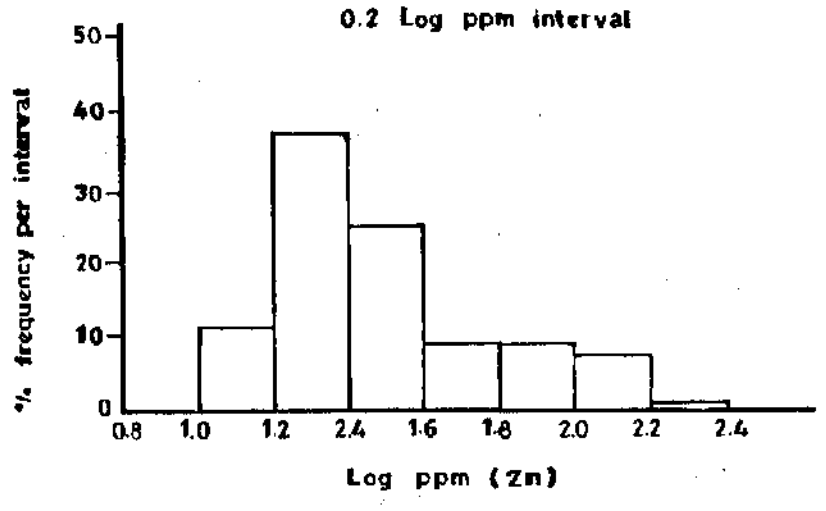


Fig. 5.1i. Histogram of (Zn) frequency distribution.

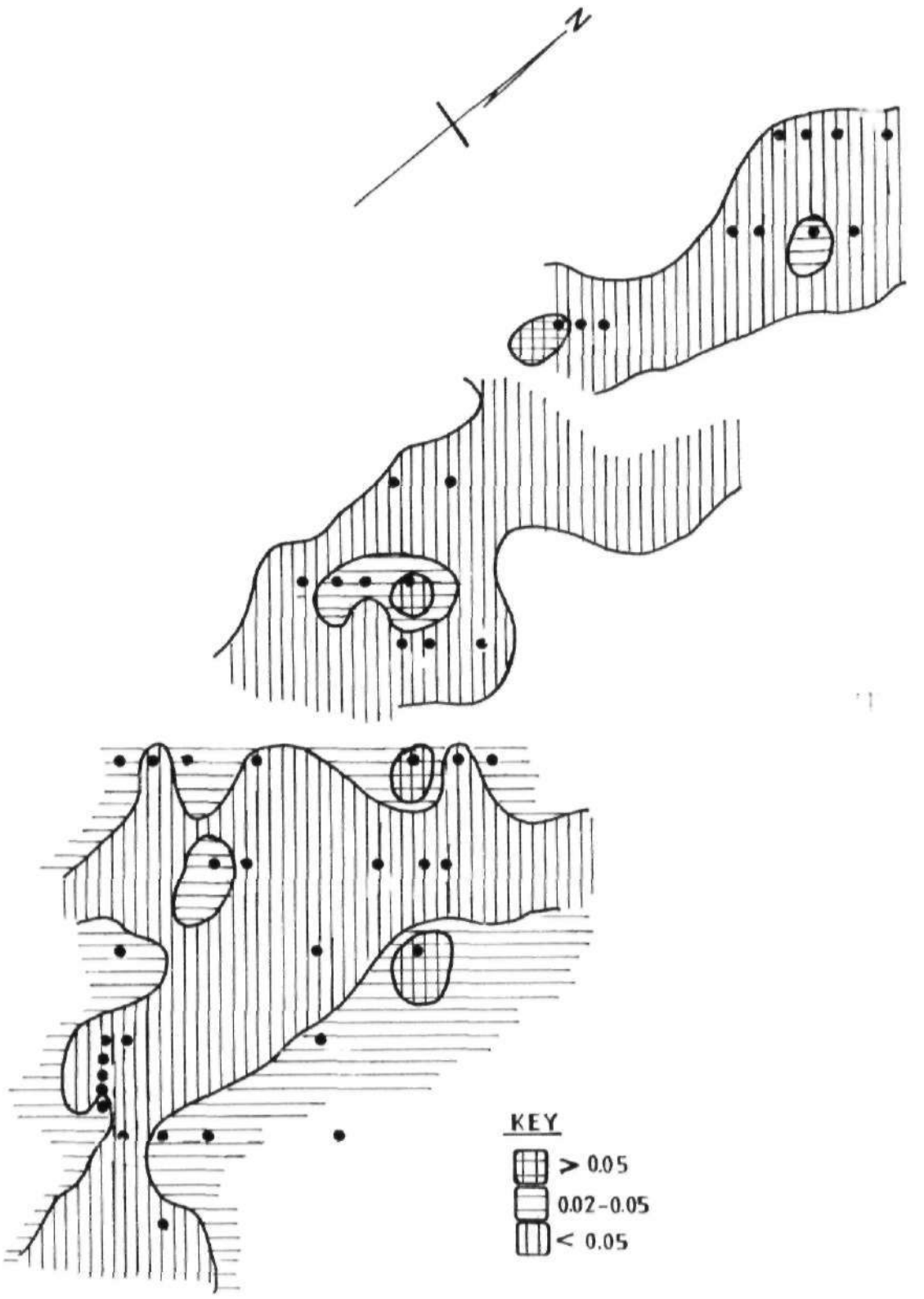


Fig.5.2h. Areal distribution of manganese (Mno) at Dinya-Koking mineralized zone.

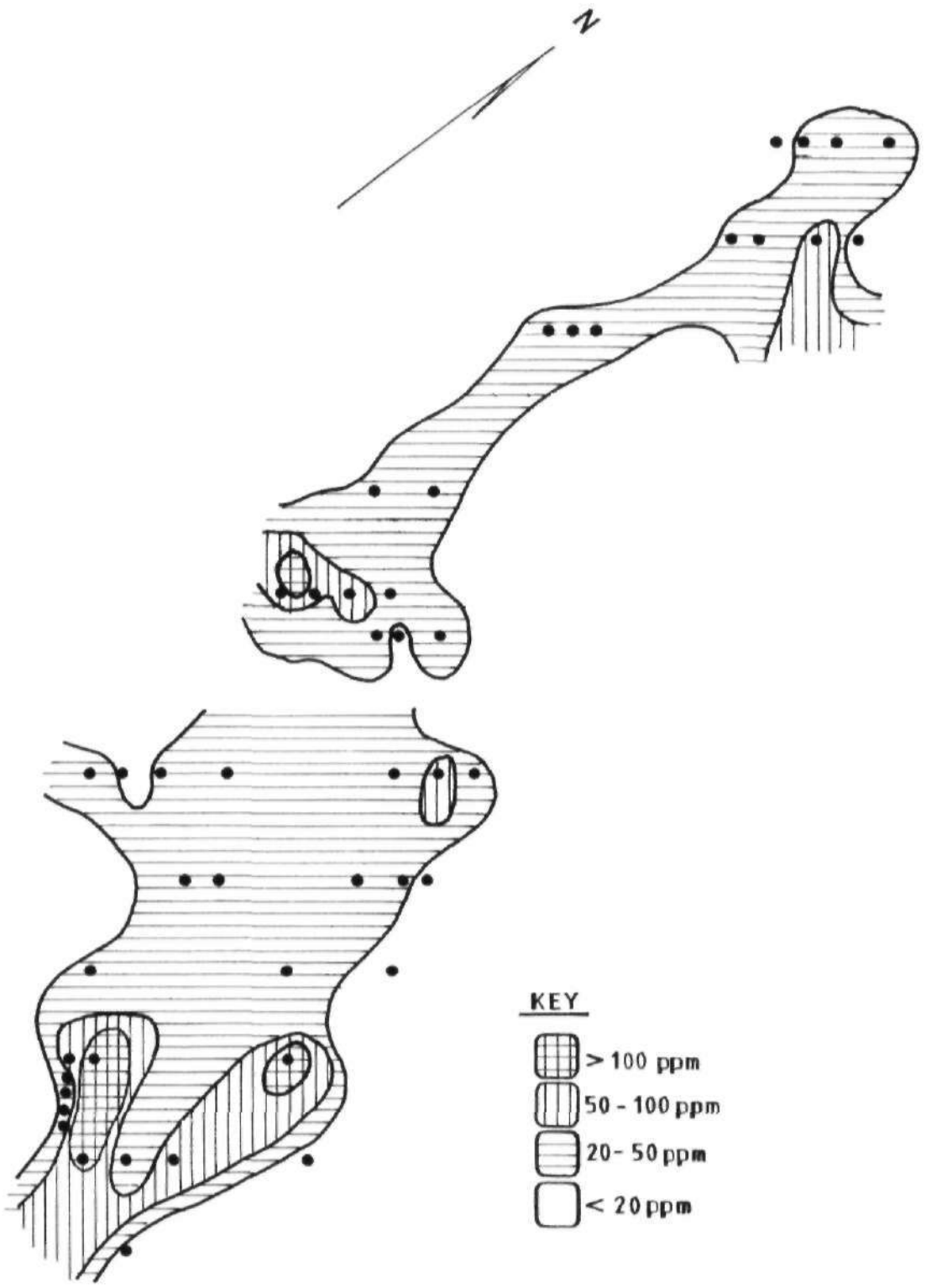


Fig. 5.2 i. Areal distribution of Zinc (Zn) at Dinya-Koking mineralized zone .

granite are 39.5 ppm and 15.7ppm respectively.

The clark value of zinc in rhyolites is 60ppm (Vinogradov, 1962) and 40ppm (Taylor, 1964) for granites. The clark value shows higher values than similar rocks in the study area.

Figure (5.2i) shows the distribution of zinc values and figure (5.2c) shows the areal distribution pattern in the mineralized zone. The distribution of zinc shows higher values in the rhyolites and the contact zones. The distribution of zinc is similar to that of iron, titanium and uranium.

Copper (Cu)

Copper values range from 1ppm to 79ppm with an average of 20.44 ppm and a standard of deviation of 14.65. The average values for copper in unaltered rhyolites and porphyritic biotite granite are 13 ppm and 13.5 ppm respectively.

The clark value of copper in rhyolites is 10 ppm (Ewart, 1968) and 10 ppm (Taylor, 1964) for granites. The clark values for rhyolites and granites indicate lower values than similar rocks in the study area.

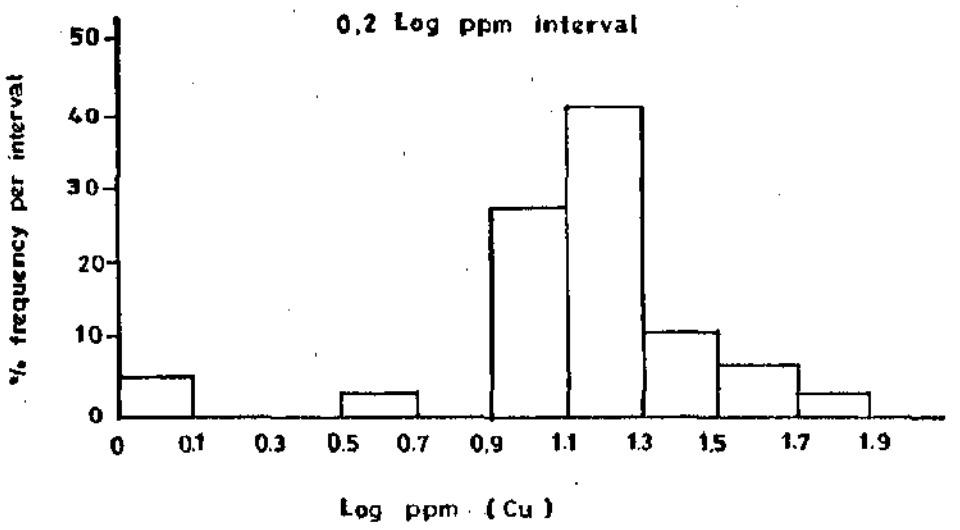


Fig. 5.1j Histogram of (Cu) frequency distribution.

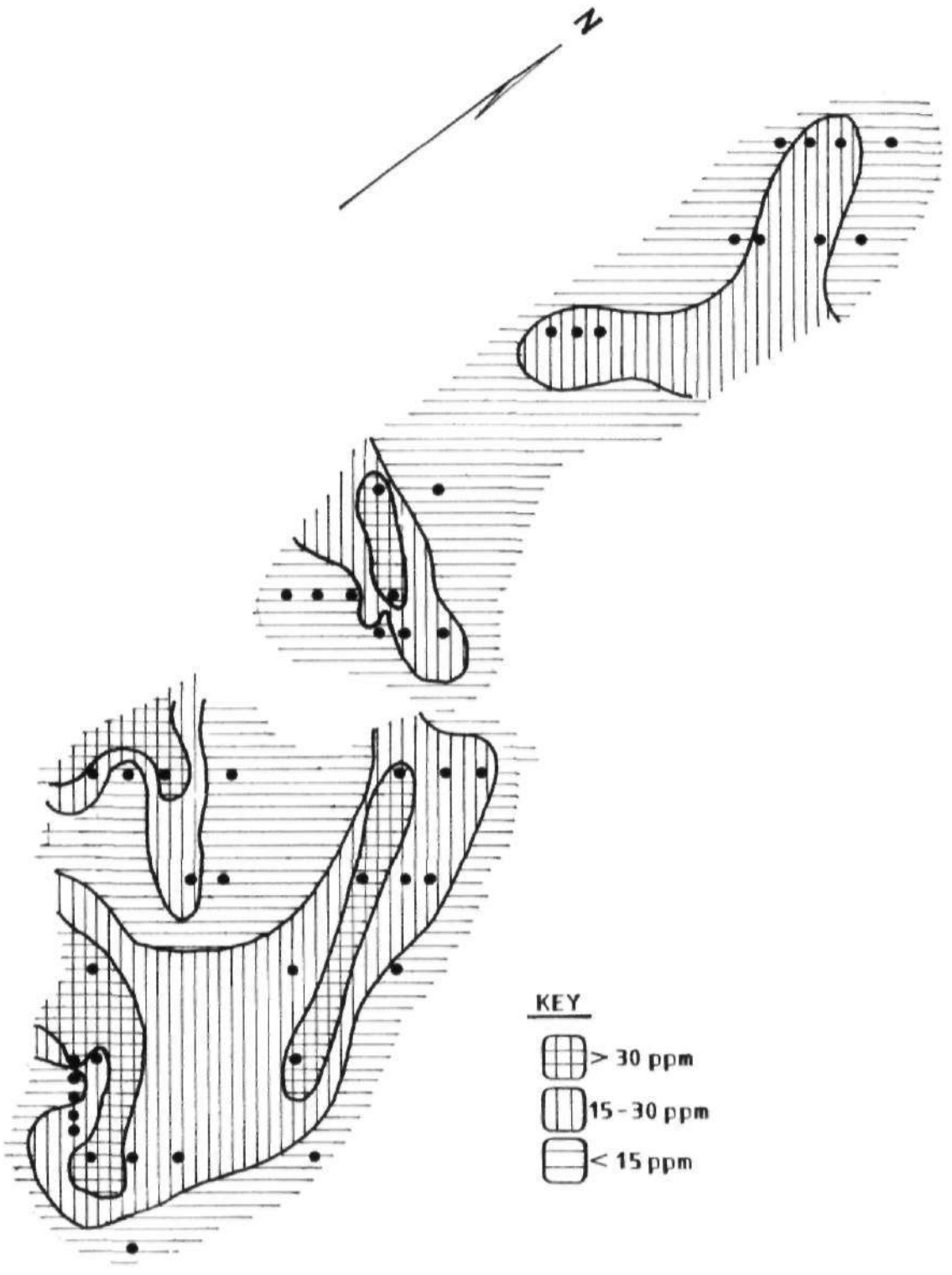


Fig. 5.2 j. Areal distribution of Copper (Cu) at Dinya-Koking mineralized zone.

Figure (5.1j) shows the distribution of copper concentration and figure (5.2j) shows the areal distribution pattern in the mineralized zone. The distribution of copper shows higher concentration in the rhyolites and along the contact. The distribution pattern is similar to the distribution pattern of iron, titanium and uranium.

Chromium (Cr)

Chromium values have a range of 11 ppm to 165 ppm, with an average of 56.10 ppm and a standard deviation of 37.31. The average values of chromium concentration in the unaltered rhyolites and porphyritic biotite granite are 68.6 ppm and 37.5 ppm respectively.

The clark values of chromium in rhyolites and granites are 80 ppm (Ewart et. al., 1968) and 4 ppm (Taylor 1964) respectively. The clark value of chromium in rhyolite indicates a higher value than the average value of chromium in rhyolites in the study area, while in the granites, the porphyritic biotite granite has higher average value compared to the clark value in granites.

Figure (5.1k) shows the distribution of chromium values and figure (5.2k) shows the areal distribution pattern of chromium in the mineralized zone. The distribution shows higher concentrations in the rhyolites especially along the contacts.

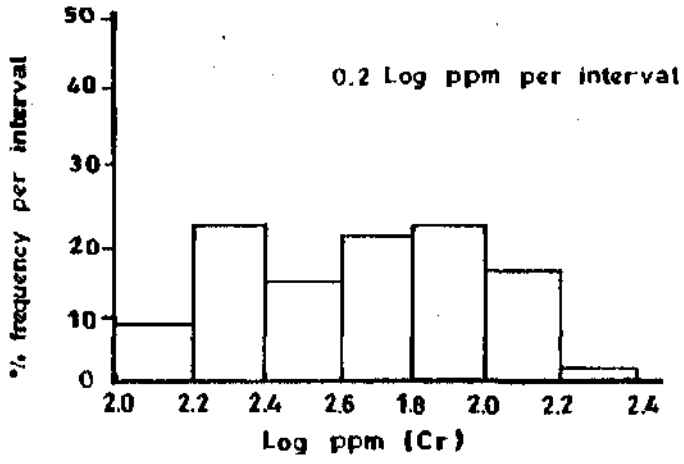


Fig. 5.1k. Histogram of (Cr) frequency distribution.

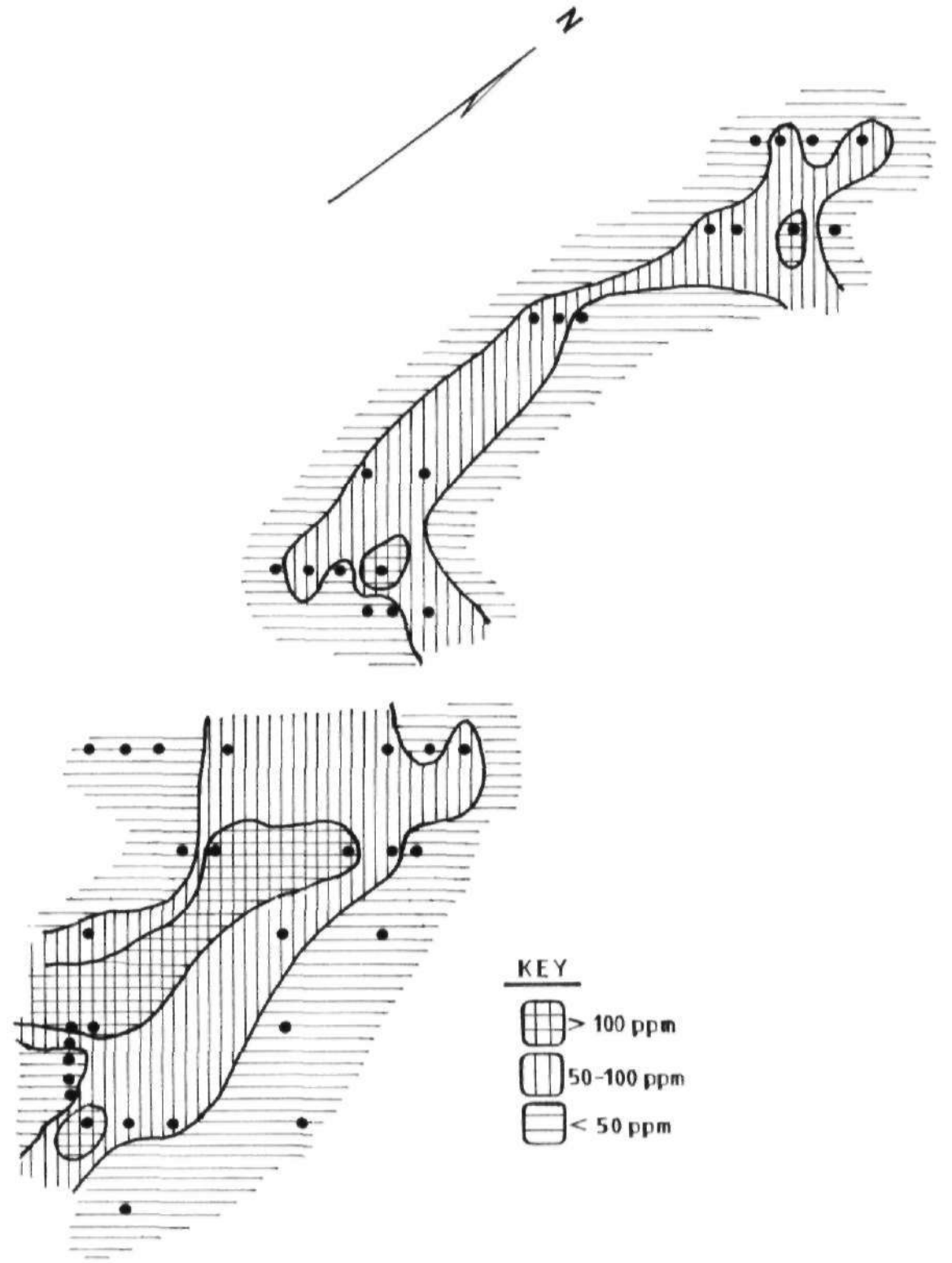


Fig. 5.2k. Areal distribution of Chromium (Cr) at Dinya-Koking mineralized zone.

Nickel (Ni)

Nickel concentration values have a range of 5 ppm to 40 ppm with an average of 16.43 ppm and a standard deviation of 9.67. The average values of unaltered rhyolites and porphyritic biotite granite are 14.8 ppm and 10 ppm respectively.

The clark value of nickel for rhyolites is 6 ppm (Ewart et. al., 1968) and 0.5 ppm (Taylor, 1964) for granites. The clark values of rhyolites and granites represent lower values than average values obtained for rhyolites and granites in the study area.

Figure (5.11) show the distribution of nickel and figure (5.21) shows the areal distribution pattern of nickel in the mineralized zone. The distribution shows high nickel values in the rhyolites and along the contact of the rhyolites and granites.

Uranium (U)

The values of Uranium have a range of 5.6 ppm to 170.9 ppm with an average of 47.19 ppm and a standard deviation of 26.57. The average value of Uranium in unaltered rhyolites is 49.6 ppm and 14.35 ppm in the unaltered porphyritic biotite granite.

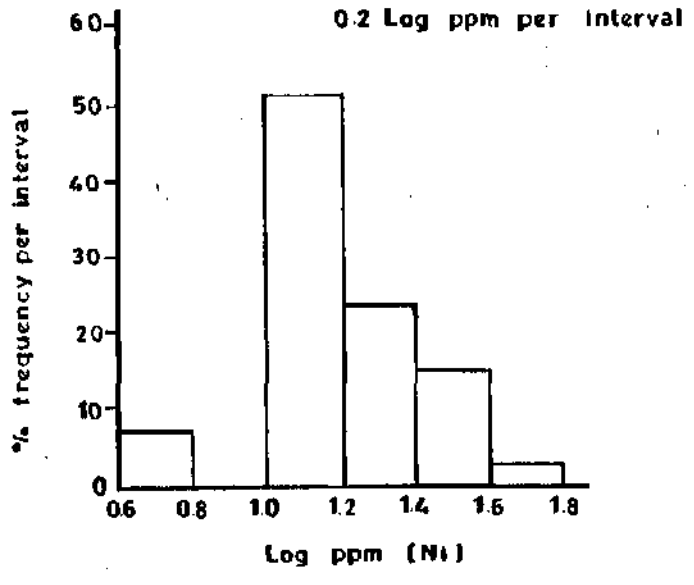


Fig. 5.1l. Histogram of (Ni) frequency distribution.

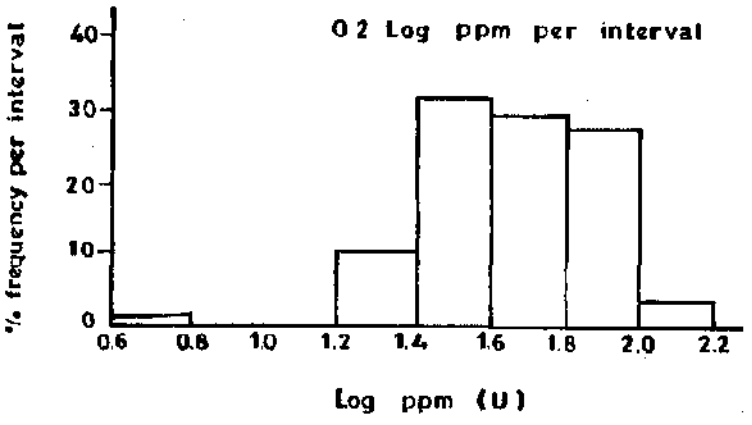


Fig. 5.1m. Histogram of (U) frequency distribution.

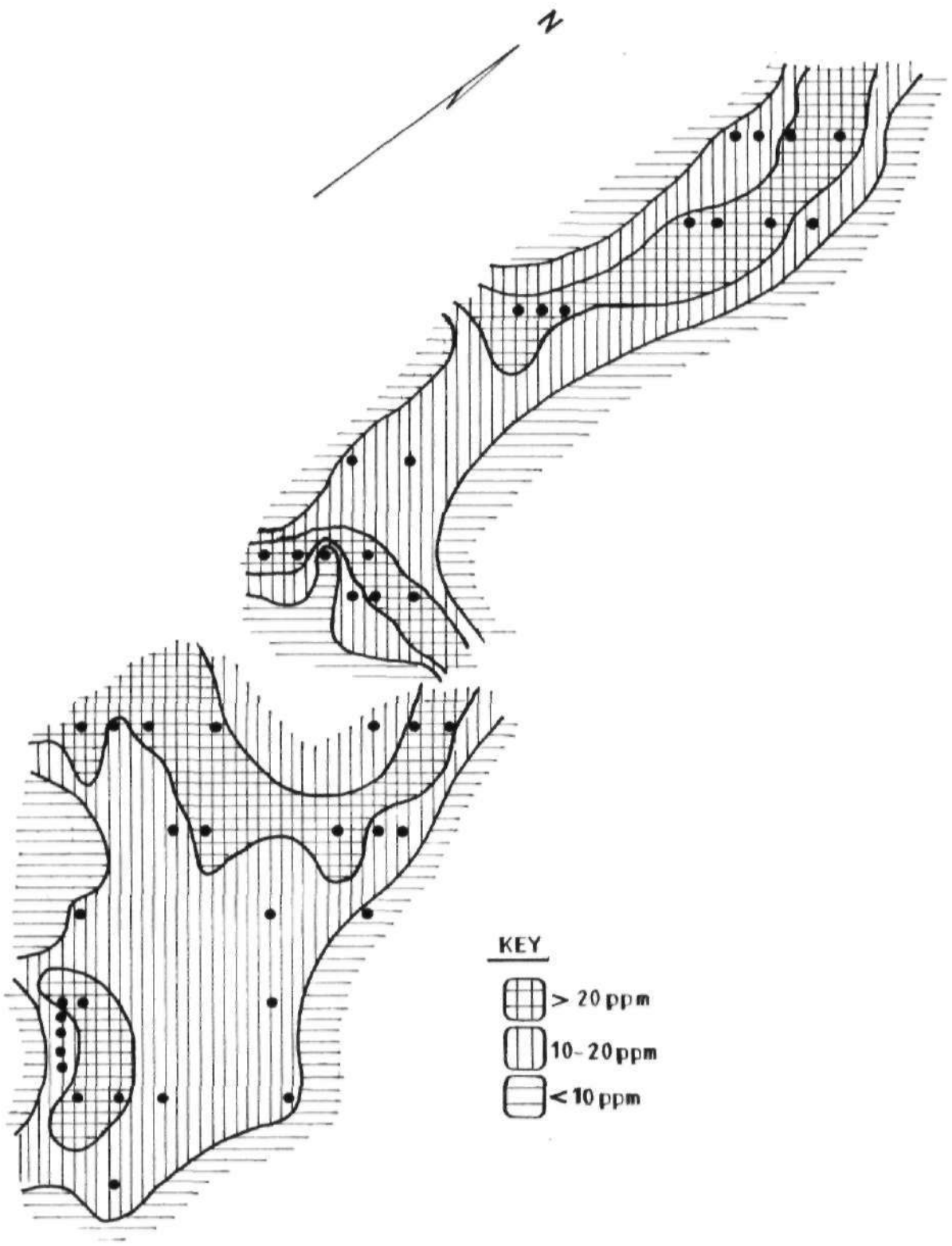
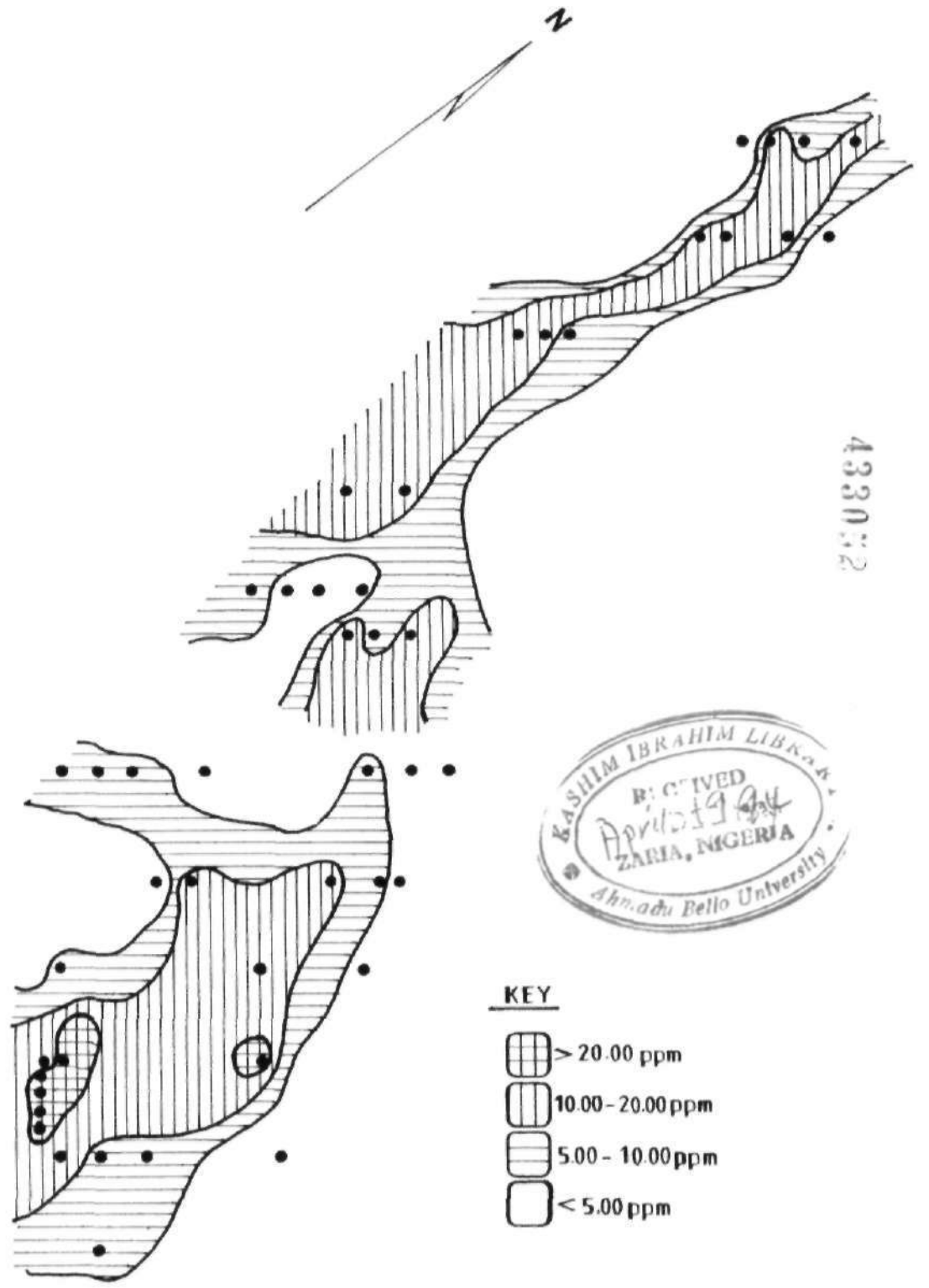


Fig. 5.21. Areal distribution of Nickel (Ni) at Dinya-Koking mineralized zone.



433052
KASHIM IBRAHIM LIBRARY
RECEIVED
April 19 94
ZARIA, NIGERIA
Ahmadu Bello University

Fig. 5.2m. Areal distribution of Uranium (U) at Dinya-Koking mineralized zone.

The average value (clark value) for Uranium in rhyolites is 5 ppm (Ewart et. al., 1968) and 4 ppm (Vinogradov 1962) for granites. The average composition of rhyolites and porphyritic biotite granite in the study area indicate higher values than the clark values in similar rocks.

Figure (5.1m) shows the distribution of Uranium concentration values and figure (5.2m) shows the areal distribution of uranium in the mineralized zone. Generally the composition of uranium is higher in the rhyolites than in the granites, with the highest values obtained along the contact of the two rocks.

5.3 Distribution trends

Elements distribution

The distribution of elements in the delineated alteration zones of the host rocks indicate that certain elements were enriched while others were depleted (Table 5.3 and 5.4). The removal or addition of these elements in the wall rocks was caused by the ingress of mineralizing fluid, which was capable of depositing or removing certain elements at prevailing p.H. and E.h. conditions. A clear picture of depletion and enrichment in the altered zones is shown in fig. (5.3 and 5.4) for the porphyritic biotite granite and fig. (5.5 and 5.6) for the rhyolites.

Elements	Unaltered porphyritic biotite granites	Mildly altered porphyritic biotite granite	Intensely altered porphyritic biotite granite	A	B
CaO	0.565%	0.03%	0.28%	-0.285	-0.285
MgO	0.272%	0.011%	0.175%	-0.261	-0.097
FeO	1.935%	3.245%	1.940%	+1.31	+0.005
K_2O	1.590%	0.161%	0.231%	-1.431	-1.359
Na_2O	1.546	0.158%	0.286%	-1.388	-1.260
P_2O_5	0.124%	0.115%	0.055%	-0.009	-0.069
TiO_2	0.02%	0.20%	0.04%	-0.18	-0.02
MnO	0.039%	0.005%	0.007%	-0.034	-0.032
Zn	15.75 ppm	19.75 ppm	18.7 ppm	+4.0	+3.05
Cu	13.5 ppm	11 ppm	17.4 ppm	-2.5	+3.9
Cr	37.5 ppm	60.0 ppm	37.4 ppm	+22.5	-0.5
Ni	10.0 ppm	17.5 ppm	12.4 ppm	+ 7.5	+2.4
U	14.35 ppm	53.6 ppm	29.0 ppm	+39.3	+14.7

Table 5.3 Loss and gain in the mildly and intensely altered porphyritic biotite granite. (Average values)

(A) Losses and gains in the mildly altered zone in % and ppm.

(B) Losses and gains in the intensely altered zone in % and ppm.

Elements	Unaltered rhyolites	Mildly altered rhyolites	intensely altered rhyolites	C	D
CaO	0.206%	0.038%	0.197%	-0.168	-0.009
MgO	0.131%	0.019%	0.114%	-0.112	-0.017
FeO	2.946%	5.686%	4.504%	+2.74	+1.558
K_2O	0.108%	0.113%	0.136%	+0.005	+0.028
Na_2O	0.232%	0.088%	0.175%	-0.144	-0.057
P_2O_5	0.123%	0.141%	0.133%	-0.018	+0.010
TiO_2	0.04%	0.05%	0.05%	+0.01	+0.01
MnO	0.005%	0.018%	0.016%	-0.013	+0.011
Zn	39.58 ppm	37.8 ppm	59.25ppm	-2.38	+19.67
Cu	13 ppm	20.18 ppm	25.8 ppm	+7.8	+12.8
Cr	68.66ppm	66.75 ppm	60.65ppm	-1.91	+8.01
Ni	14.83ppm	21.0 ppm	19.78ppm	+6.17	+4.95
U	49.6 ppm	51.49 ppm	53.07ppm	+1.89	+3.47

Table 5.4 Loss and gain in the mildly and intensely altered Rhyolites (Average values)

(C) Losses and gains in the mildly altered zone in % and ppm.

(D) Losses and gains in the intensely altered zone in % and ppm

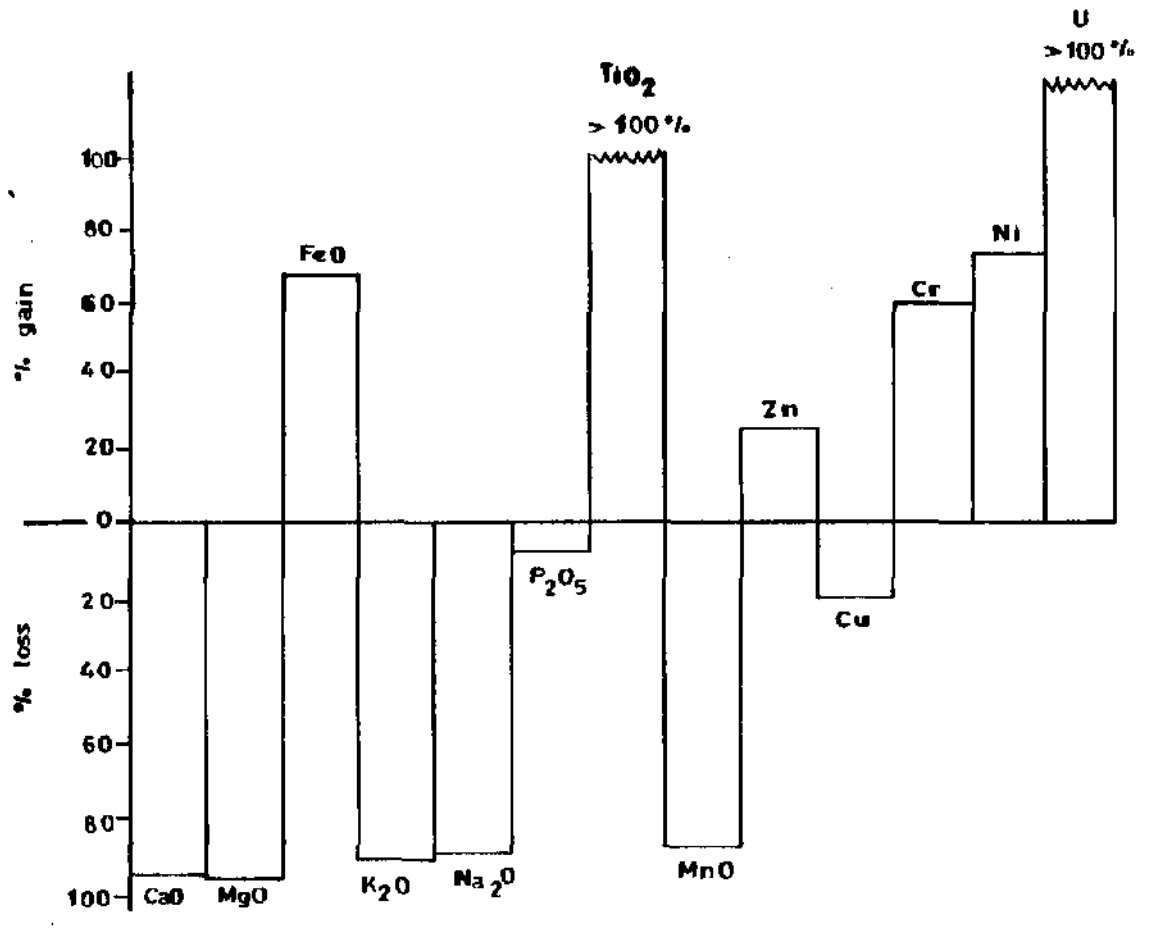


Fig.5.3. Percentage elements loss and gain in the mildly altered porphyritic biotite granite.

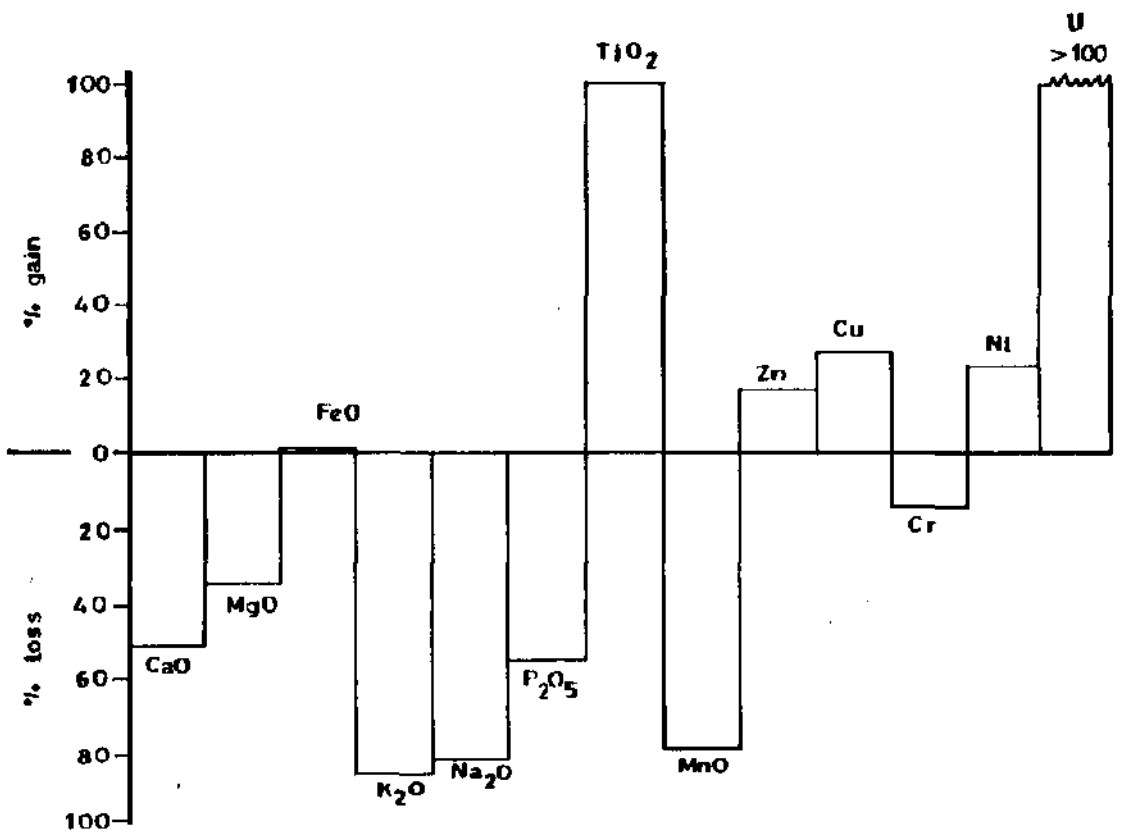


Fig.5.4. Percentage elements loss and gain in the intensely altered porphyritic biotite granite.

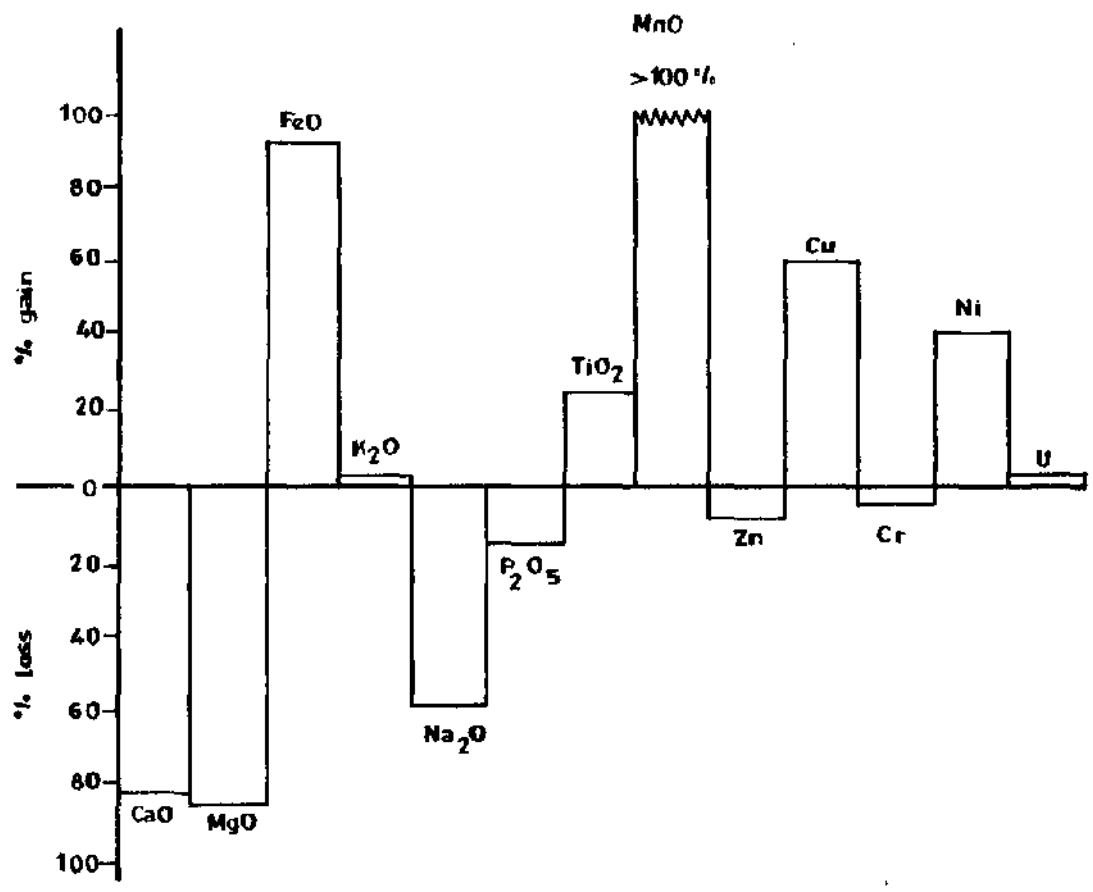


Fig. 5.5. Percentage elements loss and gain in the mildly altered rhyolites.

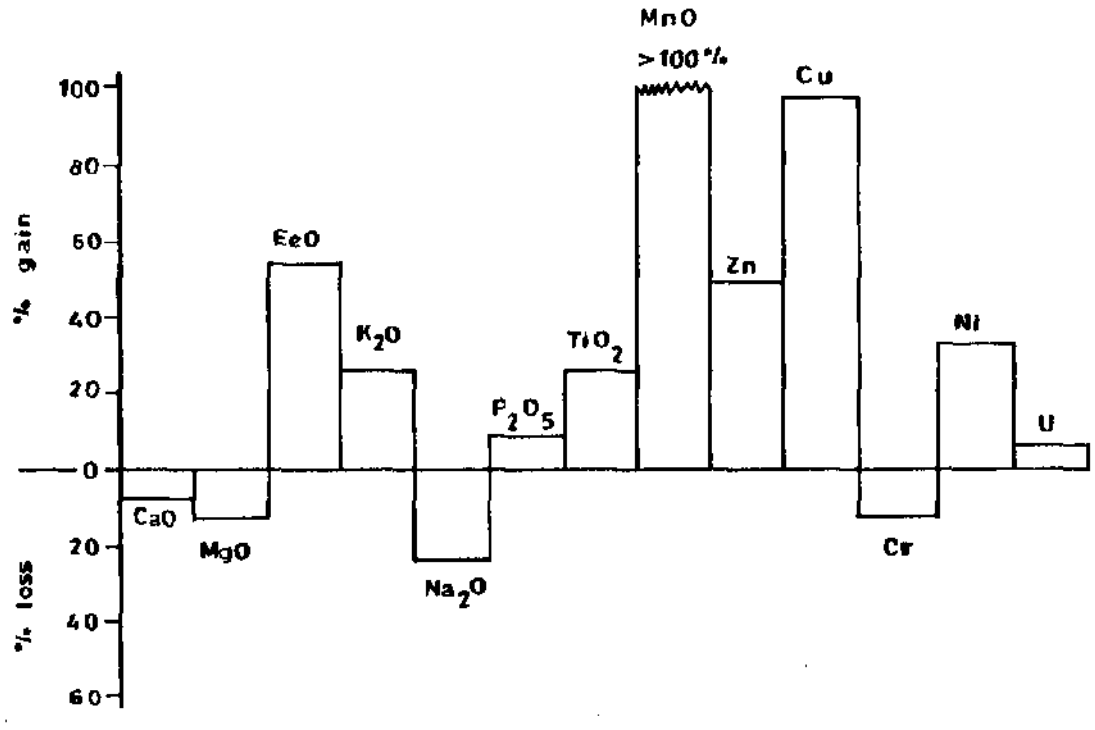


Fig. 5.6. Percentage elements loss and gain in the intensely altered rhyolites.

Depletion and Enrichment trends

Evaluation of elements distribution in the unaltered porphyritic biotite granite against the mildly and intensely altered biotite granite reveal that CaO, MgO, K_2O, P_2O_5, TiO_2, MnO and Na_2O were continuously depleted in the mildly and intensely altered zone. The depletion is however greater in the mildly altered zone. Another trend is the higher enrichment of FeO, Zn, Cu, Cr, Ni and U in the mildly altered zone with slight decrease in the intensely altered zone.

Elements distributions in the unaltered rhyolites compared with the mildly and intensely altered rhyolites reveal that CaO, MgO, Na_2O and Cr were depleted with intensity of alteration. Another trend is the enrichment of FeO, K_2O, TiO_2, MnO, Cu, Ni and U in the altered zones. Within the trend FeO and Ni depleted slightly in the intensely altered zone while K_2O, Cu and U increased steadily. MnO and TiO_2 more or less maintained a constant increase in the two zones. The last trend in the rhyolites is the Zn, and P_2O_5 which depleted in the mildly altered zone and become enriched in the intensely altered zone.

On comparative basis the average values of K_2O, Na_2O, FeO, Cr, Zn and U in the rhyolites are considerably higher than those in the granites. In the case of FeO, Cr and U, the

high values in the rhyolites are comparable to values in the mildly altered zone of the granites. It is also noted that CaO, Na_2O and K_2O values in the unaltered granites are comparatively very high.

Generally FeO, Cu, Ni and U have higher values in granites than their clark values for similar rocks while FeO, MnO, P_2O_5, Cr, Cu, Ni and U have higher values in rhyolites than their clark values in similar rocks.

5.4 Correlation Analysis

The result of correlation, calculated as correlation coefficient ranges from -1 to +1. A correlation coefficient of +1 or close to it indicates a positive correlation while a correlation coefficient of -1 or close to it indicates a negative correlation or inverse relationship with the second variable. A correlation coefficient of zero or coefficient values close to zero indicates little or no dependent relationship with the second variable.

Correlation analyses were done for the population data and the intensely altered host rocks.

Table (5.5) shows the result of correlation matrix from (40) samples of the population data.

	CaO	MgO	FeO	K_2O	Na_2O	P_2O_5	TiO_2	MnO	Zn	Cu	Cr	Ni	V
CaO	1.0000	0.9968	0.0802	-0.5259	-0.8868	-08368	-0.0880	-0.1347	0.0319	0.1335	0.0113	0.1579	-0.0271
MgO		1.0000	0.0855	0.5237	0.8548	-0.0569	-0.0932	-0.1226	0.0447	0.1252	-0.0028	0.1396	-0.0366
FeO			1.0000	0.0661	0.0912	0.4100	0.1304	0.0829	0.02487	0.5462	0.3742	0.8011	0.1671
K_2O				1.0000	0.5051	-0.1582	-0.1624	-0.0480	0.0598	0.0327	-0.1251	0.0688	-0.1519
Na_2O					1.0000	-01124	-0.0904	0.0177	0.0743	0.0498	-0.1531	-0.0331	-0.0985
P_2O_5						1.0000	0.2575	0.0433	0.0208	0.1759	0.4031	0.4293	0.5831
TiO_2							1.0000	-0.1206	-0.1093	0.0686	-0.0093	0.0246	0.1939
MnO								1.0000	0.1200	0.1534	0.1637	0.0959	0.1225
Zn									1.0000	0.2465	0.2131	0.2850	-0.0722
Cu										1.0000	0.2418	0.6012	-0.1021
Cr											1.0000	0.6392	0.5123
Ni												1.0000	0.2427
V													1.0000

TABLE 5.5 - Correlation Matrix of the Population Data.

The matrix result shows a significant positive correlation (>0.80) between CaO, MgO, Na_2O and (>0.5) correlation between CaO, MgO, Na_2O and K_2O. There is also a significant positive correlation (>0.8) between FeO, Ni, and (>0.5) correlation between FeO - Ni, Cr, and Cu. Another positive correlation (>0.5) exists between P_2O_5 - Cr and U. A negative correlation (>-0.5) does not exist between any of the elements.

Table (5.6) shows the result of the correlation matrix obtained from samples of intensely altered porphyritic biotite granite.

The result of the matrix indicates a positive correlation (>0.6) between CaO - MgO, Na_2O, Cu, Cr and U. Another positive correlation (>0.6 exists between FeO - K_2O, P_2O_5, Zn, Cr and (>0.7) correlation between Cr - FeO, Ni, Zn and U. A negative correlation (>-0.5) exists between TiO_2 - Zn, Cr, Ni, FeO and P_2O_5.

Table (5.7) shows the result of the correlation matrix obtained from samples of the intensely altered rhyolites.

	CaO	MgO	FeO	K_2O	Na_2O	P_2O_5	TiO_2	MnO	Zn	Cu	Cr	Ni	U
CaO	1.0000	.9999	.0313	.2428	.9754	.1092	- .2421	.2493	.2938	.9802	.6116	.2608	.7961
MgO		1.0000	.0348	.2506	.9758	.1134	-.2504	-.2434	.2952	.9818	.6144	.2638	.7948
FeO			1.0000	.4782	-.0301	.6063	-.6277	.0227	.9371	.0739	.7983	.9349	.2815
K_2O				1.0000	.3653	.0111	-.4688	.7603	.3181	.4215	.6001	.3275	.4772
Na_2O					1.0000	-0715	-.1489	.0503	.1925	.9871	.5771	.1424	.8493
P_2O_5						1.0000	-.8560	-.4949	.6511	.0739	.4356	.7870	-.1868
TiO_2							1.0000	.0.421	-.5884	-.3053	-.5784	.7384	-.0027
MnO								1.0000	-.2514	-.0636	-.0171	-.2618	.0853
Zn									1.0000	.2842	.8844	.9763	.4484
Cu										1.0000	.6505	.2601	.8183
Cr											1.0000	.8458	7532
Ni												1.0000	.3161
U													1.0000

TABLE 5.6 - Matrix correlation of intensely altered Porphyritic biotite granite.

	CaO	MgO	FeO	K_2O	Na_2O	P_2O_5	TiO_2	MnO	Zn	Cu	Cr	Ni	U
CaO	1.0000	.9988	.3941	.9615	.9628	.0595	.6105	-.1945	-.2973	.1991	.2254	.3274	.4053
MgO		1.0000	.4031	.9550	.9632	.0383	.6005	-.1560	-.2692	.2234	.2293	.3226	.4009
FeO			1.0000	.3583	.2769	.6179	.3818	.5229	-.3989	.6033	.5339	.5743	.5813
K_2O				1.0000	.9062	-.0224	.7578	-.3016	-.3976	.1818	.0711	.2183	.2615
Na_2O					1.0000	-.0295	.6230	-.2872	-.0626	-.0174	.0461	.1227	.2365
P_2O_5						1.0000	-.0587	.1183	-.5163	.1180	.6428	.6912	.7239
TiO_2							1.0000	-.3776	-.2112	-.0743	-.3959	-.2295	-.2091
MnO								1.0000	.1074	.7743	.5322	.3884	.3438
Zn									1.0000	-.4361	-.5118	-.6893	-.5986
Cu										1.0000	.6623	.6476	.5530
Cr											1.0000	.9718	.9653
Ni												1.0000	.9822
U													1.0000

Table 5.7 Matrix correlation of altered rhyolites

The result of the correlation matrix indicate a significant positive correlation (>0.7) between CaO-MgO, K_2O, Na_2O and a positive correlation (>0.5) exists between FeO-P_2O_5, MnO, Cu, Cr, Ni, and U. Another positive correlation (>0.6) exists between TiO_2 - CaO, MgO, K_2O and Na_2O. A negative correlation (>-0.5) exists between Zn - P_2O_5, Cr, Ni and U.

5.5 Principal Component Analysis

The Principal component analysis concerns transformation of variance to covariance of the original data. The covariance is given here as components. The components are grouped into different factors with decreasing order of the percentage variance.

Factor analysis has been extensively used in recent years by geochemists to evaluate geochemical data. This is done to measure the strength of any relationship among the variables and to show the grouping of elements into associations, due to the covariance structure of the original variables as well as the structure of the factors.

Table (5.8) below shows the result of the calculated principal component analysis and the percentage variance.

Component No	Percentage Variance	Cumulative Percentage Variance
1	25.52	25.52
2	24.74	50.26
3	11.93	62.19
4	9.03	71.22

	1st Component	2nd Component	3rd Component	4th Componen
CaO	0.46	-0.22	-0.16	0.01
MgO	0.47	-0.23	-0.16	0.02
FeO	0.28	0.35	0.15	-0.24
K_2O	0.31	-0.22	0.04	0.04
Na_2O	0.41	-0.27	-0.10	0.06
P_2O_5	0.09	0.37	-0.36	-0.01
TiO_2	-0.04	0.13	-0.33	-0.55
MnO	0.00	0.12	0.20	0.55
Zn	0.14	0.12	0.40	0.13
Cu	0.24	0.24	0.36	-0.29
Cr	0.15	0.38	-0.09	0.31
Ni	0.30	0.39	0.14	-0.08
U	0.03	0.29	-0.53	0.32

Table 5.8 Result of the Principal Component Analysis at different percentage variance.

Figure (5.7a) shows the plot between the first and second components. The plot reveals a cluster of CaO, MgO, Na_2O and K_2O in the top left quadrant and a cluster of Fe_2O_3, Cu, Zn, Cr, MnO, P_2O_5, Ni and U on the top right quadrant while TiO_2, falls, in the bottom right quadrant.

Figure (5.7b) shows the plot between the first and third components. The plot produced a cluster of MgO, CaO, Na_2O, Cr, TiO_2, P_2O_5 and U in the top left quadrant and a cluster of K_2O, FeO, Ni, Cu and Zn in the top right quadrant.

Figure (5.7c) shows the plot between the first and fourth component. The plot produced a cluster of Na_2O, MgO, CaO, K_2O, Zn and U in the top left quadrant and a cluster of FeO, Cr, Cu, Ni and P_2O_5 in the top right quadrant. TiO_2 occurs singly in the bottom left quadrant.

Figure (5.7d) show the plot between the second and third component. The plot produced a cluster of CaO, MgO, Na_2O in the bottom left quadrant and K_2O in the bottom right quadrant. P_2O_5, TiO_2 and Cr occur in the top left quadrant and FeO, Ni, MnO, Cu, Zn in the top right quadrant.

Figure (5.7e) show the plot between the second and

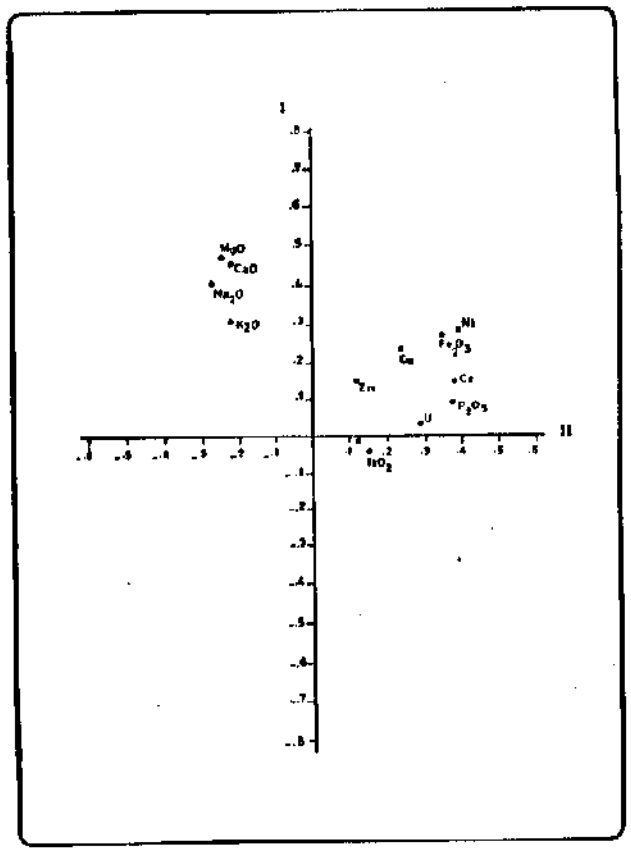


Fig. 5.7a.

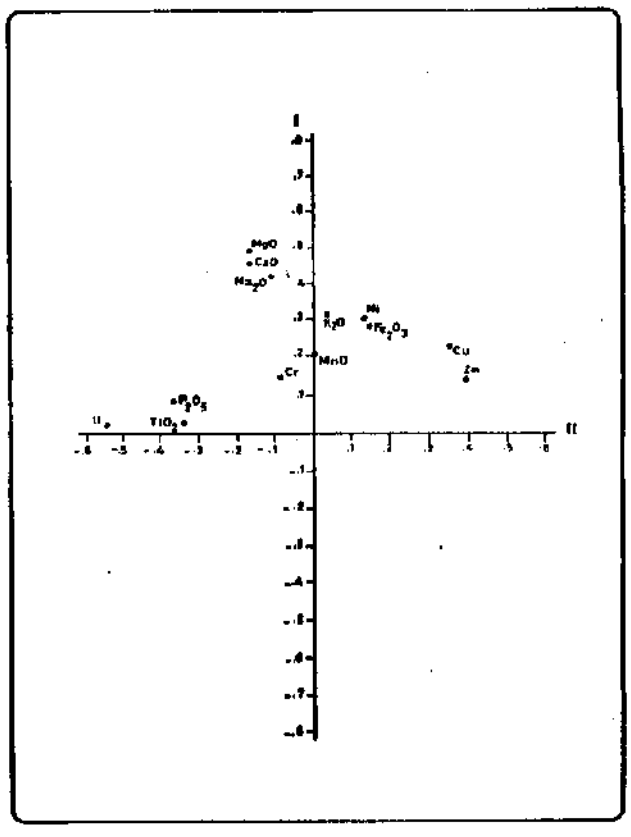


Fig. 5.7b.

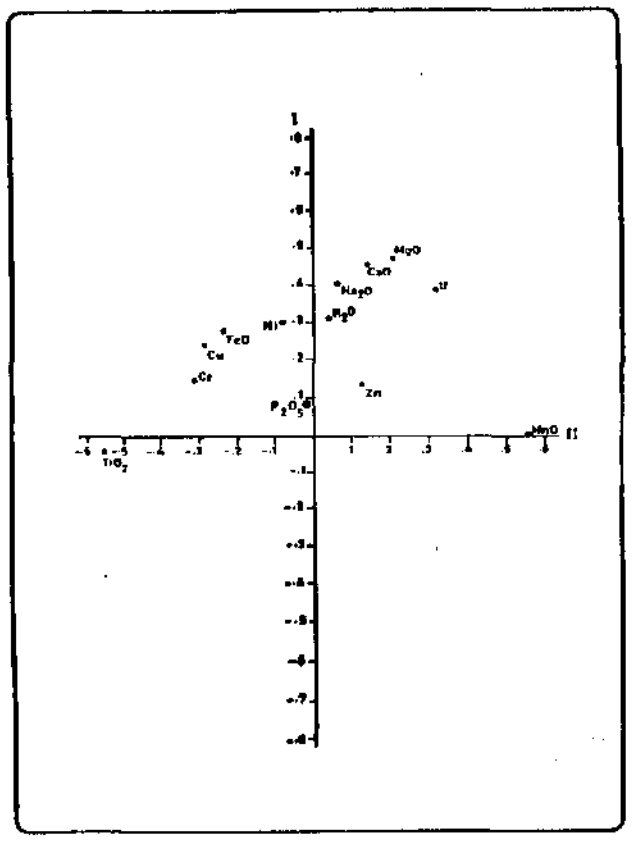


Fig. 5.7c.

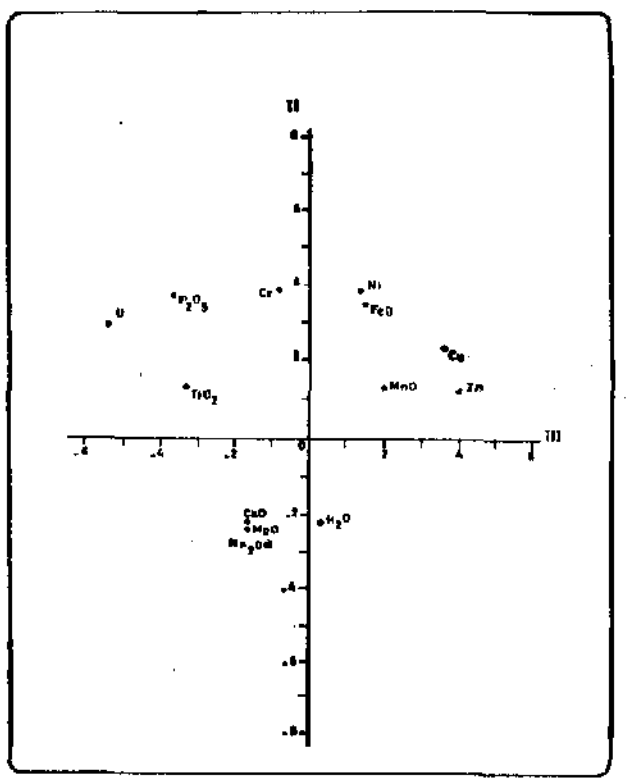


Fig. 5.7d.

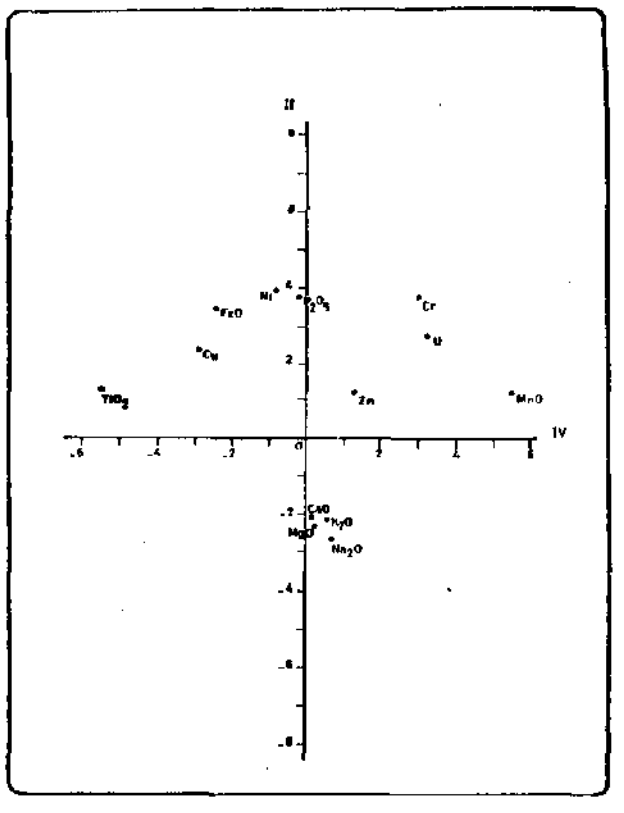


Fig. 5.7e.

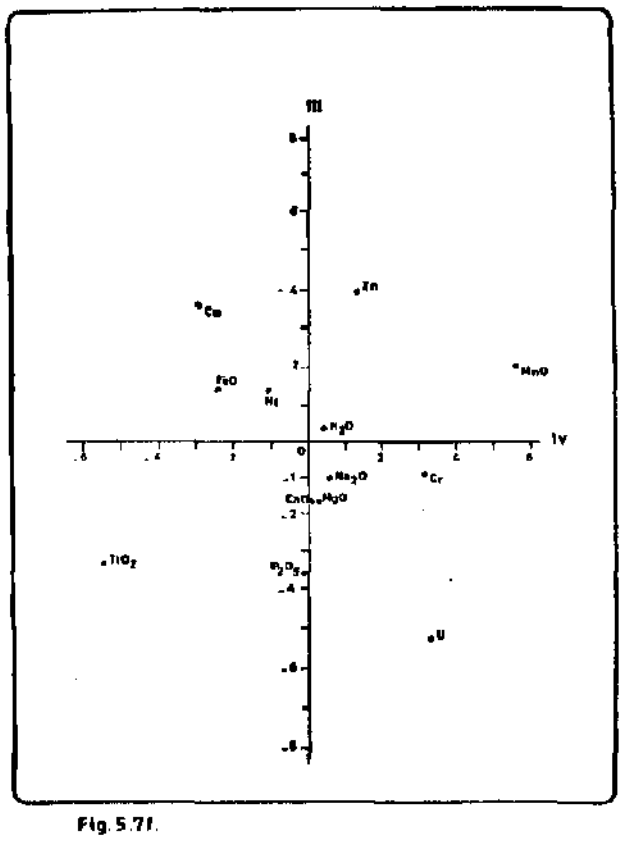


Fig. 5.7f.

fourth components. The plot produced a cluster of Cu, FeO, Ni, TiO_2 and P_2O_5 top in the left quadrant and Zn, Cr, U and MnO in the top right quadrant, while CaO, MgO, Na_2O and K_2O occur in the bottom left quadrant.

Figure (5.7f) shows plots for the third and fourth components. The plot produced Cu, Ni and FeO in the top left quadrant and Zn, MnO and K_2O in the right top quadrant while, P_2O_5 and TiO_2 occurs in the bottom left quadrant and CaO, Na_2O, MgO, Cr and U in the bottom left quadrant.

Element Association

Plots of the factors measure the strength of relationship between the elements and give rise to element associations.

Factor I

MgO-CaO-Na_2O-K_2O Association. The association is due to lithological factors and describe the rock forming minerals group. The association is similar to the depletion trend obtained from the population data. The association indicates an oxidizing environment in which the elements were removed.

Factor II

P_2O_5-U Association is a recurrent association in some of the plots. The highest factor loading is however recorded in the second factor. This association indicates mineralization. FeO-P_2O_5-Ni association is also a common association in the plots with the highest factor loading (>.35) in the second factor, the association indicates enrichment of the elements during mineralization.

Factor III

Cu-Zn Association, shows a high factor loading (>.35) in the third factor, the association is attributed, to the rhyolites and its volcanogenic origin.

The P_2O_5 - U association also has a strong relationship due to the same mineralization factors.

Factor IV

Factor IV reveals very weak association of FeO-Ni and CaO-MgO-Na_2O-K_2O.

5.6 Comparison between correlation and enrichment-depletion trends

Results of correlation analysis show that correlation exists between CaO-MgO, Na_2O and K_2O. Other elements correlation are FeO-Cr, Ni and U and the P_2O_5 - U.

The first correlated elements compare with the depletion trend in the elements while the second trend is similar to the enrichment trend. The correlation of P_2O_5 and U which falls both in the depletion and enrichment trend is as a result of secondary processes.

Results obtained from correlation of intensely altered porphyritic biotite granite show correlation between CaO-MgO,Na_2O, Cu, Cr and U. Other correlations are those of K_2O - P_2O_5, Zn, Cr and Ni and between Cr - Ni, Zn; FeO and U.

From the correlation results obtained from the intensely altered granite, the first correlation shows similarity to the depletion trend in granite. The absence of K_2O in the correlation signifies intermediate reaction between the mineralizing fluid and the wall rock as K_2O went through exchange reaction with Na_2O. The presence of Cu, Cr and U in the correlation indicates initial leaching of the elements in the early stage of interation between the mineralizing fluid and the wall rock. The second and third correlation, all represent the enrichment trends which were due to the mineralizing fluid.

Correlation results from the intensely altered

rhyolites had correlation of CaO-MgO, K_2O and Na_2O and another correlation of TiO_2-MnO, FeO, and Cr.

The first correlation compares with the CaO, MgO, Na_2O and Cr depletion trend, except for the absence of K_2O and the presence of Cr in the depletion trend. Comparison of the two trends shows that K_2O was enriched and chromium which had rather high values in the rhyolites was removed instead.

The enrichment trend in the rhyolites compares with the second correlation and confirms, that K_2O, TiO_2, MnO, FeO, Cu, Cr, Ni and U were enriched. The presence of Cr in this trend is explained by the fact that though Cr was removed from the rhyolites it was still supplied by the mineralizing fluid.

5.7 Comparison of element association with element correlation and enrichment-depletion trends

A comparison of the different elements trends obtained by different approaches may perhaps shed more light on elements interrelationship.

Table (5.9) presents all the element trends for a quick comparison.

enrichment-depletion trend	Elements	Correlation	Elements Association					
			Factor 1 & II	Factor 1 & III	Factors I & IV, II & III	II & IV	III & IV	
Sandstones	-	Ca0-Mg0,Ma_2O,K_2O	Mg0-Ca0-Ma_2O-Cr	Ma_2O-Mg0-Ca0-$-Ti0_2$ -P_2O_5-U	Ca0-Mg0-Ma_2O -K_2O-Zn-U	Ca0-Mg0-Ma_2O	Ca0-Mg0-Ma_2O	Ca0-Mg0-Ma_2O
Rhyolites	Ca0-Mg0,Ma_2O,K_2O,Cr	Ca0-Mg0,Ma_2O,K_2O	-	-	-			
			$Ti0_2$-Ca0-Mg0,K_2O Ma_2O					Depletion trends
Granites	Ca0-Mg0,Ma_2O,K_2O	Ca0-Mg0,Ma_2O,Cu, Cr and U.						
		P_2O_5,$Ti0_2$, Mn0						

TABLE 3.9 Combination of elements association, elements correlation and enrichment-depletion trends.

enrichment-depletion trend	Elements	Correlation	Factor I & II	Elements Association Factor I & III	Factors I & IV,	II & III	II & IV	III & IV
Sandstones	-	Fe0-Ni,Cr and Cu	Fe0-Cr-Cu-Zn	K_2O-Fe0-Ni-Cu- P_2O_5-U	Fe0-Cr-Cu-Ni	Fe0-Cr-Ni,	Fe0-Ni-P_2O_5	Cu-Zn, Fe0-Ni
Rhyolites	Fe0,K_2O,Ti0,Mn0,Cu Ni and U	Fe0-P_2O_5,Mn0,Cu,Cr, Ni and U	-	-	-	-		
Granites	Fe0,Zn,Cu,Cr,Ni and U	Fe0,K_2O,P_2O_5,Zn,and Cr						Enrichment trends
		Cr-Fe0,Ni,Zn and U	-	-	-	-		

TABLE 3.9 Combination of elements association, elements correlation and enrichment-depletion trends.

enrichment-depletion trend	Elements	Correlation	Elements Association Factor I & II	Factor I & III	Factors I & IV,	II & III	II & IV	III & IV
Sandstones	-	Ca0-Mg0,Ma_2O,K_2O	Mg0-Ca0-Ma_2O-Cr	Ma_2O-Mg0-Ca0-$-Ti0_2$ -P_2O_5-U	Ca0-Mg0-Ma_2O -K_2O-Zn-U	Ca0-Mg0-Ma_2O	Ca0-Mg0-Ma_2O	Ca0-Mg0-Ma_2O
Rhyolites	Ca0-Mg0,Ma_2O,K_2O,Cr	Ca0-Mg0,Ma_2O,K_2O	-	-	-			
			$Ti0_2$-Ca0-Mg0,K_2O Ma_2O					Depletion trends
Granites	Ca0-Mg0,Ma_2O,K_2O	Ca0-Mg0,Ma_2O,Cu, Cr and U.						
		P_2O_5,$Ti0_2$, Mn0						

The first element association CaO-MgO-Na_2O-K_2O, which is due to factor I is similar to the depletion trends in granites and the correlation of the same elements in the population data. The association infact compares with all the depletion trends and correlation of similar elements except for the absence of K_2O and presence of P_2O_5, TiO_2, MnO, Cu, Cr and U. The presence of these elements also appears in the plot of factor I and III and factor I and IV.

The other association P_2O_5 - U and FeO-Cr-Ni due to factor II and Cu-Zn due to factor III all compare very well w similar elements correlation and enrichment trends.

Chapter 6

DISCUSSION, CONCLUSION AND RECOMMENDATION

6.0 DISCUSSION

The metallogenic features of the Archean to Proterozoic crystalline basement of Nigeria have been discussed and attempts made by many worker's, Black (1980); Woakes and Olade (1988); and Olade and Woakes (1988); and many others to relate the distribution and origin of mineral deposits within the West African shield to major tectonic features. According to (Woakes and Olade 1988) the early Proterozoic of the Nigerian basement was characterized by gold, diamond, and manganese while tin, molydenum, tungsten, Niobium-tantalum and uranium metals were prodominantly of Proterozoic age.

According to Carter et. al., (1963); Oyawoye (1970); McCurry (1970) the granites in the study area are Proterozoic in age being product of the Pan African orogeny. The volcanic rocks around the study area are product of the continous spread of Cretaceous to Recent volcanic activity that covers the north-eastern part of the Nigerian basement, while the rhyolites in the study

area are Cenozoic in age. Wright (1976); Fitton (1987) and are clearly different from the Cretaceous volcanicity that was confined to the Benue trough.

The Structural setting of the basement rocks and rhyolites confirm that the rhyolites are younger and were emplaced later in the Proterozoic basement rocks. The shear zone, in the basement rocks being the lineaments along which the rhyolites were emplaced. Mineralization in this area is spatially related to the rhyolitic bodies especially along the shear zones and contact of the rhyolites and granites.

Nash et. al., (1981) identified that vein type deposits include all uranium deposits that occupy relatively simple faults and fracture, zones often extending to depth of 300 - 1500 metres in a variety of host rocks. In another view Ojo (1980) described certain uranium deposits as occurring in Precambrian rocks, particularly Proterozoic rocks near sedimentary basins. He pointed out that they are emplaced in shear zones in granites and metasediments with or without volcanics or basic bodies that usually form traps for uraniferous solutions. He concluded that these deposits are different from vein type deposits, both in size and origin. From

the two models, the structural setting of the mineralized area fits more closely with the model described by Ojo (1980).

6.1 Origin of mineralizing fluids

Evidences of leaching along the shear zones and contact of the rhyolites and granites, coupled with depletion of Ca, Mn and concentration of Cu and Ni indicate that the hydrothermal solution responsible for mineralization was ascending.

The origin of the mineralizing hydrothermal solution is associated with the volcanic activity which was the principal factor responsible for initial generation of hydrothermal solution during or/and after the emplacement of the rhyolitic bodies. The hydrothermal solutions were formed from basaltic magma, first by separation of the liquid fraction of the melt by gravitation and crystallization differentiation.

On the way through the fissure system the supercritical liquid fraction became cooled and condensed to hot aqueous hydrothermal solution. After formation of hydrothermal solution, Circulation around pore spaces became impossible. At this stage the deep seated

fractures, together with the shear zones provided channel ways along which the hydrothermal solution circulated to the surface.

6.2 Sources of Uranium and other Metals

Due to the leaching of the wall rocks, some certain elements were depleted while others were enriched. The two possible sources of uranium and the metals are:

(i) Through concentration of uranium and the siderophile elements, FeO, Ni and Mn in the termal fraction of the magma and

(ii) Through leaching of uranium and other Lithophilic elements mg, K_2O, Cr, Ti and the chalcophiles Cu and Zn from the crustal rocks.

The presence of Feo, TiO_2, Mno, Cu, Ni, Cr, Zn, P_2O_5 and U in the mineralizing fluid as indicated by the enrichment trend could be linked with the origin of the mineralizing fluid. There is a tendency for uranium and other metals to be concentrated in the later fraction of the magmatic differentiation. Uranium is quite mobile in metasomatic reactions, the transport of uranium to the surface was then suitable under a high fco_2 and low p.H. condition.

Uranium is lithophilic in nature, this explains its association with Cr, Mno, and (Fe). The presence of Feo and Ni together with uranium in the mineralizing fluid points to the magmatic origin of the mineralizing fluid. The association of uranium with the lithophile on the other hand, however draws attention that uranium and the associated elements were concentrated not only by differentiation.

The other source of uranium and the other metals could be associated with the basement granites, which have high values of U, Ni, Cu, and Feo above Clark values for granites. The leaching of Uranium and other elements from the granites is generally attributed to the supercritical solution which diffused and circulated in the pore spaces and scavaged uranium and other metals.

Generally the felsic minerals contain much less uranium but the presence of biotite with (1-60ppm U) and accessory minerals of zircon with (100-6,000 ppm U), allanite (30-100 ppm U) and apatite with (5-150 ppm U) (all values from Clark et. al., (1966); Rogers and Adam (1967) are identified as the minerals in the granite from which uranium was leached. Due to the chemical decomposition of the granites, the other secondary sources

of uranium and other metals in the mineralizing fluid is linked with the granites. Woakes and Olade (1988) proposed that mineralization in the Proterozoic (and in later times) were derived from crustal sources through deep seated structures as passage ways that mobilized metals in the adjoining rocks.

The elements correlation, depletion-enrichment trends and elements association all collaborate the fact that the mineralizing hydrothermal solution itself was rich in some elements which point to its association with a magmatic source. The trends also show a depletion trend which also point to the fact that the solution was ascending and was capable of leaching and concentrating uranium and the other metals.

The transport of these elements was possible under the oxidation nature of the hydrothermal solution and the metasomatic reactions that accompanied its upward movement. Deposition of uranium and the metals was primary due to changes in p.H. and E.h. conditions that prevailed at the surface. The conditions were due to the presence of hematite and reduction of fCO_2 fugacity. Deposition of uranium itself was achieved by reduction of pitchblende from the mineralizing fluid. This was

accomplished by oxidation of reduced iron in the wall rock and equilibrium of hematite with the mineralizing solution. The role of hematite in the reduction of uranium has been cited in many works. Rich (1977), Ojo (1980), Nash et. al., (1981). There was also a preference of deposition of uranium and other metals in the rhyolites due to its basic composition.

6.3 CONCLUSION

The geological setting of the Dinya-Koking mineralization is found to occur in a variety of host rocks. The setting suggests that the rhyolites were emplaced into the granites along lineaments. As regards the Structural setting the presence of structures along which fluids circulated in the mineralized zone is similar to what is obtained in classical uranium Vein-type deposits.

The origin of mineralizing solution in the study area is associated with the volcanic activity in the area. Though hydrothermal solution in vein type deposits may be generated from basaltic magma, their upward movement are not accompanied by emplacement of solid rocks. The difference in origin between the deposit in the study area and a classical vein type deposit is manifested mainly by

emplacement of rhyolites during or before the circulation of hydrothermal solutions.

In terms of mineralogy and chemistry, pitchblende deposition was accompanied or preceded by deposition of quartz and hematite. There was formation of carbonate, nickel and copper minerals with a high to anomolous concentration of Cu, Zn and Ni in the mineralized rocks. The mineralogy and chemistry of the mineralization under study is therefore similar to vein type deposits.

The two fundamental differences between the vein type uranium deposit and the mineralization under study lie largely in the size and emplacement of rhyolites along the shear zones.

In view of the writer, the vein type uranium deposit is similar to the deposit in the study area in many aspects even in origin. The writer however agrees with (Ojo 1980) that certain types including the one under study are vein-like, since they are not exactly vein type deposits.

6.4 RECOMMENDATION

Further work on the Dinya-Koking mineralization is recommended to include a wider spectrum of element analysis that could not be analysed in the present work due to lack of certain facilities. The study of polished sections will also be important to reveal the mineralogy of uranium and those of other elements.

Studies on fluid inclusion and isotopic studies are also recommended in order to understand the history of mineralization and nature of mineralizing fluid. Drilling and study of core samples would be necessary to evaluate the extent and depth of mineralization

REFERENCES

Ahren's L.H.(1954): Lognormal distribution of the elements. Geochim: Cosmochim acta 5: 49-73: 6, 121-131.

Ajayi, C.O. and Ajakaiye D.E.(1981): The origin and pecularities of the Nigerian Benue trough: another look from recent gravity data obtained from the middle Benue. Tectonophysis 80, 285-303.

Badlam, J.P.N.(1975): Mineralogy, parogenesis and origin of the Ag.-Ni-Co. Arsenide mineralization, Camsell River N.W. Canada: Mineralium Deposita Vol. 10, p.153-175.

Bawden, M.G. and Tuley, P. (1966): The Land Resources of Southern Sarduana and southern Adamawa province Northern Nigeria. In: Min overseas, Dev. Land Resources div. Land Resources study No. 7.

Baumann, L. (1976): Introduction to ore deposits. Scottish Academic Press Ltd.

Beck, L.S. (1969): Uranium deposit of the Altabaska region: Saskatchewan mineral resources report. 126, pp.139.

Benkhill, M.J. (1982); Benue trough and Benue Chain. Geol. mag. 1112, 155-168.

Beus, A.A. and Grigorian S.V. (1977) Geochemical Exploration methods for mineral deposits: Ed. A.A. Lovison, Applied publishing Ltd. Wilmette, Illinois, 287p.

Black, R. (1980): Precambrian of west Africa Episodes V. 1980. No. 4p.3.8.

Bowden, P., Bennett, J.N., Kinnaird, J.A., Whitley, J.E. Abaa, S.I. Penelope, K.H. (1981).
Uranium in the Nigeria-Nigeria Younger Granite province In mineralogical Mag. Vol. 44, pp.379-89.

Boyle, R.W. (1961. The geology, Geochemistry and origin of the gold deposit of the yellow knife district: Geol. surv. can mem. 310, 193p.

Boyle, R.W. (1979b) Geochemistry overview; In Geophysics and geochemistry in the search for metallic ores: P.J. Hood, Ed. Geol. Surv. Canada. Econ. Geol. report 31, p.25-31.

Burke, K.C. Dessauvagie, T.F.J. and Whiteman, A.J. 1970; Geological history of the Benue valley and adjacent areas. In African geology. Ed. Dessauvagie T.F.J. 1970. p.187-206.

Carter, J.D.,Barber, W., Tait, E.A. (1963). The geology of part of Adamawa, Bauchi and Bornue province in Northern Nigeria. Geol. Surv. Nigeria, Bull. NO. 30

Chukwu-Ike, I.M. (1977): Regional photogeological interpretation of the tectonic features of the central Nigerian basement complex -a statistical imagery based study. (Unpublished Ph.D. thesis. University of London).

Clark, S.P. Peterman, Z.E. and Heier (1966): Abundance of uranium, thorium and potassium: In: Clark S.P. Jr. ed. Hanbook of physical constants Revised edition, geol soc. American mem. 97, 521-541.

Cratchley and Jones, (1965): An interpretation of the geology and gravity anomalies of the Benue valley Nigeria. Overseas geol. surv. geophys paper No. 1.

Dunlop, H.M. (1983): Strontium isotope geochemistry and potassium-argon studies on volcanic rocks from the Cameroon Line. West Africa. Ph.D. thesis University of Edinburgh (Unpublished).

Earth material 1971; Open University Press.

Elegba, S.B. Okujeni, C.D. and Mustapha, A.O. (1988); Geobotanical exploration based on bark samples from savanna trees - feasibility study. Uranium 4pp. 219-225.

Ewart, A. (1968): Trace and minor element geochemistry of the volcanic rocks, Central North Island, New Zealand. In: Handbook of Geochemistry Vol.I and II Wedepohl, K.H. 1978.

Falconer, J.D. (1911): The geology of the plateau tinfields. Bull. geol. Surv. Nigeria. No. 1.

Farrington, J.L. (1952). A primary description of the Nigerian lead-zinc field. Econ. geol. 47, 583-608.

Fitton, J.G. (1987): The Cameroon Line, West Africa: A comparison between oceanic and continenetal alkaline volcanism In: Alkalini igneous Rocks Ede Fitton and Upton, B.G.J. Geol. Soc. Special publication No. 30, pp.273-291.

Funtua, I.I. (1988): The geology and Genesis of uranium mineralization at Kanawa, Gubrunde Horst N.E. Nigeria. M.Sc. Thesis, Ahmadu Bello University (unpublished).

Funtua, I.I., Okujeni, C.D., Abaa, S.I. and Eleqba, S.B. (1992a). Geology and genesis of uranium mineralization at Kanawa, Gubrunde horst N.E. Nigeria. In Nigeria Journal of mining geol. Vol. 28. No. 1.

Funtua, I.I., Eleqba, S.B., and Mustapha, A.O. (1992b): Biogeochemical methods applied in uranium exploration. In: Nig. journal of Min. Geol. Vol. 28. No. 2

Garret, R.M. and Christ, C.L. (1959): Behaviour of uranium minerals during oxidation. U.S. Geol. Surv. Prof. paper 320, pp.81-89.

Gayer, K.H. and Leider, H. (1955): The solubility of uranium trioxide UO_2. H_2O, in solution of hydroxide and perchloric acid at $25^{O}C$. Journal Amer. Chem. Soc. 77, 1448-1450.

Grant, N.K., Rex, D. and Freeth, S.J. (1972): Potassium-argon ages and strontium isotope ratio measurement from volcanic rocks in Northeastern Nigeria. Contr. Mineral Petrol. 35 pp. 277-92.

Green, I. (1959): Geochemical tables of the elements for 1959, Geol. Soc. Am. Bull. 70, 1127-1184.

Holland, H.D. (1965): Some application of thermochemical data to problems of ore deposits II. Mineral assemblage and composition of ore forming fluids Econ. Geol. 60, 1101-1166

Hasteller, P.B. and Garrel, R.M.(1962): Transformation and precipitation of uranium and Vanadium in low temperatures with special reference to sandstone uranium deposits. Econ. Geol. Vol. 57, p.137-169.

Hubert, L.B. (1979): Geochemistry of hydrothermal ore deposits. 2nd ed. John Wiley and Sons., Inc.

Lancelot, J.R., and Maurin, J.C. (1985): Occurrence of Upper Jurassic and Neogene uranium mineralization in N.E. Nigeria as indicated by u/pb dating:13th colloqium of African geology. St. Andrews Scotland.

Longmuir, D.(1978): Uranium solution, mineral equilibra at low temperatures with application to sedimentary ore deposits. Geochim et. Cosmochim Acta, V.42, p.527-570

Maurin, J.C. Lancelot, J.R. (1987): Origine des mineralization de pb-Zn de la Vallaee de la Benoue. (Nigeria) d'apres la composition en pb des galenas et de L'anceissan miner. deposita 22 pp.99-108.

McCurry, P. (1970): The geology of degree Sheet 21 (Zaria) M.Sc. Thesis, Ahmadu Bello University (Unpublished)

McCurry, P. (1976): The Geology of the Precambrian to Lower Proterozoic rocks of Northern Nigeria - A review. In Geology of Nigeria (ed. Kogbe C.A.) pp.15-59. Elizabethan Pub. Co.

Mieseh, A.I. (1977): Log transofmations. Maths. Geol. 9, p.191-198.

Miller, L.J.(1958): The Chemical environment of Pitchblende. Econ. Geol. 53, 531-545.

Nash, J.T., Granger, H.C. and Adams, S.S. (1981): Geology and Concept of Genesis of important types of uranium deposits Econ. geol. 75th Ann. Vol. pp.63-116.

Nockolds, S.R. (1954): Average chemical composition of some igneous rocks, Geol. Soc. Am. Bull. 65, p.1007-1032.

Ofoegbu, C.O. (1985). A review of the geology of the Benue trough; Nigeria. In: Journal of African Earth Sciences Vol. 3 No. 3 (ed. Kogbe, C.A.).

Offodile, M.E. (1976): A review of the geology of the Cretaceous of the Benue trough in: Geology of Nigeria (ed. Kogbe, C.A.) Elizabethan Press Lagos.

Ogunleye, P.O. (1991): Geology and Geochemistry of Zona uranium Mineralization and Laboratory benefication study of uranium ore from Kanawa, N.E. Nigeria.

Okeke, P.I. (1980): Petrology of igneous and metamorphic rocks in the area around Awazo, N.E., Nigeria. M.Phil Thesis. University of Edinburgh (unpublished).

Okujeni, C.D. (1987): Biogeochemical investigation into possible use of leaf and bark samples of some Savanna trees in prospecting for uranium in the Upper Benue trough, Nigeria. Nig. Journ. Scientific vol. I No. 1.

Okujeni, C.D., Funtua, I.I., Ogunmoduwa, O., Baba, I. and Edegbo, S. (1988). A geochemical orientation survey of uranium in the Peta Syncline and Gubrunde horst, Upper Benue trough, Nigeria. Nig. journal. Scientific research vol. I. No. 2.

Olade, M.A. (1976): On the Genesis of lead-zinc deposits in Nigeria Benue rift (aulocogen): A reinterpretation Nig. Journal min. geol. 13. pp.20-27.

Olade, M.A. and Woakes, M. (1988): Geotectonic evolution and tectonic features of the West African Shield. In. International Meeting on Proterozoic Geology and high grade terrains.

Olatunji, J.A. Cuff, C., (1977): Physiochemical characteristic of chlorite wall alteration. A North Queensland Example. In Abstract volume of preceeding and presidential address; 13th Ann Conf. of Nigerian Mining, geological and metallurgical society.

Ojo, O.M. (1980): Prospects of finding uranium deposits in Nigeria: Journal min. geol. vol. 17, pp.1-2.

Oshin, I.O. (1984): Distribution of uranium and thorium in the basement complex rocks of S.W. Nigeria. Nig. Journ. Min. Geol. Vol. 21. Nos. 1 & 2:27-33.

Oshin, I.O. and Rahaman, M.A.(1986). Uranium favourability study in Nigeria, journ. African earth Science. Vol.5,No. 2. 167-175.

Oyawoye, M.O. (1970). The Basement complex of Nigeria. In: African geology (ed. Dessauvagie, T.F.J. and Whiteman A.J.) Ibadan Univ. Press.

Reyment, R.A.(1965). Aspects of the Geology of Nigeria Ibadan University Press, pp.133.

Rich, R.A., Holland, H. D. and Peterson, U. (1977): Hydrothermal uranium deposits. Elsevier Scientific Publishing Co.

Riley, J.P. (1958): The Rapid analysis of Silicate rocks and minerals, Anal Chim Acta 19, p.413-428.

Robinson, B.W. and Ohomoto, H. (1973); Mineralogy, fluid inclusions and stable isotopes of the Echo-bay, U-Ni-Ag-Cu deposits, Northwest territories, Canada; Econ. geol. v. 68. pp.635-656.

Roger, J.J.W. and Adam, J. (1967); Uranium in: Wedpohl, K.H. ed, Handbook of geochemistry, v. 2. pt. Chapter 92 pp.50., Springer-Verlag, Berlin.

Rose, A.W., Hawkes, H.E., Webb, J.S. (1979). Geochemistry in Mineral Exploration. 2nd Ed. Academy Press.

Sergeyeva, E.I., Nikitin, A.A., Khodakovskiy, I.L. and Naumov, G.B. (1972): Experimental investigation of the equilibra in the system Uo_2-Co_2-H_2O in 25°C-2000°C temperature interval. Geochim. International, 9,900-910

Siegel, F.R. (1974): Applied geochemistry. A Wiley Interscience Publication.

Sinclair, A.J. (1974): Selection of thresholds in geochemical data using probability graphs. Journal geochem. Explor. 3, 129-149.

Sinclair, A.J. (1976); Probability graph. Association of Exploration geochemist. Special Vol. No.4, pp.95.

Skinner, B.J. (1979). The many origin of hydrothermal deposits. In: Geochemistry of hydrothermal ore deposits (Ed. Huber, L.B. (1979) 2nd Edition. John Wiley and Sons Inc.

Smith, E.E.N. (1974): Review of current concept Regarding Vein deposits of Uranium in: Formation of Uranium ore deposits: proceeding of a Symposium Athens,6-10, May IAEA pp.515-529.

Taylor, S.R. (1964): Abundance of Chemical elements to the Continental Crush, a new table: Geochim, Cosmochim Acta 28, 1273-1286.

Tennant, C.B. and White M.L. (1959): Study of distribution of some geochemical data Econ. geol. 54, 1281-1290.

Uranium (1983): Geology, Exploration, Mining and Milling an environmental aspects Vol. II. No. 1 Elsevier.

Woakes, M. and Olade, M.A. (1988): Metallogny of Nigerian basement in: International Meeting on Proterozoic geology and high grade terrains.

Wright, J.B. (1976): Volcanic Rocks in Nigeria. In: geology of Nigeria ed. Kogbe, C. A. pp.93-142. Elizabethan Press Lagos.

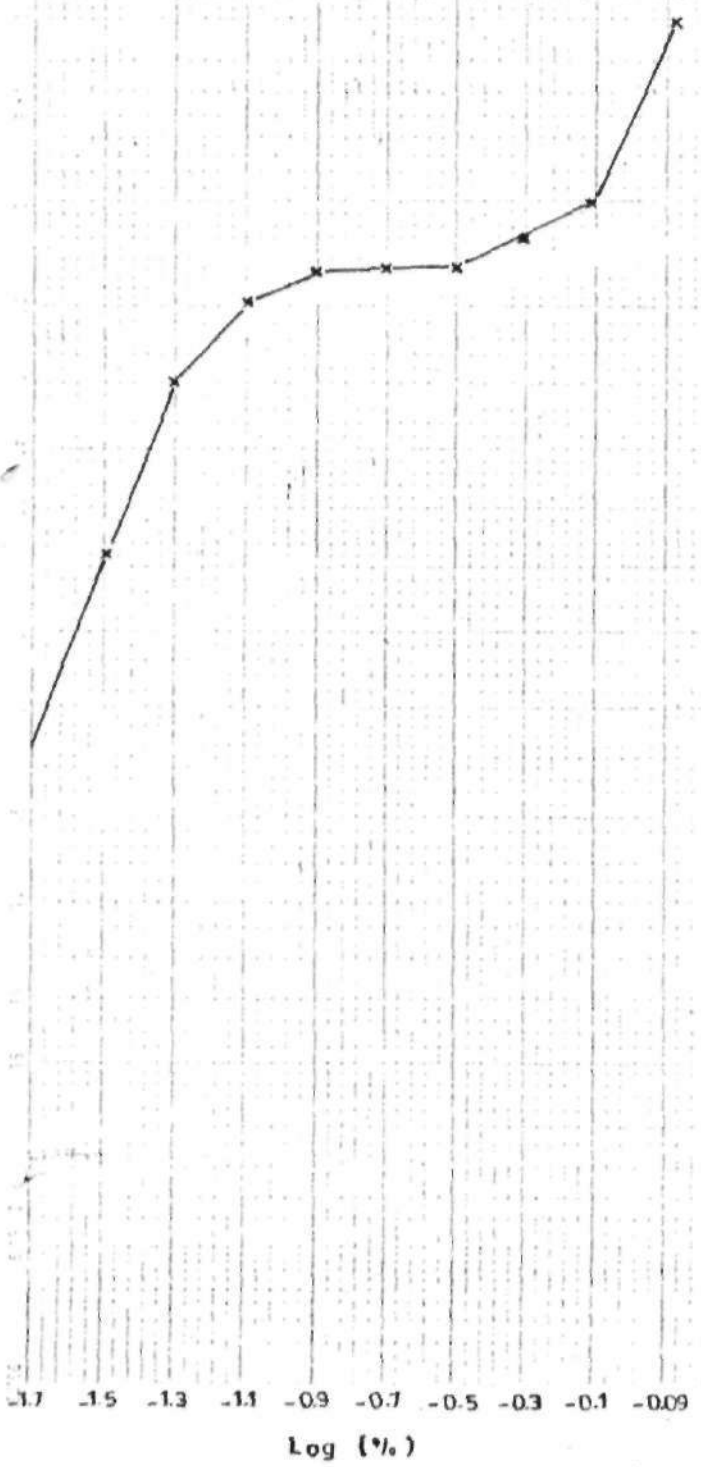
Wright, J.B. (1976) Origin of the Benue trough: A critical review. In: Geology of Nigeria (ed. Mogbe C.A.). Elizabethan Press, Lagos.

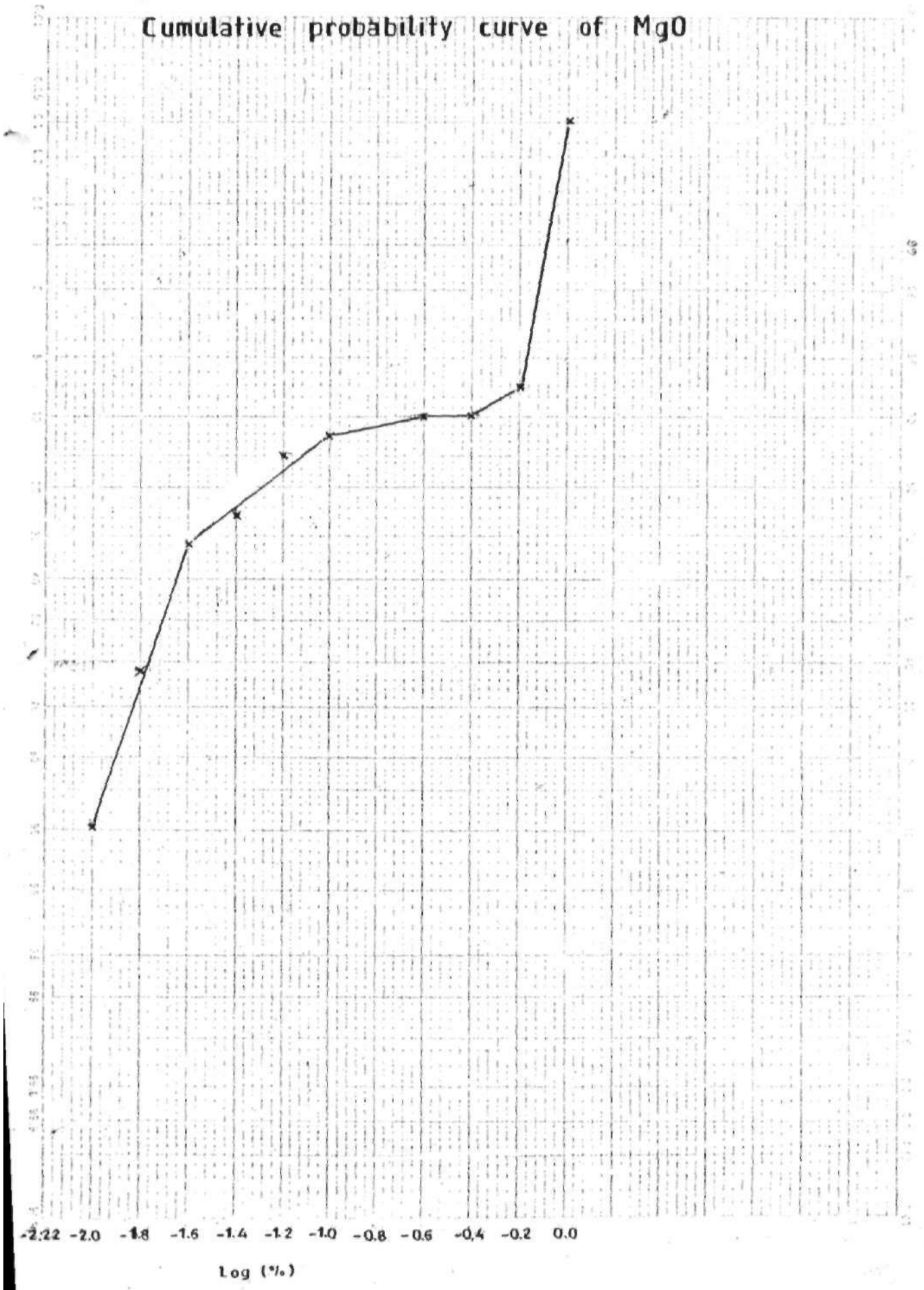
	CaO	MgO	FeO	K_2O	Na_2O	P_2O_5	TiO_2	MnO	Zn	Cu	Cr	Ni	U
1.	1.10	0.53	2.95	2.18	3.00	0.20	0.02	0.07	24	16	55	15	23
2.	0.03	0.01	0.92	1.00	0.09	0.05	0.02	0.01	7.5	11	20	5	5.6
3.	0.78	0.57	11.35	0.25	1.02	0.14	0.08	0.01	38.5	42	115	35	53.5
4.	0.03	0.02	4.1	0.05	0.54	0.08	0.08	0.03	21.0	26	75	15	66.1
5.	1.23	0.82	2.0	0.30	0.84	0.06	-	0.02	23.0	38	55	15	35.0
6.	0.04	0.02	2.25	0.12	0.06	0.23	0.08	0.01	12.0	16	50	10	47.3
7.	1.20	0.70	1.3	0.30	0.80	0.05	0.08	0.01	127.5	44	30	10	92.2
8.	0.07	0.03	0.7	0.12	0.10	0.04	0.14	0.03	36.0	16	20	10	47.3
9.	0.04	0.01	1.50	0.12	0.07	0.05	0.14	0.01	17.5	11	30	10	29.0
10.	1.08	0.7	5.0	0.26	0.84	0.14	0.16	0.01	22.5	16	85	19	66.1
11.	0.03	0.01	7.0	0.42	0.06	0.12	0.16	0.01	23.5	11	85	25	47.3
12.	0.03	0.01	4.2	0.14	0.06	0.16	0.32	0.01	23.5	11	85	25	66.1
13.	0.03	0.01	0.48	0.06	0.07	0.18	0.02	0.01	27	11	100	20	66.1
14.	0.03	0.01	6.75	0.07	0.07	0.33	0.10	0.01	23	16	97	20	66.1
15.	0.03	0.03	14.45	0.10	0.08	0.28	0.12	0.12	70	16	165	40	66.1
16.	0.03	0.01	2.29	0.18	0.25	0.07	0.08	0.01	16	11	35	10	41.2
17.	0.03	0.01	6.5	0.06	0.06	0.32	0.10	0.06	44	16	100	30	85.6
18.	0.05	0.01	6.75	0.09	0.09	0.14	0.10	0.01	38.5	16	100	20	79
19.	0.07	0.04	0.7	0.12	0.09	0.04	0.14	0.01	36	16	20	10	47.2
20.	0.04	0.01	5.0	0.07	0.07	0.09	0.24	0.01	44	31	80	15	66.1
21.	0.03	0.01	2.9	0.05	0.06	0.15	0.08	-	36	11	65	15	66.1
22.	0.03	0.01	0.60	0.09	0.06	0.01	0.08	-	100	11	15	5	41.2
23.	0.05	0.02	2.6	0.05	0.07	0.02	0.16	0.02	23.5	13	65	20	29.0
24.	0.03	0.01	6.75	0.07	0.07	0.33	0.10	0.01	23	16	97	20	66.1
25.	0.03	0.01	10.0	0.15	0.08	0.05	0.06	0.06	25	31	130	31	29.0
26.	0.03	0.02	7.25	0.08	0.06	0.07	0.14	0.01	22	6	35	10	53.5
27.	0.05	0.02	0.63	0.05	0.06	0.15	0.22	0.01	12.5	11	22.4	10	29
28.	0.06	0.02	3.35	0.05	0.10	0.08	0.06	0.01	24	21	60	25	53.5
29.	0.04	0.02	17.4	0.06	0.254	0.303	0.12	0.02	44	79	21	40	35
30.	0.03	0.04	2.0	0.11	0.29	0.05	0.12	0.01	13.5	6	40	10	47.3
31.	0.04	0.02	7.5	0.08	0.07	0.18	0.14	0.02	38.5	36	11	25	41.2
32.	0.05	0.02	3.45	0.20	0.08	0.09	-	0.01	30.5	11	50	20	29
33.	0.03	0.03	2.5	0.08	0.06	-	0.02	0.06	37.5	41	55	15	35
34.	0.07	0.69	13	0.31	0.72	0.13	0.12	0.01	75	16	15	30	29
35.	0.03	0.01	6.25	0.06	0.07	0.10	0.02	0.02	23	31	90	25	41.2
36.	0.03	0.01	1.05	0.05	0.06	6.0	0.06	0.01	30	18	25	12	23.1
37.	0.02	0.01	8.0	0.05	0.06	0.5	0.08	0.01	42.5	11	120	30	66.1
38.	0.78	0.42	2.5	0.25	0.06	0.14	0.08	0.01	28.5	41	115	35	53.5
39.	0.03	0.01	3.65	0.06	0.06	0.11	0.10	0.01	21	16	70	15	41.2
40.	0.03	0.01	2.35	0.48	0.23	0.04	-	0.02	17.5	16	40	12	29
31.	1.23	0.82	2.0	0.31	0.84	0.06	-	0.01	23.0	38	55	15	35
42.	0.03	0.02	2.5	0.08	0.33	0.08	0.10	0.12	37.5	16	53	10	59.6
43.	0.05	0.02	0.75	0.09	0.20	0.01	0.18	0.01	10	11	20	5	29
44.	0.03	0.01	10.75	0.06	0.06	0.21	0.24	0.01	82.5	76	135	35	35
45.	0.03	0.02	1.86	0.09	0.09	0.05	0.12	-	14	1	32	12	29
46.	0.04	0.02	1.0	0.06	0.06	-	0.08	0.01	27.5	1	30	10	29

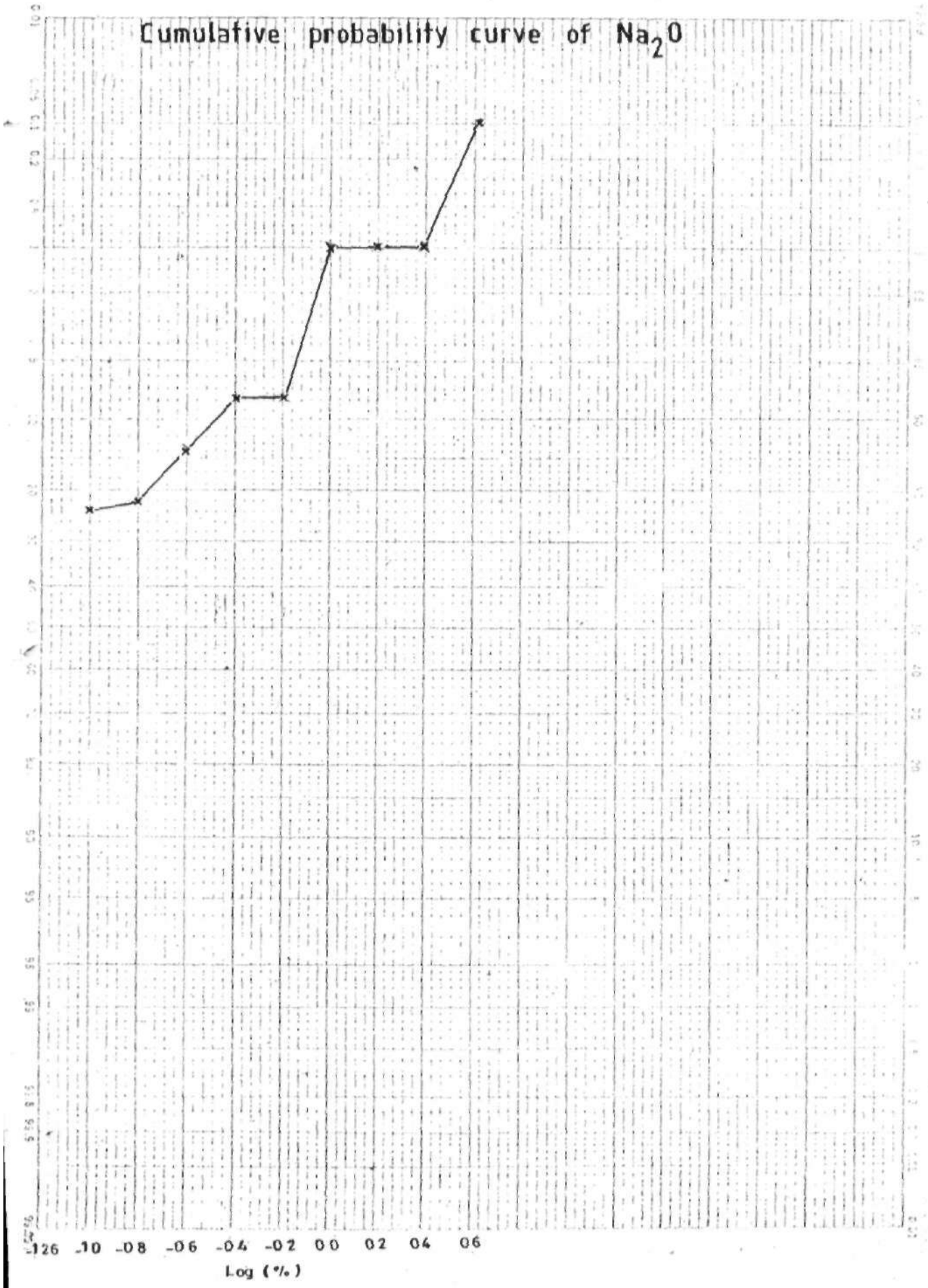
	CaO	MgO	FeO	K_2O	Na_2O	P_2O_5	TiO_2	MnO	Zn	Cu	Cr	Ni	U
47.	0.03	0.02	3.68	0.08	0.08	0.73	0.24	0.03	27.5	21	70	15	72.5
48.	0.04	0.02	1.45	0.07	0.06	-	0.14	0.01	21.8	16	30	12	23.1
49.	0.09	0.07	6.7	0.21	0.21	0.09	0.06	0.04	235	36	104	30	35
50.	0.06	0.03	1.85	0.06	0.06	0.05	0.12	0.02	130	23	25	15	170.9
51.	1.20	0.70	1.30	0.76	0.80	0.05	0.08	0.01	127.5	44	30	10	92.2
52.	0.07	0.04	10.25	0.07	0.07	0.37	0.14	0.02	115	41	137	35	66.1
53.	0.03	0.03	1.10	0.18	0.18	0.03	-	0.01	28.5	13	20	10	113.6
54.	0.03	0.04	3.30	0.07	0.07	0.01	0.06	0.01	57.5	23	80	15	47.7
55.	0.04	0.01	1.15	0.08	0.08	0.08	0.02	-	12.5	11	20	10	23.1
56.	0.03	0.03	2.40	0.25	0.15	0.04	0.14	0.03	20.0	16	40	15	35.0
57.	0.06	0.04	2.60	0.16	0.06	0.07	0.12	0.03	21.5	21	50	25	41.2
58.	0.48	0.47	5.25	0.26	0.10	0.08	0.08	0.18	38.0	31	75	20	29.0
59.	0.05	0.05	3.45	0.20	0.08	0.09	-	0.03	30.5	11	50	20	29.6
60.	0.03	0.03	1.10	2.18	0.18	0.03	0.02	0.03	28.5	13	20	10	11.4

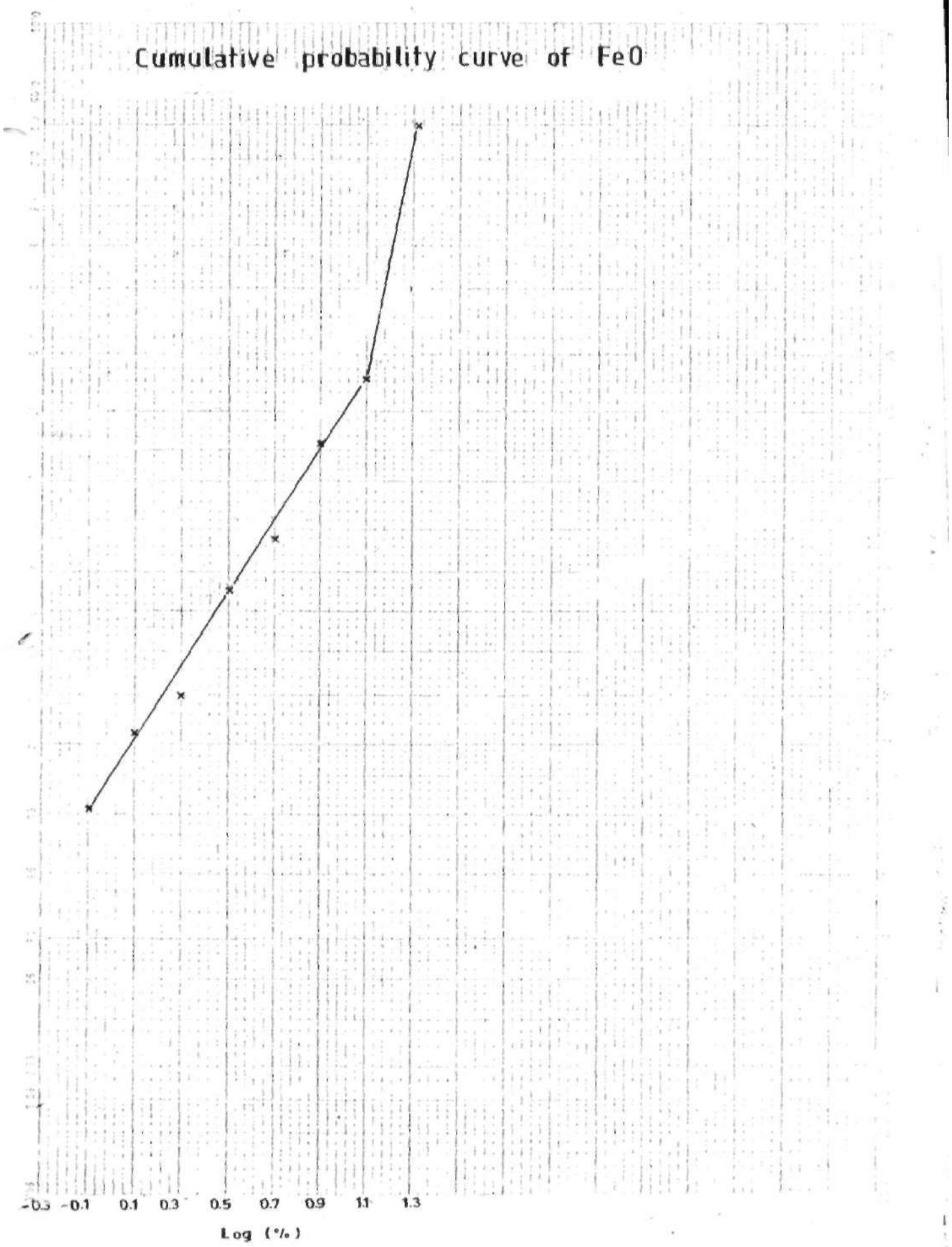
APPENDIX II

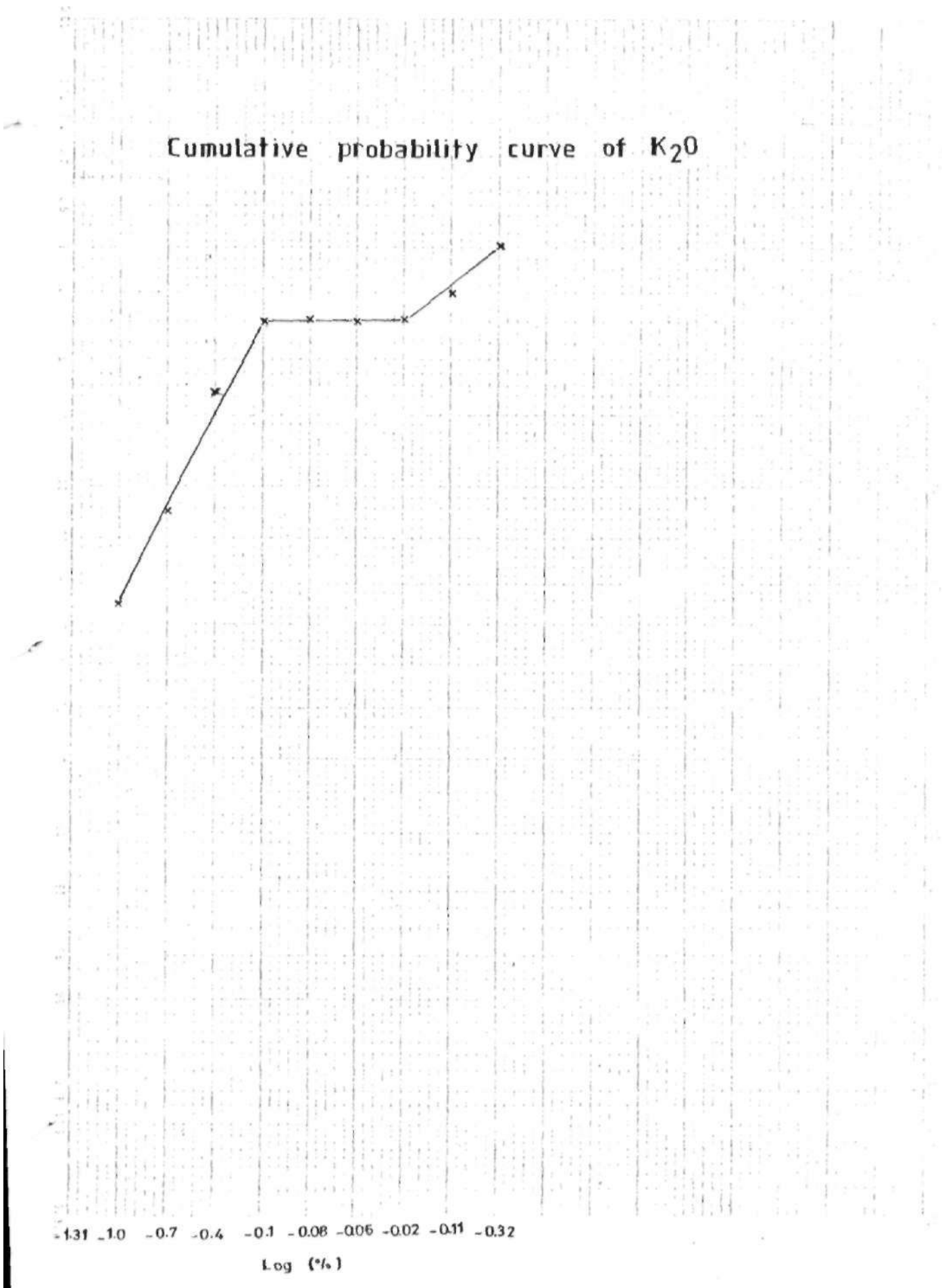
Cumulative probability curve of CaO



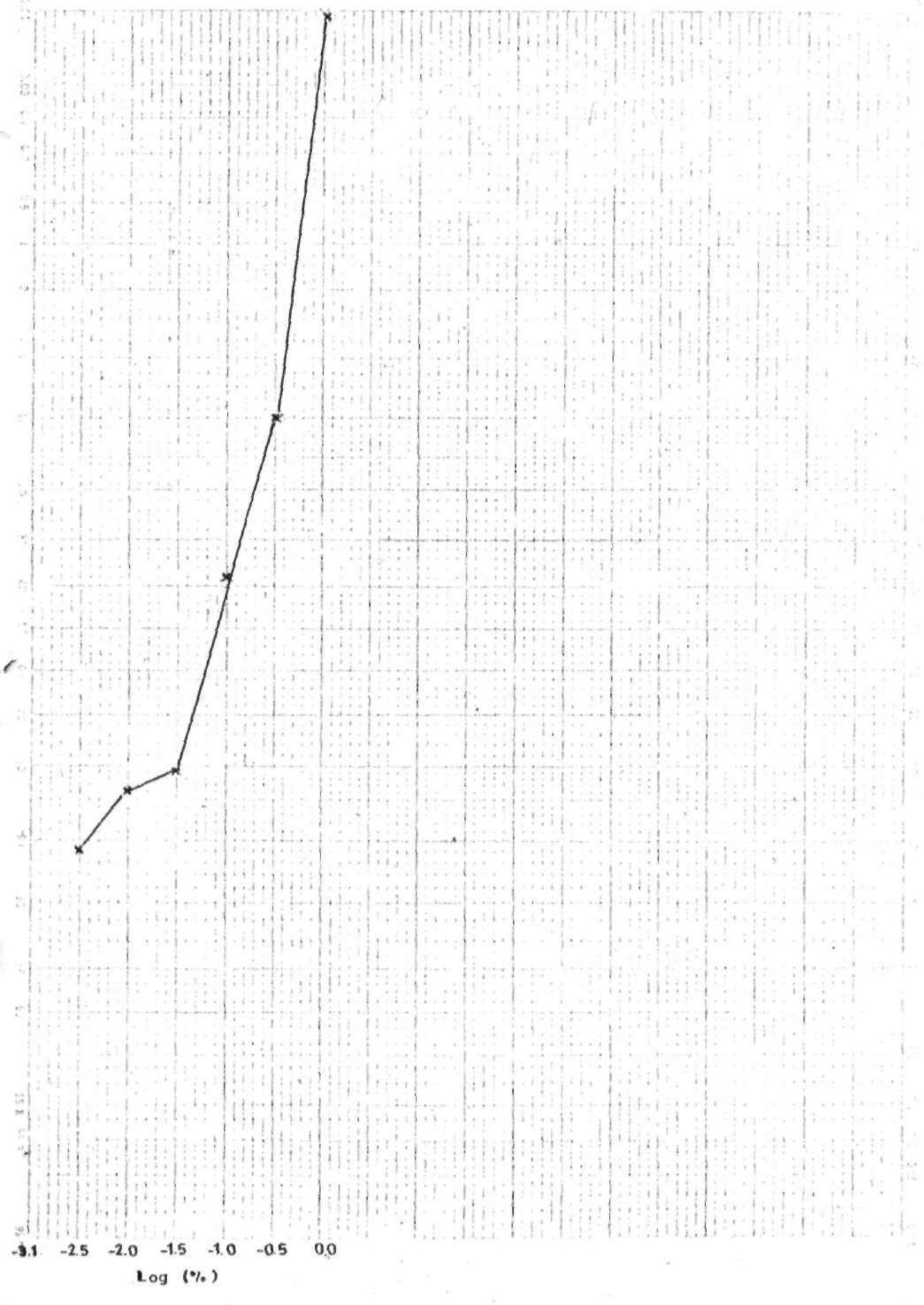

Cumulative probability curve of MgO
-2.22 -2.0 -1.8 -1.6 -1.4 -1.2 -1.0 -0.8 -0.6 -0.4 -0.2 0.0
Log (%)


Cumulative probability curve of Na_2O
-126 -10 -08 -06 -04 -02 00 02 04 06
Log (%)

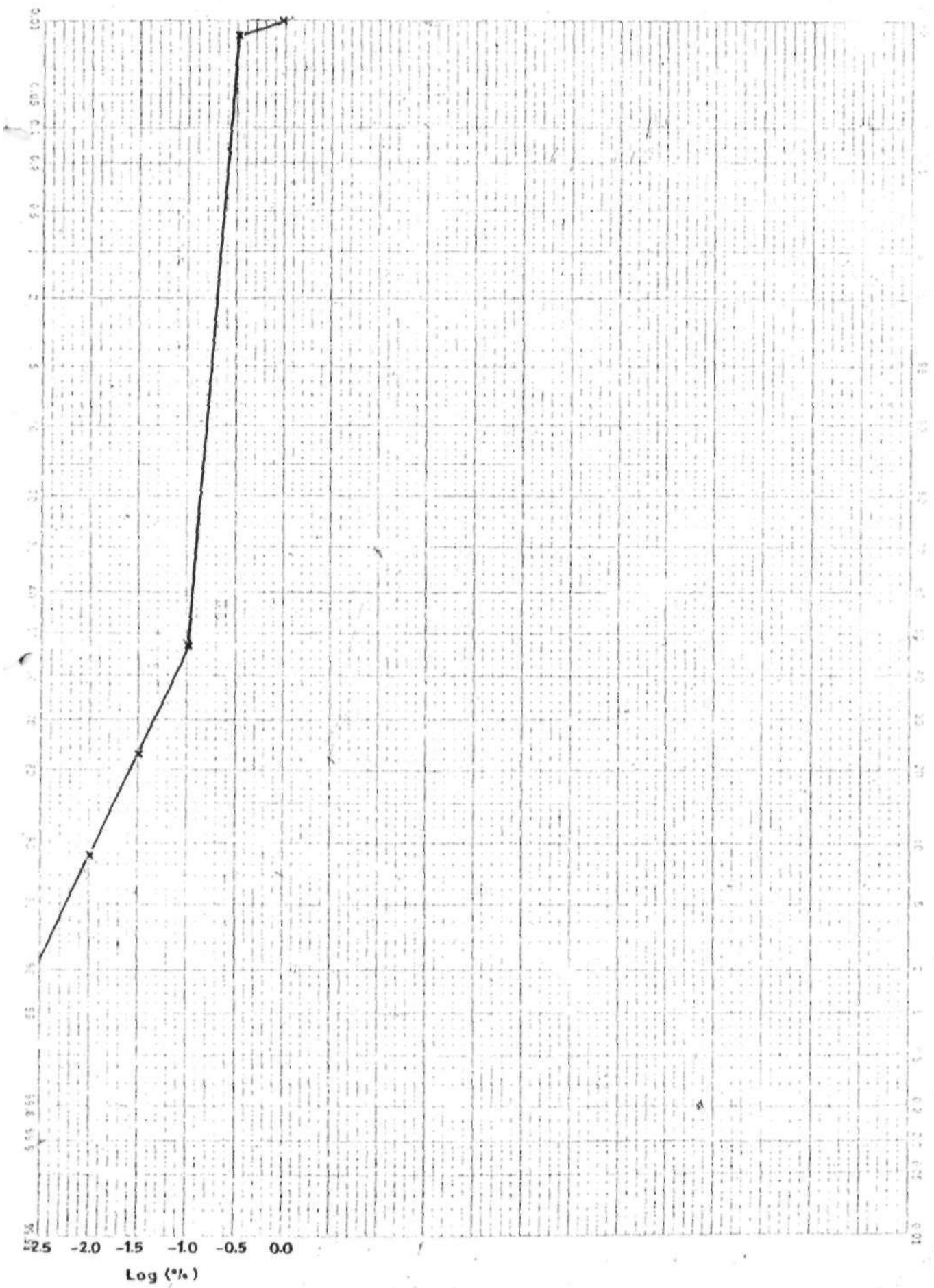

Cumulative probability curve of FeO
-0.3
-0.1
0.1
0.3
0.5
0.7
0.9
1.1
1.3
Log (%)

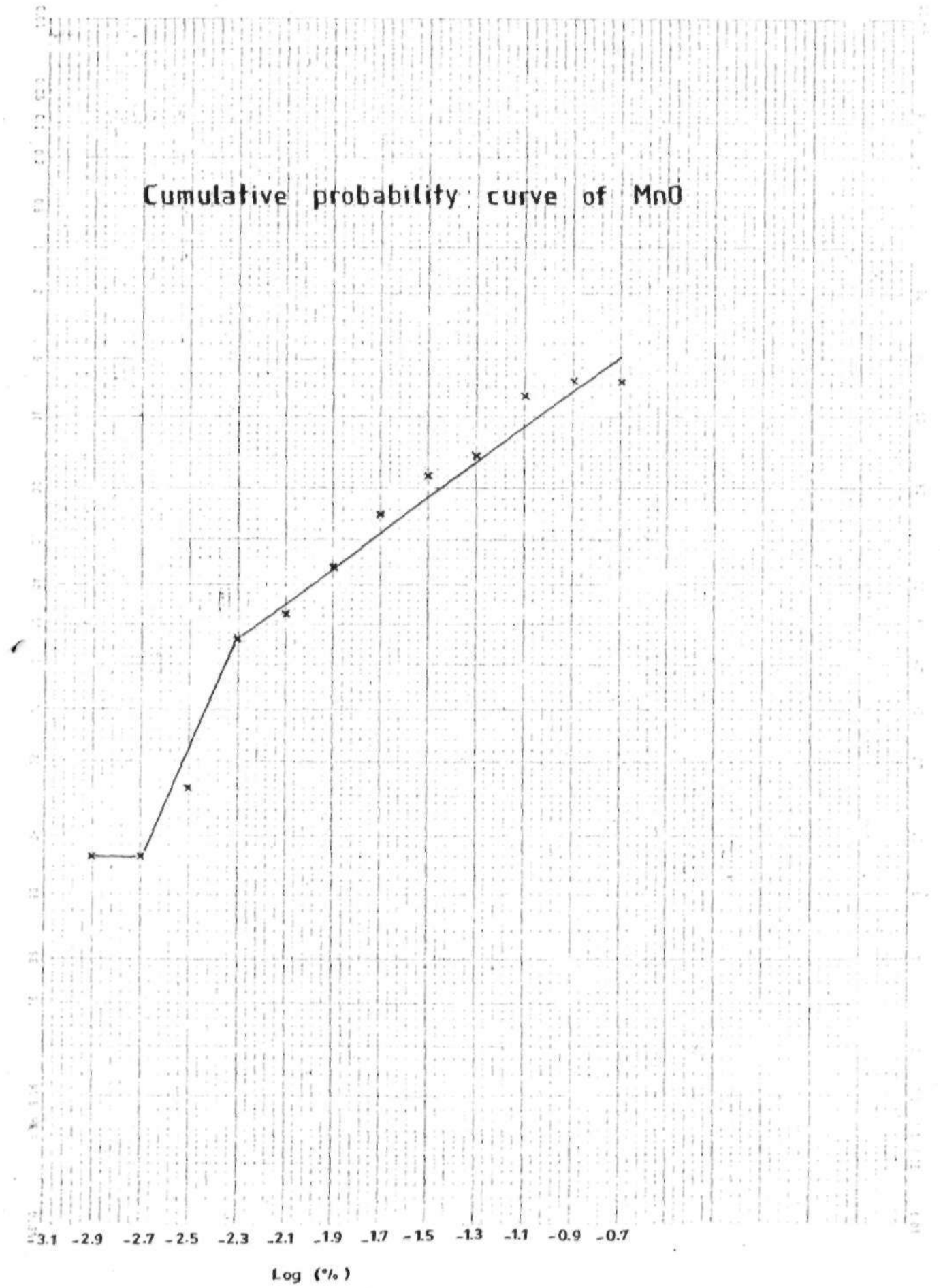

Cumulative probability curve of K_2O
-1.31 -1.0 -0.7 -0.4 -0.1 -0.08 -0.06 -0.02 -0.11 -0.32
Log (%)

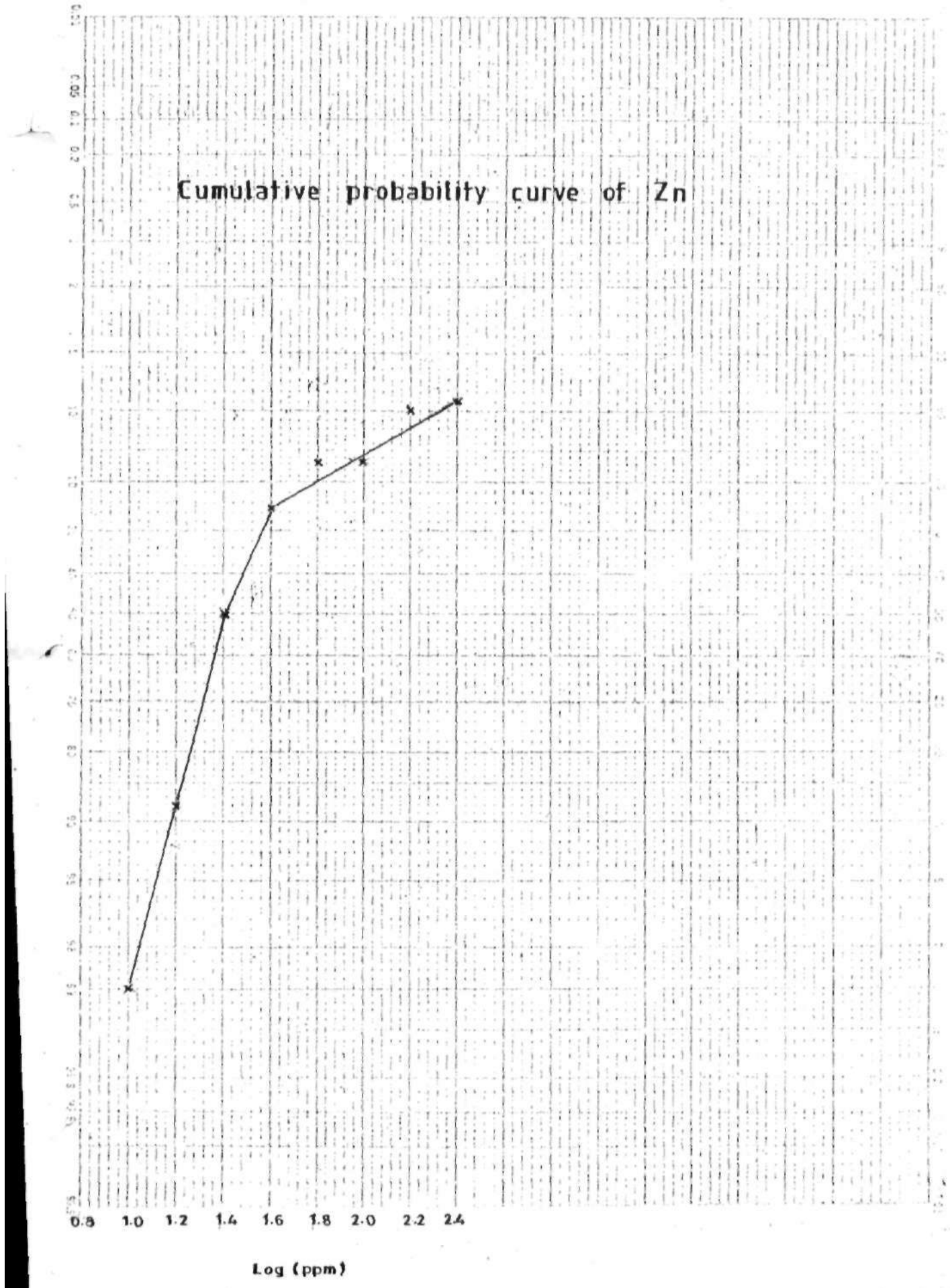
Cumulative probability curve of P_2O_5



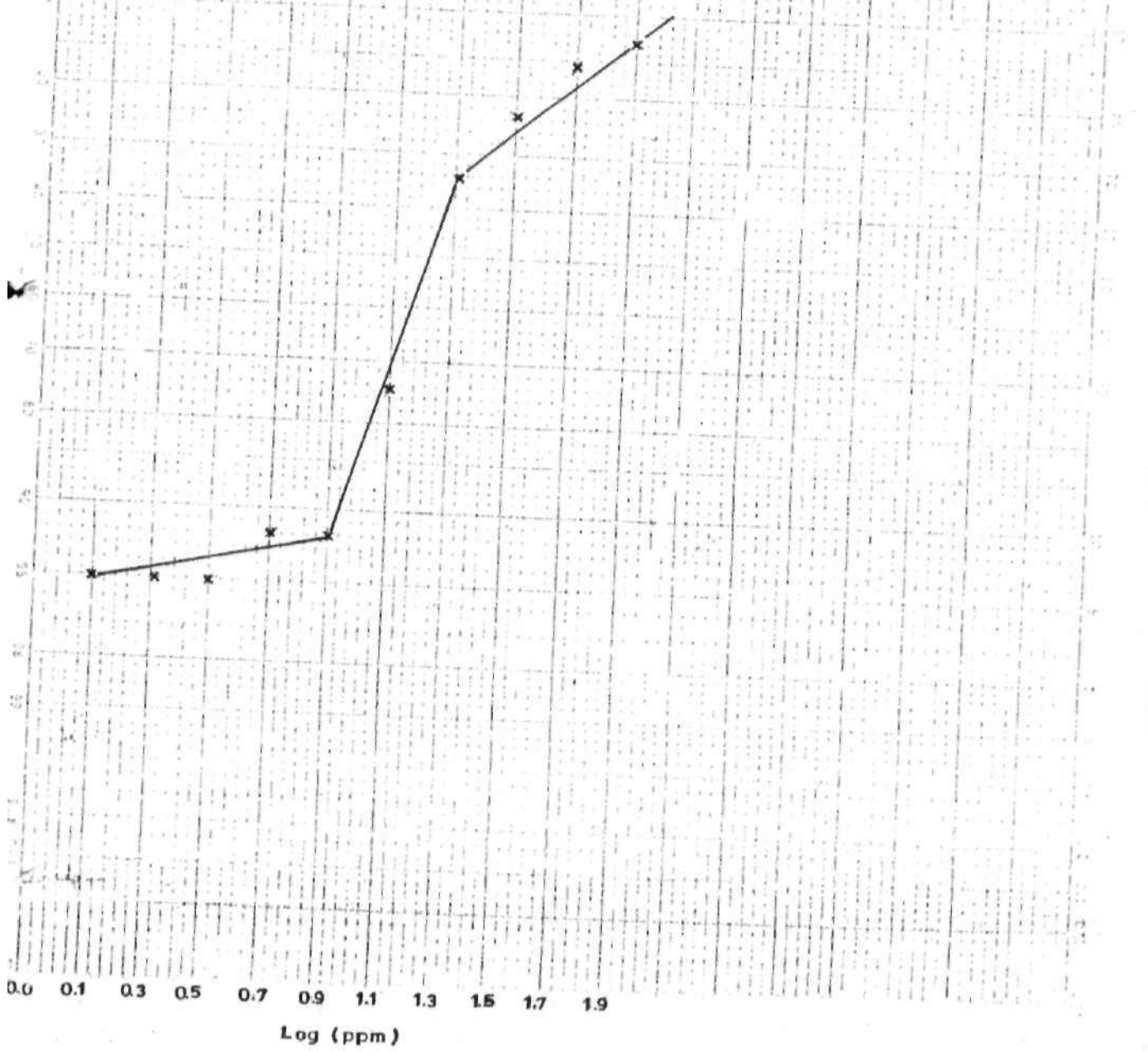
Cumulative probability curve of TiO_2



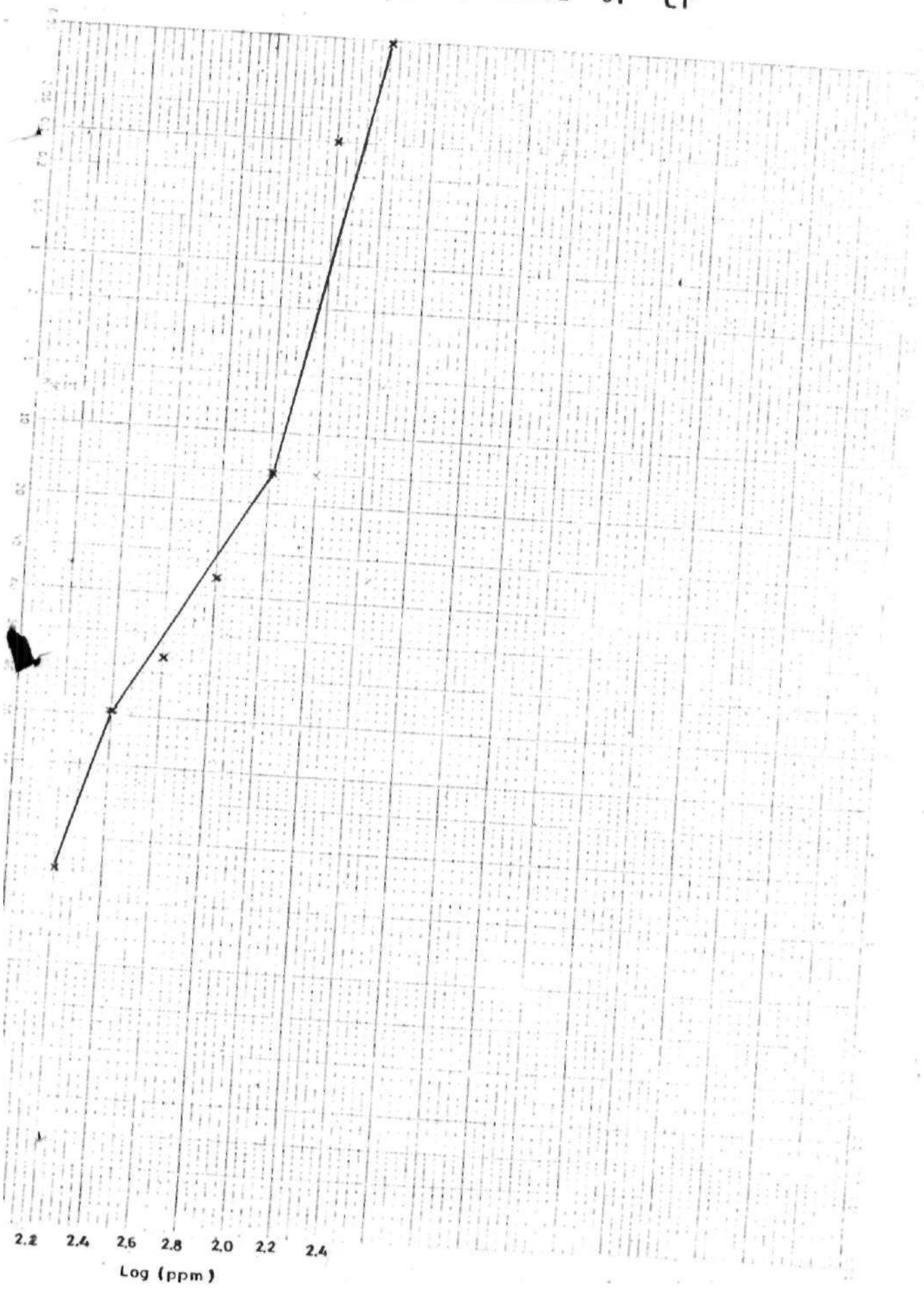

Cumulative probability curve of MnO
-3.1 -2.9 -2.7 -2.5 -2.3 -2.1 -1.9 -1.7 -1.5 -1.3 -1.1 -0.9 -0.7
Log (%)

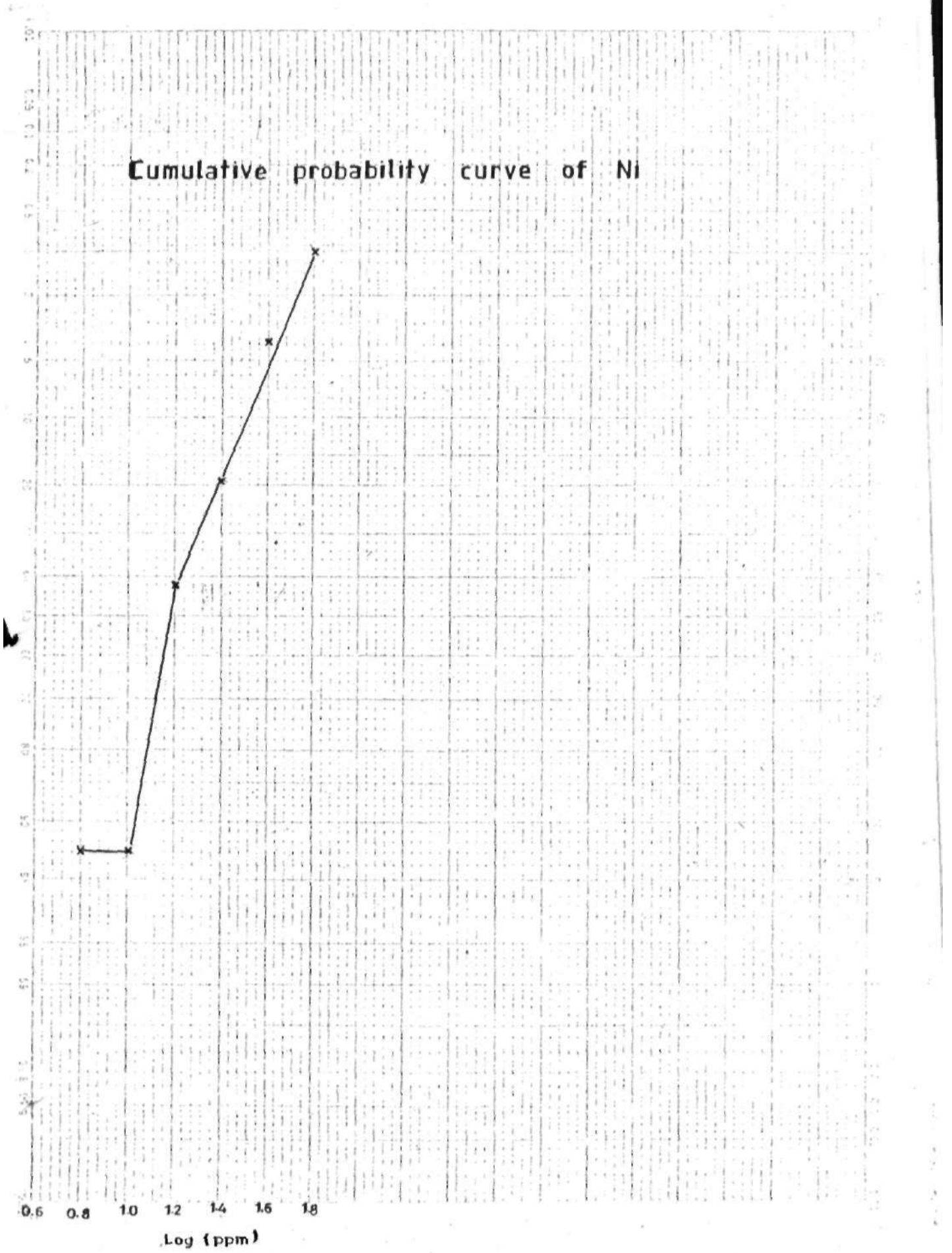

Cumulative probability curve of Zn
0.8
1.0
1.2
1.4
1.6
1.8
2.0
2.2
2.4
Log (ppm)

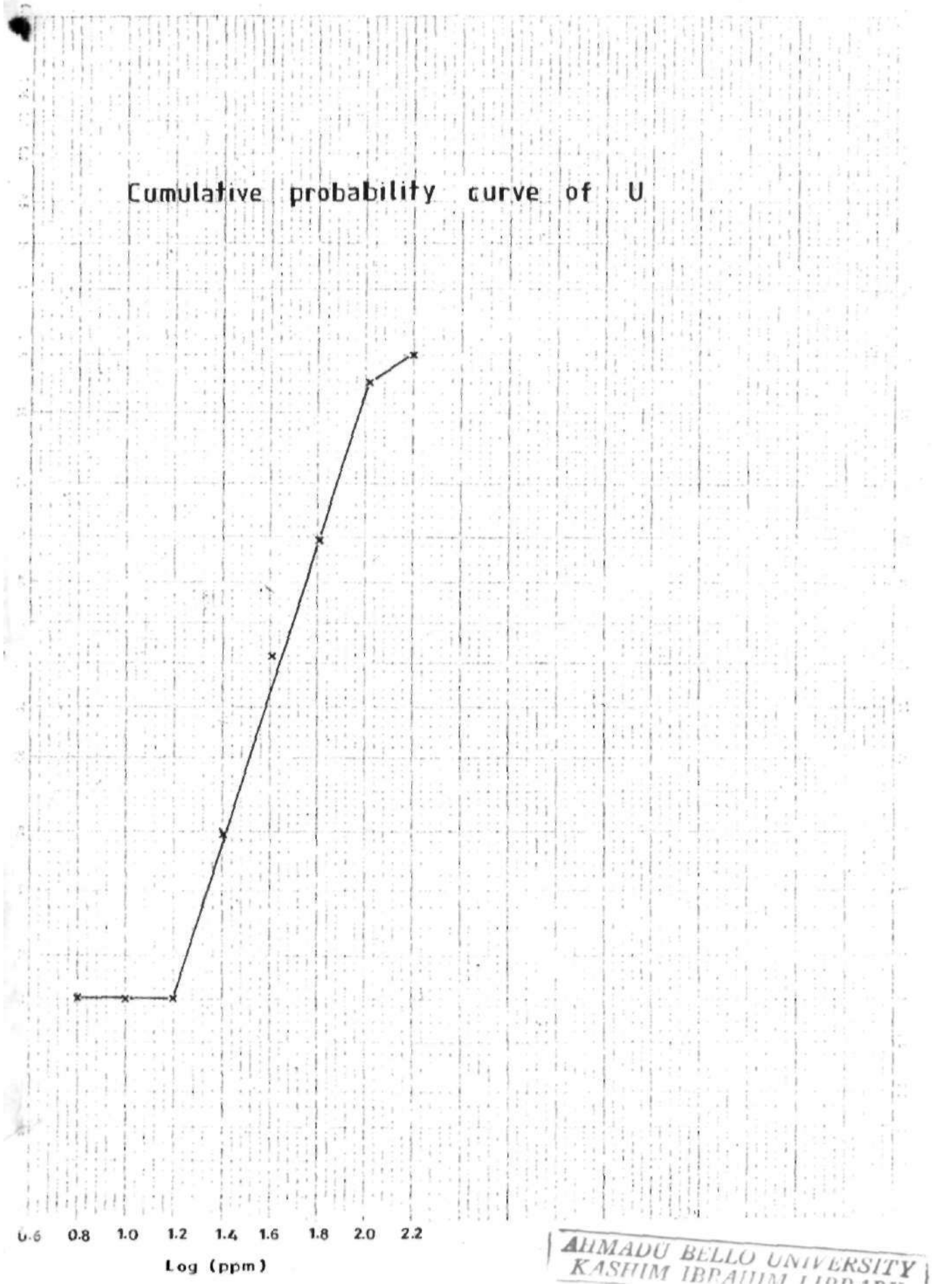
Cumulative probability curve of Cu



Cumulative probability curve of Cr




Cumulative probability curve of Ni
0.6
0.8
1.0
1.2
1.4
1.6
1.8
Log (ppm)



AHMADU BELLO UNIVERSITY
KASHIM IBRAHIM LIBRARY

FIG. 3.1. GEOLOGICAL MAP OF PART OF MONKIN (SHEET 126 N.W.)

